Molecular Analysis of Chordomas and Identification of Therapeutic Targets

A thesis submitted to the University College London (UCL) for the degree of Doctor of Philosophy

by

Asem Ali Esmaeil Shalaby

June 2010

Institute of Orthopaedics and Musculoskeletal Sciences

(IOMS)

Brockley Hill, Stanmore,
Middlesex, HA7 4LP

I, Asem Ali Esmaeil Shalaby, confirm that the work presented in this thesis is my own. Where information has been derived from other sources, I confirm that this has been indicated in the thesis.

ABSTRACT

Chordoma is a rare malignant bone tumour, showing notochordal differentiation, which occurs in the axial skeleton. Brachyury, a molecule involved in notochordal development, is a highly specific and sensitive marker for chordoma. It is hypothesised that *brachyury* or genes involved in its activation are implicated in the pathogenesis of chordoma. As there is currently no effective drug therapy for chordoma the aim of this study was to identify genetic events involved in chordoma pathogenesis with a view to identifying potential therapeutic targets.

One hundred chordomas (50 skull-based, 50 non-skull based) were studied. Immunohistochemistry showed that the PI3K/AKT/TSC/mTOR pathway was activated in 65% of chordomas, thereby providing a rationale for testing mTOR inhibitors for the treatment of selected cases. DNA sequencing revealed no mutations in *PI3KCA* or *RAS homologue enriched in brain (Rheb)* in 23 tumours. Immunohistochemistry and Western blotting showed activation of the fibroblastic growth factor receptor (FGFR)/RAS/RAF/MEK/ERK/ETS2/brachyury pathway in more than 90% of cases, but no mutations were found in the genes analysed (*FGFR*s, *KRAS*, *BRAF* and *brachyury*) in 23 tumours. Three percent of cases revealed *brachyury* amplification but nearly half of the cases showed chromosomal abnormalities involving the *brachyury* locus. Knockdown of *brachyury* was achieved in the U-CH1 chordoma cell line using shRNA and resulted in premature cell senescence. These findings demonstrate that *brachyury* plays an important role in chordoma pathology.

FISH analysis showed *EGFR* copy number gain in 45% of chordomas, including 6% with amplification and 39% with high level polysomy. The EGFR inhibitor, tyrphostin (AG1478) significantly inhibited growth of the chordoma cell line, and Western blotting showed this was associated with reduced phosphorylation of EGFR in a dose dependent manner. This study provides evidence for the first time that selected chordomas may be susceptible to treatment with EGFR inhibitors.

ACKNOWLEDGEMENTS

First and foremost, I would like to express my utmost gratitude to **God**, the most Gracious, the most Merciful and Compassionate.

I would like to thank everyone who offered me help and encouragement throughout my PhD project and the writing of this thesis.

I am very grateful to my supervisor Professor Adrienne Flanagan. She has been a source of practical council and support throughout. She provided me with invaluable guidance and inspiration. I am indebted to her for her time and patience. Without her guidance, I would never have got to the end.

I would like to thank Dr Helen Birch, my second supervisor and Dr Vivek Mudera for their guidance and academic support through my project.

I would like to thank each member of Professor Adrienne Flanagan's group for their friendship and advice and for providing a wonderful working environment. In particular, I would like to thank Dr Nadège Presneau for her endless help and advice throughout the entire project.

I would like to show my deep thanks to Dr Bernadine Idowu who generously helped me and provided a lot of support during my difficult times.

Many thanks to my Fellow student, Miss Laure Duhamel for her help during the long hours of laboratory work.

Many thanks to the staff of the pathology department at the Royal National Orthopaedic Hospital, Stanmore, especially Mr Steve Crane, Mrs Margaret Byers, Mr Fitim Berisha and Miss Dina Halai for their valuable help.

A special thanks to Dr Tim Diss who helped me a great deal especially during my early days in the laboratory and for reviewing my thesis.

I am extremely thankful and appreciative to all my friends especially Dr Samir Sayed who gave me a lot of encouragement.

Most of all, I wish to extend my endless thanks and appreciation to my family; Omnia, Omar and Fatima, for their help, inspiration and support.

PUBLICATIONS

(Resulting in part from the work presented in this thesis)

I. Research papers

1. Analysis of the Fibroblastic Growth Factor Receptor-RAS/RAF/MEK/ ERK-ETS2/brachyury Signalling Pathway in Chordomas.

   Asem Shalaby, Nadège Presneau, Bernadine Idowu, Lisa Thompson, Timothy Briggs, Roberto Tirabosco, Timothy Diss and Adrienne M Flanagan. August 2009. Modern Pathology (2009) 22, 996-1005.

2. Potential Therapeutic Targets for Chordoma: PI3K/AKT/TSC1/TSC2/ mTOR pathway.

   Presneau N, Shalaby A, Idowu B, Gikas P, Cannon SR, Gout I, Diss T, Tirabosco R, Flanagan AM. April, 2009. British Journal of Cancer (2009) 100, 1406–1414.

3. Epidermal Growth Factor Receptor as a Potential Therapeutic Target in Chordomas.

   Asem Shalaby, Hongtao Ye, Bernadine Idowu, Tim Diss, Thomas Jacques, Roberto Tirabosco, Nadege Presneau, Adrienne Flanagan (In preparation).

4. Frequent Chromosomal Abnormalities Involving *Brachyury* Locus in Sporadic Chordomas.

   Nadège Presneau, Asem Shalaby, Nischalan Pillay, Hongtao Ye, Bernadine Idowu, Dina Halai, Roberto Tirabosco, Thomas Jacques, Fred Mertens, Lars-Gunnar Kindblom, Karoli Szuhai, Pancras Hogendoorn, Adrienne M Flanagan (In preparation).

II. Oral and poster presentations

1. PI3K/AKT/mTOR Pathway Implicated in Pathogenesis of Non-Skull Based Chordomas.

   Asem Shalaby, Nadège Presneau, Bernadine Idowu, Lisa Thompson, Adrienne M Flanagan. Pathological Society Summer Meeting, Leeds, 1-4 July 2008 (oral presentation).

2. Involvement of FGFR/RAS/MAPK Pathway in Non Skull Base Chordoma.

   Asem Shalaby, Nadège Presneau, Adrienne M Flanagan. Pathological Society Winter Meeting, London, 8-9 January 2009 (poster presentation).

3. Potential Therapeutic Target for Chordoma: PI3K/AKT/TSC1/TSC2/ mTOR Pathway.

   Asem Shalaby, Nadège Presneau, Adrienne M Flanagan. ICR Centenary Conference, London, 8-10 June 2009 (poster presentation).

4. Activation of Receptor Tyrosine Kinases and PKC theta in Non Skull Base Chordoma.

   Asem Shalaby, Nadège Presneau, Bernadine Idowu, Adrienne M Flanagan. Pathological Society Summer Meeting, Cardiff, 30 June-3 July 2009 (oral presentation).

5. Analysis of Epidermal Growth Factor Receptor Status in Sporadic Chordomas

   Asem Shalaby, Hongtao Ye, Bernadine Idowu, Tim Diss, Thomas Jacques, Roberto Tirabosco, Nadège Presneau, Adrienne M Flanagan. EMSOS 2010 conference, Birmingham, 5-7 May 2010 (poster presentation).

6. *In Vivo* and *In Vitro* Implications of the Transcription Factor *T* (*Brachyury*) in Pathogenesis of Sporadic Chordomas.

   Asem Shalaby, Nadege Presneau, Nischalan Pillay, Hongtao Ye, Bernadine Idowu, Dina Halai, Roberto Tirabosco, Thomas Jacques, Fred Mertens, Karoli Szuhai, Lars-Gunnar Kindblom, Pancras Hogendoorn, Adrienne M Flanagan. Pathological Society Summer Meeting, St Andrews, 29 June-1 July 2010 (oral presentation).

7. Epidermal Growth Factor Receptor as a Potential Therapeutic Target in Chordomas.

   Asem Shalaby, Hongtao Ye, Bernadine Idowu, Tim Diss, Thomas Jacques, Roberto Tirabosco, Nadège Presneau, Adrienne M Flanagan. Pathological Society Summer Meeting, St Andrews, 29 June-1 July 2010 (oral presentation).

Table of Contents

List of Figures

List of Tables

List of Abbreviations

A431	Epidermoid carcinoma cell line
aCGH	Array comparative genomic hybridisation
AR	Androgen receptor
ATP	Adenosine triphosphate
BAC	Bacterial artificial chromosome
bp	Base pair
BCA	Bicinchoninic acid
bFGF	Basic fibroblastic growth factor
BNCT	Benign notochordal cell tumour
BSA	Bovine serum albumin
cAMP	Cyclic adenosine monophosphate
CASP9	Caspase 9
CD24	Cluster of differentiation 24
CDK	Cyclin dependent kinase
CDKN	Cyclin dependent kinase inhibitor
cDNA	Complementary DNA
CEA	Carcinoembryonic antigen
CEP	Chromosome enumeration probes
CGH	Comparative genomic hybridisation
Chdm	Chordoma
CHN2	Chimaerin 2
CK19	Cytokeratin 19
COREC	Central Office for Research Ethics Committees
COX2	Cyclo-oxygenase-2
CPVL	Probable serine carboxypeptidase
CREB	cAMP response element binding
CSPG4	Chondroitin sulfate proteoglycan 4
CT	Computed tomography
d	Day
DAB	Diaminobenzidine
DAPI	4',6'-diamidino-2-phenylindole
DDR1	Discoidin domain receptor 1
dHPLC	Denaturing high performance chromatography
DMEM	Dulbecco's Modified Eagle's Medium
DMSO	Dimethylsulfoxide
DNA	Deoxyribonucleic acid
dNTP	Deoxyribonucleotide triphosphate
dsRNA	Double-stranded ribonucleic acid
DVL1	Dishevelled homolog

E-Cadherin	Epithelial Calcium-dependent adhesion protein
ECL	Chemiluminescence
EDTA	Ethylenediamine tetraacetic acid
eFGF	Embryonic fibroblastic growth factor
EGF	Epidermal growth factor
EGFR	Epidermal growth factot receptor
eIF-4E	Euokaryotic Initiation factor 4E
EMA	Epithelial membrane antigen
EphB2	Ephrin A2
ERG	Ets related gene
ERK	Extracellular signal-regulated kinase
ER	Estrogen receptor
ETS2	v-ets erythroblastosis virus E26 oncogene homolog 2
F	Forward
FACS	Fluorescence activated cell sorting
FBS	Fetal bovine serum
FDA	Food and Drug Administration
FGF	Fibroblastic growth factor
FGFR	Fibroblastic growt factor receptors
FISH	Fluorescent *in situ* hybridisation
FRAP1	FK506 binding protein 12-rapamycin associated protein 1
FRS2α	Fibroblast growth factor receptor substrate 2 alpha
FSRT	Fractionated stereotactic radiation therapy
GAP	Guanosine activating proein
GAPDH	Glyceraldehyde phosphate dehydrogenase
GDP	Guanosine diphosphate
GFAP	Glial fibrillary acidic protein
GFP	Green fluorescent protein
Grb2	Growth factor receptor bound 2
GTP	Guanosine triphosphate
Gy	Gray (unit of absorbed radiation dose)
GβL	G protein β subunit-like
h	Hour
H&E	Haematoxylin and eosin
HEK293T	Human Embryonic Kidney 293T cell line
HeLa	Cervical carcinoma cell line
HER2	Human Epidermal growth factor Receptor 2
HLXB9	Homeobox-containing gene 9
HMW-MAA	High molecular weight melanoma-associated antigen
HRP	Horseradish peroxidise
IgG	Immunoglobulin G
IMDM	Iscove's Modified Dulbecco's Medium
IMRT	Intensity modulated radiation therapy

kDa	Kilodalton
L	Litre
LB	Luria-Bertani medium
LOH	Loss of heterozygosity
mAb	Monoclonal antibody
MAPK	Mitogen activated protein kinase
MAPKK	Mitogen activated protein kinase kinase
mCGH	Metaphase comparative genomic hybridisation
MEK	Mitogen activated extracellular signal-regulated kinase Kinase
MET	Met proto-oncogene (hepatocyte growth factor receptor)
min	Minute
mM	Millimolar
MMP	Matrix metalloproteinase
MRI	Magnetic resonance imaging
mRNA	Messenger ribonucleic acid
MSI	Microsatellite instability
mTOR	Mammalian target of rapamycin
mTORC	mammalian target of rapamycine complex
MTS	3-(4,5-dimethylthiazol-2-yl)-5-(3-carboxymethoxyphenyl)-2-(4-sulfophenyl)-2H-tetrazolium, inner salt
NCAM	Neural cell adhesion molecule
NGF	Nerve growth factor receptor
nmol	Nanomole
NSCLC	Non-small cell lung cancer
O/N	Over night
ORF	Open reading frame
p-	Phospho-
p70 S6K	P70S6 kinase
RSK	Ribosomal s6 kinase
PAGE	Polyacrylamide gel electrophoresis
PAX7	Paired box gene 7
PBS	Phosphate buffered saline
PBS-T	Phosphate buffered saline-Tween
PC	Pressure cooking
PCR	Polymerase chain reation
PDGFR	Platelet-derived growth factor receptor
PDK	Phosphoinositide-dependent kinase
pH	Potential of hydrogen
PI3K	Phosphoinositide-3-kinase
PI3KCA	Phosphoinositide-3-kinase, catalytic, alpha polypeptide
PIP2	Phosphatidylinositol-4,5-bis phosphate
PIP3	Phosphatidylinositol-3,4,5-tris phosphate
PKC	Protein kinase C

PLCγ	Phospholipase C gamma
pmol	Picomole
PMS	Phenazine methosulfate
PTEN	Phosphatase and tensin homolog
PVDF	Polyvinylidene Fluoride
R	Reverse
RAF	Raf murine sarcoma viral oncogene homolog
RAS	Rat sarcoma viral oncogene homolog
rb1	Retinoblastoma 1
Rheb	RAS homologue enriched in brain
RIPA	Radioimmunoprecipitation assay
RISC	RNA-inducing silencing complex
RNAi	RNA interference
rpm	Rotations per minute
RPMI-1640).	Roswell Park Memorial Institute medium 1640
RPS6	S6 ribosomal protein
RTK	Receptor tyrosine kinase
RT-PCR	reverse transcriptase polymerase chain reaction
RUNX3	Runt-related transcription factor 3
s	Second
SA-β Gal	Senescence-associated beta-Galactosidase staining
SD	Standard deviation
SDS	sodium dodecyl sulfate
Ser	Serine
SH2	Src-homology domain 2
SHH	sonic hedgehog gene
shRNA	short hairpin ribonucleic acid
shRNAmir	microRNA-adapted shRNA
siRNA	small interfering RNA
SKOV3	Ovarian carcinoma cell lie
SNP	Single nucleotide polymorphism
SOS	Son of sevenless
SOX-9	Sry-related HMG box
SRS	Stereotactic radiosurgery
SSC	Saline-sodium citrate
STAT3	signal transducers and activators of transcription 3
TBE	Tris/Borate/EDTA
TBS	Tris-buffered saline
TBX	T-box transcription factor
TEAA	triethylammonium acetate;
TGF	Transforming growth factor

Thr	Threonine
TKI(s)	Tyrosine kinase inhibitor(s)
TMA(s)	Tissue microarray(s)
TOR	Target of rapamycin
TORKinibs	Target of rapamycin blocking agents
TrkA	Transforming tyrosine kinase protein A
TSC	Tuberous sclerosis complex
Tyr	Tyrosine
U/µl	Unit/microlitre
U/ml	Unit/millilitre
U-CH1	Ulm-Chordoma 1 cell line
UCL	University College London
WIBR	Wolfson Institute for Biomedical Research
Xbra	Xenopus brachyury
µL	Microlitre
µM	Micromolar
µm	Micrometer
℃	Degree Celsius

1. INTRODUCTION

1.1 GENERAL INTRODUCTION

Chordoma is a rare low to intermediate grade malignant bone tumour that occurs along the axial skeleton and is thought to arise from cellular remnants of notochord (Bjornsson et al., 1993; Mirra et al., 2002).

1.1.1 History

Chordoma was first described by Luschka (1856) and Virchow (1857) who gave the name ecchondrosis physaliphora to this tumour believing it to be of cartilaginous origin. Müller (1858) was the first to suggest the tumour to be of notochordal origin based on the presence of notochordal remnants in the skull base and the coccyx and he changed the name to ecchordosis physaliphora. Ribbert (1894) confirmed this view and introduced the term chordoma. One year later, Ribbert (1895) showed experimental evidence by puncturing the intervertebral discs of rabbits that the escaped nucleus pulposus after a time showed evidence of mass formation with histological structure similar to that of chordoma. Congdon (1952) replicated this experiment using a similar model.

The first report of a symptomatic chordoma was made by Klebs, (1864) in the spheno-occipital region. The sacro-coccygeal chordoma was first described in 1900 by Henning while the first intervertebral chordoma was described by Raul and Diss in 1924. Dedifferentiated

chordoma was first identified in the literature and described as malignant chordoma by Davison and Weil (1928). The chondroid variant of chordoma was first described as an entity by Heffelfinger et al., (1973) although Virchow (1857) first described the resemblance of chordoma to cartilage.

1.1.2 Incidence

Chordomas represent 1-4% of all primary malignant bone tumours (Heffelfinger et al., 1973; Ishida and Dorfman, 1994; Mirra et al., 2002) and are the fourth most common malignant bone tumour (Gottschalk et al., 2001; Ishida and Dorfman, 1994). The general incidence of chordoma in the population is approximately 0.08 per 100,000 per year (Ishida and Dorfman, 1994; McMaster et al., 2001).

Most chordomas arise in the axial skeleton with very few chordomas arising in extra axial locations. Chordomas are nearly evenly distributed along the axial skeleton with 32% arising in the cranium, 33% in the whole spine, and 29% in the sacrum and coccyx (Ishida and Dorfman, 1994; McMaster et al., 2001). The frequently reported anatomical distribution of 50% sacral, 35% cranial and 15% vertebral was based on small studies while the more even distribution was found in a population based study (Heffelfinger et al., 1973; Eriksson et al., 1981; Dahlin and Unni, 1994; McMaster et al., 2001). Generally, no racial predilection has been reported. However, McMaster et al., found that chordoma is four times more common in white than in black

populations. There is a male predominance (2:1) for sacral presentation while the skull-based chordomas shows no difference in gender distribution (Weber et al., 1995; McMaster et al., 2001).

Chordoma can present at any age from infancy to very late during the 8th or 9th decades, however, skull-based chordomas tend to present earlier, predominantly in the third and fourth decades. The median age for sacral chordoma is around 60 years (Perzin and Pushparaj, 1986).

1.1.3 Risk factors

There are no reported associations with irradiation or other environmental factors. However, irradiation may be a predisposing factor for dedifferentiated chordoma, an aggressive variant of chordoma (Saito et al., 1998; Hanna et al., 2008b).

A small percentage of chordomas have a familial pattern of inheritance. Eight families have been reported to have more than two affected members (Foote et al., 1958; Enin, 1964; Kerr et al., 1975; Chetty et al., 1991; Stepanek et al., 1998; Dalpra et al., 1999; Miozzo et al., 2000; Kelley et al., 2001). Recently, abnormalities in *brachyury*, a gene involved in notochordal development, have been shown to confer a high susceptibility for familial chordomas (Yang et al., 2009b).

Chordoma has no association with any of the inherited tumour predisposition syndromes apart from six cases of chordomas occurring in patients with tuberous sclerosis complex (TSC) syndrome (Dutton

and Singleton, 1975; Schroeder et al., 1987; Borgel et al., 2001; Lee-Jones et al., 2004; Lountzis et al., 2006). A case of chordoma with Crohn’s disease has been reported and although Crohn's disease and chordoma share common chromosomal abnormalities in 1p, 3p, and 7q, there is no obvious genetic relation between the two conditions (De Jesus-Monge et al., 2004).

1.1.4 Clinical presentation:

Clinically, chordomas are slow-growing tumours resulting in local destruction and invasion. Pain and neurological symptoms from local compression are the main presenting symptoms. Sacral chordomas manifest late, so the tumour is often huge at diagnosis. The symptoms include low back pain, anaesthesia, paraesthesia and sometimes intestinal obstruction. Headache and diplopia are the most common symptoms related to skull-based chordoma (Rich et al., 1985; York et al., 1999).

Local recurrence occurs in about 70% in cases where negative margins are not achieved after surgical resection as radical surgical excision is rarely feasible because of the extensive local infiltration and the presence of vital structures in the vicinity of the tumour. In contrast, local recurrence affects only 10-20% of patients with tumours resected with appropriate negative margins (Chambers and Schwinn, 1979; Volpe and Mazabraud, 1983; Kaiser et al., 1984; Sundaresan et al., 1987; Boriani et al., 2006).

Distant metastases occur in 20-48% of patients with chordomas of the spine (Volpe and Mazabraud, 1983; McPherson et al., 2006; Vergara et al., 2008) and in less than 10% of patients with skull-based tumours (Gay et al., 1995). The most common sites of distant metastases are the lungs, liver, bones, lymph nodes and skin (Bergh et al., 2000). The metastases occur mostly from sacral chordomas due to late presentation compared to skull-based chordomas (Higinbotham et al., 1967; Chambers and Schwinn, 1979; Sundaresan, 1986; Vergara et al., 2008). Metastases usually occur within three years from the initial diagnosis; however, the range varies from 3 months to more than 10 years (Bergh et al., 2000; Asano et al., 2003; Baratti et al., 2003).

1.1.5 Radiological appearance

Radiographically, chordoma appears as a destructive bony lesion geneally with a large soft tissue mass. Intra-tumoural amorphous calcification is seen in sacral chordomas in about 30-70% of cases as detected by X-ray and has been described as one of the cardinal radiological signs of sacral chordoma (Hsieh and Hsieh, 1936; Bergh et al., 2000; Llauger et al., 2000).

Computed tomography (CT) scanning is essential for evaluation of bone destruction, and calcification and/or bone fragments within the lesion. Chordomas appear on CT as homogeneous lytic lesions, with a density comparable to that of muscle. On contrast enhancement, the tumour appears heterogeneous and frequently shows low attenuation

within the soft tissue component reflecting the myxoid nature of the stroma (Firooznia et al., 1986).

Magnetic resonance imaging (MRI) is the best means of evaluating the extent of the tumour (Murphy et al., 1998). On MRI, chordomas are lobulated tumours, with low to intermediate signal intensity on T1-weighted images and heterogeneous high signal intensity on T2-weighted images (Sze et al., 1988; Leproux et al., 1993; Doucet et al., 1997; Murphy et al., 1998).

1.1.6 Treatment of chordoma

1.1.6.1 Surgery

Surgery is the main line of treatment for chordomas. The radical resection gives better local control and survival. However, adequate excision has major sequelae with loss of urogenital and rectal function in case of bilateral section of nerve roots, as well as cranial nerve impairments after resection of skull-based chordomas. Magrini et al., showed that radical resection is possible in average of 10-20% of cases arising at different sites (Magrini et al., 1992). Recent advances in imaging techniques improve the prognosis of chordoma by discovering small intra-osseous tumours which can be easily treated by en block resection (Smolders et al., 2003). Postoperative radiotherapy, both by linear accelerator, or proton therapy or combination can provide better control of the disease after surgery (Agrawal et al., 2006; Torres et al., 2009).

1.1.6.2 Radiotherapy

Radiation therapy alone is the second choice of treatment if surgery is not feasible although chordoma is a relatively radio-resistant tumour. In 1952, Dahlin and MacCarty, first reported the beneficial role of radiotherapy in treatment of skull-based chordomas. The dose of conventional photon radiotherapy required for the best response is relatively high (60-70 Gy) being restricted by the low radiation tolerance of the adjacent vital structures and so other types or modalities may be better tolerated (Dahlin and MacCarty, 1952; Park et al., 2006; Takahashi et al., 2009).

Proton beam radiotherapy can be used to maximize the dose of radiation to the tumour, while sparing adjacent critical structures. Proton radiotherapy is mainly used for skull based-chordomas, and results in the best long-term control and is associated with fewer complications (Munzenrider and Liebsch, 1999; Amichetti et al., 2009; Takahashi et al., 2009). Hug (2001) reported treatment of 33 patients with proton beam radiotherapy and found increased survival rate in comparison to other types of radiotherapy (Hug et al., 1999; Munzenrider and Liebsch, 1999; Hug, 2001). Carbon-ion radiotherapy characterised by high biologic effectiveness can be also used to treat chordomas with promising results of phase II clinical trials as measured by good local tumour control and an associated mild reaction in the normal tissue (Schulz-Ertner et al., 2003b; Imai et al., 2009; Mizoe et al., 2009).

New modalities of delivering focal photon radiotherapy, including fractionated stereotactic radiation therapy (FSRT), intensity modulated radiation therapy (IMRT) and stereotactic radiosurgery (SRS) allow delivery of higher and more conformal doses to the tumour while protecting the surrounding normal tissue (Foweraker et al., 2007; Gabriele et al., 2003; Henderson et al., 2009; Munzenrider and Liebsch, 1999; Debus et al., 2000; Mizoe et al., 2009; Chang et al., 2001).

1.1.6.3 Chemotherapy

Chordomas are generally considered to be resistant to standard cytotoxic chemotherapy. Dedifferentiated chordoma, a high grade form of chordoma with rapidly dividing cells has shown a limited response to chemotherapeutic drugs such as doxorubicin, ifosfamide, cisplatin and etoposide which are active in sarcomas (Fleming et al., 1993; Scimeca et al., 1996).

1.1.6.4 Targeted Drug therapy

1.1.6.4.1 Kinase inhibitors

The tyrosine kinase inhibitor, imatinib mesylate has shown a partial anti-tumour clinical and radiological response in a limited number of patients with chordoma, most probably through inactivation of platelet-derived growth factor receptor-β (PDGFR β) (Casali et al., 2004). Adding cisplatin has been shown to have synergistic activity and can re-establish a tumour response in advanced chordoma patients

progressing on imatinib mesylate alone (Casali et al., 2007; Stacchiotti et al., 2009).

Three cases of advanced chordomas have been reported to respond to inhibitors of epidermal growth factor receptor (EGFR), suggesting that inhibition of this molecule may be useful therapeutically for the treatments of chordomas (Hof et al., 2006; Singhal et al., 2009; Linden et al., 2009). Recent reports suggested c-Met oncoprotein inhibitors (Ostroumov and Hunter, 2008), and signal transducers and activators of transcription 3 (STAT3) inhibitors as potential drug targeted therapy for chordoma (Yang et al., 2009a) Although these targets are interesting, detailed preclinical *in vitro* and *in vivo* studies are required before using these drugs in the clinical management of the disease.

1.1.6.4.2 PI3K/AKT/TSC/mTOR pathway inhibitors

The activation of the PI3K/AKT/TSC/mTOR pathway has also been demonstrated in a small number of tumour samples (Han et al., 2009). In line with these data, Stacchiotti et al., (2009) reported a partial tumour response in 7 out of 9 advanced chordoma patients with the combined use of sirolimus, an mTOR inhibitor, and imatinib myselate a receptor tyrosine kinase inhhibitor. The PI3K/mTOR pathway inhibitor, PI-103 has also been shown to exhibit *in vitro* effects on a chordoma cell line U-CH1 in the form of reduction of proliferation and induction of apoptosis (Schwab et al., 2009a; Stacchiotti et al., 2009).

1.1.7 Prognosis

1.1.7.1 Survival rate

Median survival for patients with chordoma has been reported as 6 to 7 years, and the overall survival rates 70% at 5 years, and 40% at 10 years (Naka et al., 2003; McMaster et al., 2001; Stacchiotti et al., 2010). In general, patients with sacral chordomas have a better survival rate than those with skull-based chordomas. Complete surgical resection offers the best chance for long-term survival (Gay et al., 1995). Post-operative radiation therapy can increase the local control and prolong survival. The best results are reported with aggressive surgical treatment and proton-beam postoperative radiotherapy with a disease-free survival rate up to 77% at 5 years and 69% at 10 years (Rosenberg et al., 1999; Crockard et al., 2001).

Local recurrence markedly decreases the chances of achieving a cure and is considered as the most important predictor of mortality in chordoma patients (Bergh et al., 2000; Colli and Al-Mefty, 2001). Five-year survival of 35% is reported with incomplete resection even when followed by conventional photon radiation therapy (Zorlu et al., 2000). Detection of metastases markedly decreases the median survival time to less than a year (Bergh et al., 2000; Asano et al., 2003; McPherson et al., 2006).

1.1.7.2 Prognostic factors:

1.1.7.2.1 Clinical factors

The prognosis of chordoma is affected by many clinical factors, and poorer outcome has been associated with skull-based location, larger tumour size, invasion of the surrounding muscle, female gender, and age over 40 years (Forsyth et al., 1993; O'Connell et al., 1994; Thieblemont et al., 1995; Chen et al., 2010). The resectability and the quality of surgical margins represent the main prognostic factors (Forsyth et al., 1993; Bergh et al., 2000; Boriani et al., 2006; Osaka et al., 2008; Chen et al., 2010).

1.1.7.2.2 Histopathologic and genetic factors

The important histopathological factors which have been found to be associated with reduced survival include nuclear pleomorphism (Chambers and Schwinn, 1979; Naka et al., 2003), proliferation index of more than 5% as assessed by MIB-1 expression, increased mitotic activity and microscopic tumour necrosis (Matsuno et al., 1997; Matsuno and Nagashima, 2000; Naka et al., 2003). The presence of a dedifferentiated component is associated with a markedly poor prognosis compared to the conventional variant (Hanna et al., 2008a; Saito et al., 1998).

Low expression of E-cadherin and over-expression of TP53 are considered to be predictors of poor prognosis (Mori et al., 2002; Naka et al., 2005; Saad and Collins, 2005). Expression of matrix

metalloproteinases is also associated with unfavourable prognosis (Naka et al., 2004). Among the genetic markers, isochromosome 1q has been suggested as a marker of aggressiveness in skull-based chordomas (Sawyer et al., 2001) and loss of heterozygosity (LOH) at the *Rb1* gene locus 13q14 has been shown to be associated with aggressive chordomas (Eisenberg et al., 1997).

Although numerous studies have tried to use histological features as predictors for prognosis and biologic behaviour, none has been proved satisfactory and therefore are not used in clinical or diagnostic settings and the relationship between histological features and biological behaviour remains controversial (Kaiser et al., 1984; Bjornsson et al., 1993; Naka et al., 1996). Most of these studies were based only on a small number of specimens resulting in divergent results (Matsuno et al., 1997; Holton et al., 2000). Owing to low incidence and slow growth rate of chordomas, the reports were based on patient cohorts being treated over a long time span: different markers were used in attempt to predict outcome and different therapeutic modalities were also employed. These various issues have resulted in failure to develop a reliable prognostic marker for chordomas (Kaiser et al., 1984; Rich et al., 1985; York et al., 1999).

1.2 PATHOLOGY OF CHORDOMA

Chordoma is classified according to the histological appearance into three different variants. These are conventional, chondroid and dedifferentiated. A component of the conventional type is virtually always present in the chondroid variant and small chondroid areas are commonly found in the conventional variant. By definition a conventional or chondroid component must be present in a dedifferentiated chordoma (Gottschalk et al., 2001; Rosenberg et al., 1994).

Macroscopically, conventional chordoma is a soft, tan-grey lobulated mass with a gelatinous cut section. Foci of haemorrhage and necrosis are common especially in the large tumours. The chondroid chordoma is less gelatinous and is more firm giving the lesion a chondral appearance. The dedifferentiated component of a chordoma is fleshy and does not show the gelatinous or chondral appearance described above (Batsakis et al., 1980; Mirra et al., 2002).

1.2.1 Conventional chordoma

Microscopically, conventional chordoma is formed of nests, cords, lobules or clusters of cells separated by homogeneous amorphous myxoid stroma. The cells show great variability in size from small polyhedral or stellate cells to intermediate cells and larger cells with abundant cytoplasm and numerous intra-cytoplasmic vacuoles giving a ‘bubbly’ appearance and described as physaliphorous cells by Virchow (1857). The physaliphorous cells are characteristic of chordoma but are

not pathognomonic as they may be found in other tumour types including carcinoma, chondrosarcoma, epithelioid hemangio-endothelioma and liposarcoma. The nuclei of the neoplastic cells are of moderate size, dark staining and may contain small nucleoli or pseudo-inclusions. Additional morphologic features include significant nuclear pleomorphism, spindling of the tumour cells and physaliphorous cells with a single large cytoplasmic vacuole. Foci of necrosis and haemorrhage are common, especially in larger tumours (Naka et al., 2003).

Based on the degree of cellularity, conventional chordoma has been divided into two histological subtypes; the non-solid type which is composed of cord-like structures and the solid type composed of diffuse sheets of tumour cells (Naka et al., 2003). A representative histological section of conventional chordoma is shown in Figure 1.1A, while the characteristic physaliphorous cells containing multiple clear cytoplasmic vacuoles can be seen in Figure 1.1B.

Histochemistry is rarely, if ever used, for diagnosing chordomas as it is of limited value since the advent of immunohistochemistry. The cytoplasm of chordoma cells contains periodic acid-Schiff diastase-sensitive glycogen granules, although the cytoplasmic vacuoles are glycogen free. The myxoid stroma is rich in acidic and sulphated mucopolysaccharides and stains faintly with mucicarmine, and strongly with alcian blue which is not significantly reduced by prior digestion with

hyaluronidase.The stroma does not stain with phosphotungstic acid haematoxylin and reticulin stains whereas cartilaginous ground substance is strongly impregnated by these reagents (Crawford, 1958).

The immunoreactivity of conventional chordomas shows high expression of the nuclear transcription factor brachyury: this is highly sensitive and specific for chordoma and is absent in a wide range of other various epithelial and mesenchymal tumours apart from hemangioblastoma, known to derive embryologically from the posterior mesoderm (Glasker et al., 2006; Vujovic et al., 2006).

Chordomas also express epithelial markers including cytokeratins (especially cytokeratins 8, 18 and 19), and epithelial membrane antigen (EMA) (Salisbury and Isaacson, 1985; Vujovic et al., 2006). The combination of brachyury nuclear immunoreactivity and immunoreactivity for cytokeratin 19 (CK19) is diagnostic for chordoma and used to differentiate chordomas from other histologically similar tumours including chondrosarcomas (Tirabosco et al., 2008). An example of brachyury and CK19 immunoreactivity in chordomas is shown in Figure 1.1 C and D.

Immunoreactivity for S100 protein is variable from 30-90% in the literature (O'Donnell et al., 2007; Rosenberg et al., 1994; Walker et al., 1991). Vimentin is expressed in most cases while immunoreactivity to carcinoembryonic antigen (CEA) and glial fibrillary acidic protein (GFAP) is variable (Harrowe and Taylor, 1981; Bouropoulou et al., 1989). The

matrix of chordoma contains predominantly type I collagen and to a lesser extent type II collagen. Basement membrane proteins such as collagen type IV and laminin are present on the surface of cellular cords (Gottschalk et al., 2001; Taniguchi et al., 1984; Ueda et al., 1992).

Ultrastructurally, the neoplastic cells have epithelial features including villous-like projections, intra-cytoplasmic lumina, tonofilament-like bundles of intermediate filaments and well developed desmosomes (Murad and Murthy, 1970). The cells show abundant cytoplasmic glycogen, mitochondria-rough endoplasmic reticulum complexes and attenuated mitochondriae. The vacuoles in the physaliphorous cells represent either dilated rough endoplasmic reticulum, cytoplasmic inclusions of the extracellular space or intracellular lumina (Spjut and Luse, 1964; Erlandson et al., 1968).

1.2.3 Chondroid chordoma

Chondroid chordoma was originally defined in 1973 by Heffelfinger et al., as a tumour that contains areas of conventional chordoma as well as chondroid areas resembling low-grade hyaline-type chondrosarcoma (Heffelfinger et al., 1973).

Chondroid chordoma has a predilection for the skull base but can occur in the spinal and sacro-coccygeal regions. It represents 5%-15% of all chordomas and up to one third of the skull-based chordomas (Chugh et al., 2007).

It was originally thought that chondroid chordoma were associated with a better survival than conventional chordoma (Heffelfinger et al., 1973; Raffel et al., 1985; Rich et al., 1985). However subsequent studies showed that there is no difference in the overall survival (Forsyth et al., 1993; Mitchell et al., 1993; O'Connell et al., 1994; Rosenberg et al., 1994; Almefty et al., 2007). The marked discrepancies in the results can be attributed to inclusion of some chondrosarcomas into the chondroid chordoma group due the absence of immunohistochemistry in the earlier studies (Almefty et al., 2007; O'Connell et al., 1994).

The controversy following the initial description of chondroid chordoma regarding its existence as a variant of chordoma was first raised by Brooks et al., (1987) and was based on failure to demonstrate epithelial marker immunoreactivity as seen in conventional chordoma. However Mitchell et al., (1993) showed epithelial immunoreactivity in a subset of chondroid chordoma and argued that the tumours that were negative for epithelial markers are in fact low-grade chondrosarcoma. This issue is now resolved as the chondroid areas have been shown to express brachyury and CK19 (Vujovic et al., 2006) and therefore should be classified as chordomas.

Microscopically, the chondroid regions in chordomas merge with or abruptly appose the surrounding conventional component. The chondroid areas are composed of neoplastic cells distributed individually

in lacunar-like spaces surrounded by solid appearing hyalinised matrix similar to hyaline cartilage. The quantity of the chondroid component in any individual tumour is variable and a tumour is now only classified as a chondroid chordoma when at least 60% of the tumour has a chondroid appearance. However, in some cases; it is so abundant that it may be difficult to distinguish the tumour from chondrosarcoma (Heffelfinger et al., 1973; Rosenberg et al., 1994). A histological section of chondroid chordoma is shown in Figure 1.1 E.

The tumour cells in the chondroid areas of chordoma exhibit the same epithelial characteristics as those in conventional foci and exhibit the same immunohistochemical and ultra-structural features. This supports the view that the chondroid appearance in these tumours represents a morphologic difference in the extra-cellular matrix rather than the presence of hyaline cartilage in a chordoma which only contains Type II collagen (Ishida and Dorfman, 1994; Rosenberg et al., 1994).

1.2.4 Dedifferentiated chordoma

Dedifferentiated chordoma was defined by Meis et al., (1987) as a tumour characterised by a sharp demarcation between a conventional chordoma and a high-grade sarcomatous component. Dedifferentiated chordoma comprises less than 5% of all chordomas and most frequently complicates sacro-coccygeal tumours (Hanna et al., 2008b). The dedifferentiation is suspected to occur as a result of ongoing cumulative

mutations in conventional chordoma cells and may arise within a primary tumour as opposed to arising in a recurrence or secondary to radiotherapy (Ikeda et al., 1997; Saito et al., 1998).

Grossly the dedifferentiated component of chordoma is fish flesh-like in appearance, and morphologically it is usually distinct from the areas of conventional chordoma. The light microscopic features, immunohistochemical phenotype and ultrastructural characteristics of the dedifferentiated component usually are those of a pleomorphic sarcoma or fibrosarcoma, although rarely there is osteosarcomatous or rhabdomyosarcomatous differentiation present (Meis et al., 1987; Morimitsu et al., 2000; Bisceglia et al., 2007).

The importance of identifying a dedifferentiated chordoma is that it behaves aggressively. It has the worst prognosis of all chordoma types and is usually rapidly fatal with systemic spread occurring in approximately 90% of cases. The size of the dedifferentiated component is a significant predictor of survival (Hanna et al., 2008b). A representative histological image of dedifferentiated chordoma is shown in Figure 1.1 F.

1.2.5 Extra-axial chordoma:

A small number of chordomas arising outside the axial skeleton in bone and soft tissue has been reported. These reports were based on the identical morphological features as those seen in conventional axial chordoma (McMaster et al., 2001; DiFrancesco et al., 2006; van Akkooi

et al., 2006; Tirabosco et al., 2008). Tirabosco et al., (2008) have recently shown immunoreactivity for brachyury and CK19 in eight extra-axial skeletal and two soft tissue cases, providing a strong evidence for the first time, that these were similar tumours. These extra-axial tumours were first described by Laskowski (1955) as chordoma periphericum and by Dabska in 1977 who labelled them as parachordoma (Laskowski, 1955; Dabska, 1977; Scolyer et al., 2004; Tirabosco et al., 2008). Soft tissue tumours with a morphological phenotype of chordoma which do not express brachyury are now considered to represent mixed tumour/myoepithelioma/parachordoma (Tirabosco et al., 2008).

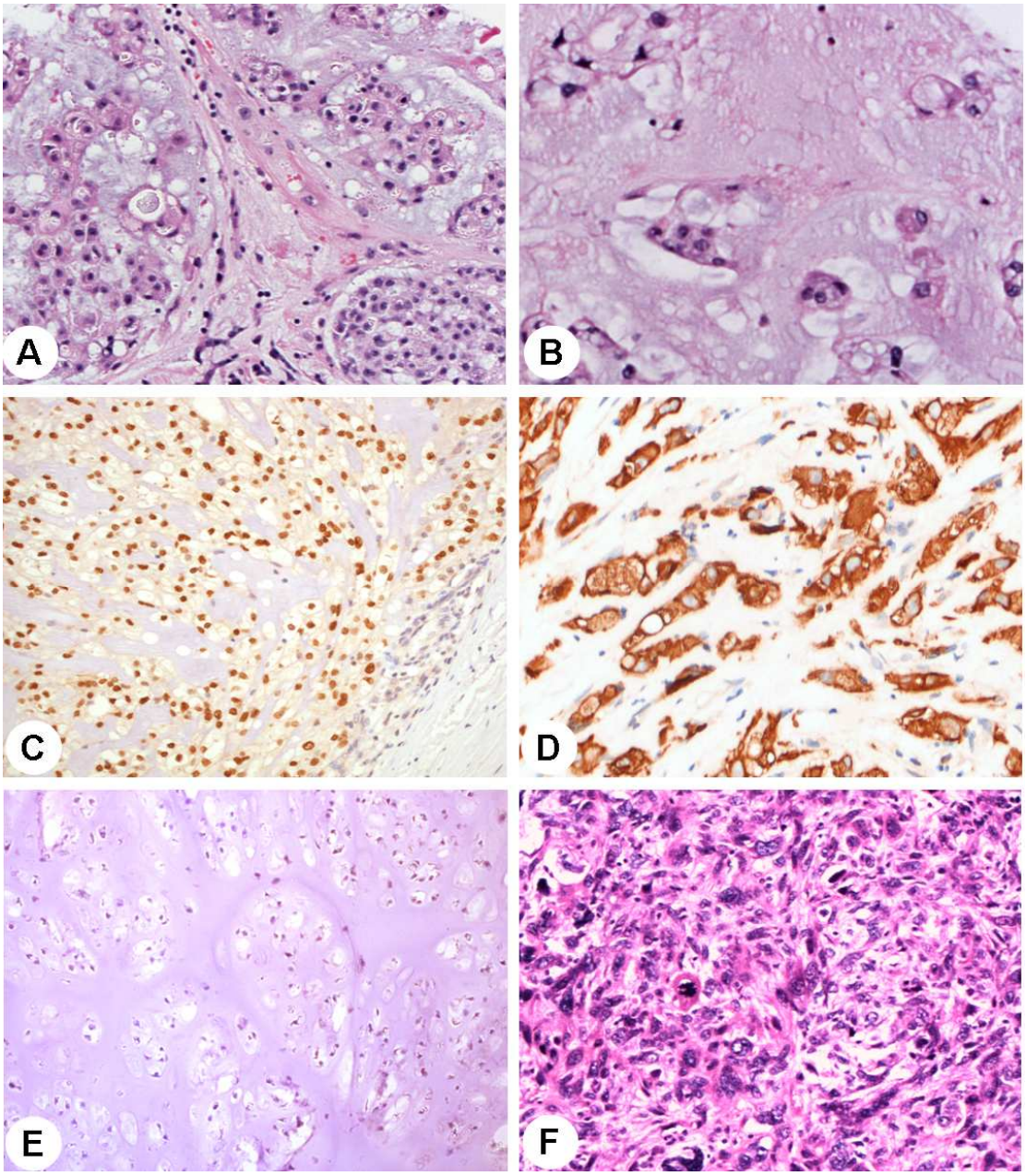

Figure 1.1 Histology of chordoma. H&E section of a conventional chordoma (A), with the characteristic physaliphorous cells (B). Immunohistochemistry for brachyury (C) and CK19 (D). H&E section of a chondroid chordoma (E) and a dedifferentiated chordoma (F).

1.3 ORIGIN OF CHORDOMA

1.3.1 Origin of axial chordoma

Chordoma shows evidence of notochordal differentiation and the most accepted theory is that chordoma arises from notochordal remnants in the vertebral bodies as evidenced by the histological, immunohistochemical and ultrastructural similarities to the notochord. The sites of notochordal vestiges correspond closely with the distribution of chordomas as evidenced by the complex irregularities and forking at both ends in the three dimensional reconstruction of the notochord (Persson et al., 1991; Salisbury, 1993; Salisbury et al., 1993; Yamaguchi et al., 2004b).

Cappell (1928) has pointed out that the great variation in histological appearance of chordoma is consistent with the histological appearances of the notochord in its various stages of development. A relatively recent theory has suggested that chordoma develops from a benign notochordal tumour. As supporting evidence for this theory, a few chordomas associated with a benign notochordal cell tumour have been reported (Yamaguchi et al., 2002; Deshpande et al., 2007).

Historically trauma to notochordal rests was suggested for the development of a chordoma. This theory was based on Ribbert's experiments in 1895 when he pierced the nucleus pulposus of rabbits and reported the development of tumours similar to chordoma. In line

with this theory, there is a report of a thoracic vertebral chordoma associated with a preceeding history of injury (Husain, 1960).

1.3.2 Origin of extra-axial chordoma

It has been suggested that the extra-axial chordomas arise from heterotopic notochordal remnants left during embryogenesis and then undergo neoplastic transformation (Fisher and Miettinen, 1997; Fisher, 2000; DiFrancesco et al., 2006; O'Donnell et al., 2007). However, developmentally this is very unlikely as there are no notochordal remnants found in extra-axial sites. Therefore, it may be that notochordal differentiation has occurred at the site of the extra-axial chordomas, although the molecular signals or mutations that would induce such differentiation are not known.

1.3.3 Notochord

The notochord in humans is a transient embryonic rod-like midline structure arising from the ectoderm at the rostral end of the primitive streak and first appears around the second gestational week and extends along much of the embryo's length (Stemple, 2005).

The functions of the notochord include acting as an early structural support and induction of the surrounding cells to construct the vertebral column (Fleming et al., 2001). During embryologic development, most of the notochordal cells disappear and become replaced with bone of the vertebral bodies and by the nucleus pulposus in the intervertebral discs. There is a great risk of incomplete involution

at the caudal and rostral ends due to a high rate of complicated folding (Salisbury et al., 1993).

The most classic form of notochordal vestiges is known as ecchordosis physaliphora, a collection of notochordal cells found at the skull base in 2% of autopsies. Microscopic intra-osseous notochordal vestiges persisting in adults within the vertebral bodies have been identified and these remnants were found mostly in the clival and sacro-coccygeal areas with a few found in the cervical and lumbar vertebrae (Ulich and Mirra, 1982; Yamaguchi et al., 2004b; Wang et al., 2008).

1.3.4 Brachyury

The *brachyury* gene is the prototypic member of the T-box family of related genes encoding transcriptional factors. *Brachyury* plays a crucial role in notochordal development and the early specification of the posterior mesoderm (Smith et al., 1991; Wilkinson et al., 1990; Muller and Herrmann, 1997). *Brachyury* has also been shown to be involved in the differentiation of mesenchymal stem cells into the chondrogenic lineage (Hoffmann et al., 2002) while the related *TBX3*, a member of the T-box family of transcription factors, induces osteogenic differentiation in human adipose tissue stromal cells (Lee et al., 2007).

Brachyury expression is induced by fibroblastic growth factor (FGF) and activin and the activation of these pathways is required for its expression (Herrmann and Kispert, 1994). The Wnt signalling pathway may also play a role in brachyury regulation (Arnold et al., 2000).

Loss of function of *brachyury* was reported more than 80 years ago when mice with heterozygous deletion exhibited a short tail phenotype. The homozygous deletion was lethal: an abnormal notochord, absent somites, and reduced allantois were reported (Gruneberg, 1958). In humans, genetic variations in *brachyury* have been shown to be associated with many neural tube defects (spina bifida and anencephaly) and sacral agenesis (Meisler, 1997; Jensen et al., 2004). One report has implicated missense mutation in *brachyury* in the development of congenital vertebral malformations including hemivertebra, vertebral bars, supernumerary vertebrae, butterfly and wedge-shaped vertebrae (Ghebranious et al., 2008).

1.3.5 Benign notochordal cell tumour

Benign notochordal cell tumour (BNCT), previously known as giant notochordal rest or hamartoma is a distinctive notochordal collection of cells that has an indolent course (Yamaguchi et al., 2008). The vast majority are asymptomatic incidental findings detected during careful dissection at autopsy or in clinical imaging studies of the axial skeleton. At autopsy, approximately 11.5% have been found in the clivus, 5% in the cervical vertebrae, 12% in the sacro-coccygeal region and 2% in the lumbar vertebra (Yamaguchi et al., 2004a).

Morphologically, BNCT consists of sheets of large polyhedral cells with abundant clear to pale pink cytoplasm and mildly pleomporphic round nuclei containing fine or homogeneously dense chromatin with no

mitoses. Some cells contain periodic acid-Schiff positive, diastase-resistant variable sized hyaline globules, which may be encountered in small extracellular cystic spaces. The lack of typical physaliphorous cells and myxoid stroma can differentiate histologically between BNCT and chordomas. Immunohistochemical profile of BNCT includes positive immunoreactivity for epithelial membrane antigen, pancytokeratin, cytokeratin 18 and S100 protein. The expression of brachyury has not been studied in the published cases (Yamaguchi et al., 2005, Yamaguchi et al., 2008).

1.4 GENETICS OF CHORDOMA

Genetic studies performed on chordomas include chromosome analysis, metaphase comparative genomic hybridisation (mCGH), array comparative hybridisation (aCGH), assessment of telomere reduction and telomere activity, fluorescent *in situ* hybridisation (FISH), DNA micro-satellite analysis, loss of heterozygosity (LOH), and clonality studies (Butler et al., 1995; Klingler et al., 2000; Scheil et al., 2001; Riva et al., 2003; Chugh et al., 2007; Hallor et al., 2008).

1.4.1 Cytogenetics, fluorescent *in situ* hybridisation (FISH) and comparative genomic hybridisation (CGH)

Chordoma is a genetically heterogeneous multiclonal tumour lacking consistent structural chromosomal aberrations as detected by the use of cytogenetic G-banding, metaphase and array comparative

genomic hybridisation and fluorescent *in situ* hybridisation (Hallor et al., 2008; Klingler et al., 2006).

Most cytogenetically investigated chordomas have a near diploid or moderately hypodiploid karyotype with several numerical and structural rearrangements. However, Scheil et al., (2001) found that 33% of tumours were hyperdiploid by using CGH technique. They suggested that failure to detect this hyperdiploid pattern by karyotyping was caused by the method used to prepare the cells for karyotyping by gowing them in tissue cultures, where the hypo- or near diploid cell populations dominate as they have *in vitro* growth advantages (Scheil et al., 2001). DNA flow cytometry studies suggested that hypoploidy is not a feature of chordoma (Hruban et al., 1990).

The identified recurrent chromosomal aberrations include loss or rearrangement of 1p and 9p and gain of chromosome 7, loss of chromosomes 3, 4, 10 and 13. The commonest reported losses are 3p and 1p (Mertens et al., 1994; Scheil et al., 2001; Brandal et al., 2004). Isochromosome 1q has been found to be a recurrent chromosome aberration and a marker of aggressiveness (Sawyer et al., 2001). Two chordomas have been shown by cytogenetics to have a translocation involving 21q22 where the transcription factors *ERG* and *ETS2* are located (Gibas et al., 1992). All chordomas analysed using aCGH were found to harbour chromosomal imbalances in contrast to the studies performed using karyotyping which reported that some chordomas had

normal karyotype which can be explained by *in vitro* growth advantage of the normal cell population (Scheil et al., 2001; Hallor et al., 2008).

The aCGH study of chordomas showed that chromosomal losses are more common than chromosomal gains and that there are no high level amplifications. The most common deletion found in this study was at 9p21 where *CDKN2A* and *CDKN2B* are located. More than 70% of the chordomas examined (16/21) showed deletion of the region covering *CDKN2A* icluding 13 cases with heterozygous deletion and cases of homozygous deletion. Loss of *CDKN2A* expression in chordomas has been also reported using immunohistochemistry (Hallor et al., 2008; Naka et al., 2005).

Loss or rearrangement at 1p36 is a common finding in sporadic chordomas and has been linked to hereditary chordoma suggesting the existence of a tumour suppressor gene (Riva et al., 2003). A minimally deleted region in 1p36.31-p36.11 where the transcription factor *RUNX3* is located was found in 57% of chordomas. The chromosomal region containing *TP53* gene was lost in 48% of chordomas using aCGH (Hallor et al., 2008).

The most common gains included chromosome 5, 7, 12 and 20. Frequently gained regions included 7p15.1 which contains the genes *CREB5*, *CPVL* and *CHN2* none of which could be related to chordoma or notochordal development. There is also a consensus gained region on chromosome 7 at 7q36 which includes homeobox-containing gene

HLXB9 and sonic hedgehog gene (*SHH*), both of which are expressed during notochordal development (Ross et al., 1998; Scheil et al., 2001). Kelley et al., (2001) performed a linkage analysis study in the family reported by Stepnak et al, and mapped minimal disease lesion to a locus 7q33. However, no loss of heterozygosity was found at any markers residing in this 7q critical region suggesting the presence of an oncogene (Kelley et al., 2001).

The locus of *TGFB1* at 5q31.1-q31.2 was gained in five of the cases and there is some evidence that this gene product is involved in cartilage development. The chromosomal region harbouring *FGFR4* on chromosome 5 (5q35.1-q35.3) also showed gain in 33% (7/21) of cases. The chromosomal region 6q27 containing *brachyury* gene showed gain in 29 % (6/21) of chordomas (Hallor et al., 2008).

Recently, another aCGH study on familial chordomas identified *brachyury* copy number variation in four out of seven analysed families suggesting its major role in susceptibility for familial chordoma (Yang et al., 2009b).

1.4.2 Loss of heterozygosity (LOH), microsatellite instability (MSI) and clonality studies in chordoma

The first LOH study on chordomas examined the *Rb1* locus (13q14) where LOH was detected in 2 out of 7 cases (Eisenberg et al., 1997). This finding is consistent with the frequently reported loss of chromosome 13 as detected by cytogenetics and CGH studies. Another

LOH study showed loss of 17p and 9p where known tumour suppressor genes (*TP53, CDKN2A*) are present (Klingler et al., 2000).

Based on the identification of LOH at the chromosomal region 1p36.13 in one family with familial chordoma and the frequent loss of 1p in chordomas, a targeted LOH study was performed by Riva et al., (2003). It showed that 85% (25/27) of chordomas had LOH at 1p36.13. Putative tumour suppressor genes at this locus include *CASP9*, *EPHA2*, *PAX7*, *DAN* and *DVL1*. Expression studies of these genes showed that out of 8 chordomas, *EPHA2*, *DVL1*, and *CASP9* were absent in 1, 4, and 5 tumours respectively (Dalpra et al., 1999; Riva et al., 2003). The limitations of this study are the high gene density in this region and its common loss in many solid tumours suggesting a possible non specific role in chordomas (Larizza et al., 2005).

In a single study, MSI and LOH were performed on 12 chordomas. MSI was detected in 50% of the chordomas at one or more loci and LOH was identified in two chordomas, one of which had MSI (Klingler et al., 2000).

A limited study has revealed telomere lengthening in 4 out of 4 chordomas in contrast to telomere length reduction that has been reported in most cancers and during *in vitro* senescence of human fibroblasts (Butler et al., 1996). The activity of telomerase, the enzyme responsible for telomere length maintenance has been demonstrated in about half of the chordomas studied (Butler et al., 1995).

A clonality study has been performed on seven sacral chordomas using an X chromosome inactivation protocol and a polymorphic human androgen receptor gene (AR) located on the X chromosome as a marker and demonstrated that chordoma is polyclonal in origin. Like in other solid tumours, this polyclonality may be caused by imbalanced chromosomal alterations and added more difficulties to the use of molecular targeted therapy in comparison to monoclonal tumours like haematopoietic malignancies (Klingler et al., 2006).

1.5 GENE EXPRESSION IN CHORDOMAS

1.5.1 Gene expression microarrays

The chordoma gene expression pattern was found by gene expression microarrays to cluster closely with cartilaginous neoplasms including chondrosarcomas, chondroblastomas and chondromyxoid fibromas (Henderson et al., 2005; Schwab et al., 2009b). Among various types of sarcomas, chordoma and chondrosarcoma grouped together in a genomic cluster distinct from that of other types of sarcoma. Both tumours showed higher levels of expression of genes characteristic of extracellular matrix and hyaline cartilage such as *collagen II*, *aggrecan*, *cartilage linking protein*, *cartilage oligomeric matix protein*, the chondrogenic transcription factor *SOX9*, *fibronectin*, *MMP9* and *MMP19* than other connective tissue tumours (Henderson et al., 2005; Schwab et al., 2009b).

The genes expressed in chordomas and not in cartilagenous neoplasms include *brachyury*, *CD24*, *cytokeratins 8*, *15*, *18*, *19*, *discoidin domain receptor 1* (*DDR1*) and *periplakin* (Schwab et al., 2009b; Vujovic et al., 2006). Over-expression of *EGFR* and its ligand, *EGF* was found in chordomas relative to the nucleus pulposus (Schwab et al., 2009b). Chordomas were not found to express high levels of *collagen X* implicated in cartilage calcification, *platelet-derived growth factor alpha*, a mitogen for connective tissue cells or *reticulocalbin 3*, a putative endoplasmic reticulum protein (Vujovic et al., 2006).

1.5.2 Protein expression studies

Many expression studies have been performed to investigate the possible roles of various molecules in chordoma biology. Expression of tyrosine kinases has been investigated using immunohistochemical and reverse transcription polymerase chain reaction techniques and demonstrated that platelet-derived growth factor receptor beta (PDGFR β) was expressed in virtually all chordomas (Tamborini et al., 2006; Fasig et al., 2008). This provided a basis for the phase II clinical trial of imatinib mesylate in chordomas (Casali et al., 2007; Ferraresi et al., 2010).

In a study of 21 chordomas, EGFR has been reported to be expressed in 67% (14/21). KIT and c-MET were detected in 33% and 66% of examined specimens while HER2 was not detected in any of the cases. The active phosphorylated forms of the transduction molecules;

ERK, AKT and STAT3, indicative of tyrosine kinase activity, were detected in 86%, 76% and 67% of cases (Fasig et al., 2008). In another study of 12 chordomas, Weinberger et al., (2005) reported expression of EGFR and c-MET in all of the 12 chordomas while HER2 expression was detected in only 7 chordomas. The expression of nerve growth factor receptor (TrkA) and nerve growth factor (NGF) was significantly higher in chordomas than in notochordal cells (Park et al., 2007).

Cyclo-oxygenase-2 (COX2) has been detected in 90% (19/21) of chordomas, oestrogen receptor beta (ERβ) in all the 21 tested cases and the androgen receptor has been detected in 90% of cases (19/21) while oestrogen receptor alpha (Erα) or progesterone receptors have not been detected (Fasig et al., 2007). Expression of high molecular weight melanoma-associated antigen (HMW-MAA), also known as chondroitin sulphate proteoglycan 4 (CSPG4), a possible target of immune therapy has been detected in 62% of 21 chordomas (Schwab et al., 2009b).

Expression of the adhesion molecules E-cadherin, α-catenin, β-catenin, γ-catenin and neural cell adhesion molecule (NCAM) in chordoma has been detected in chordomas and are thought to be associated with the formation and maintenance of chordoma tissue architecture but these are not related to the microscopic characteristics or prognosis (Naka et al., 2001). Horiguchi et al., suggested that nuclear expression on E-cadherin is a characteristic feature of chordoma while

Mori et al., suggested E-cadherin is a diagnostic marker for chordomas (Mori et al., 2002; Horiguchi et al., 2004).

1.6 AIMS

The overall aim of this work was to understand the pathogenic mechanisms underlying the development of chordomas and to attempt to link the findings to possible therapeutic applications.

The first aim of this work was to investigate the role of the PI3K/AKT/TSC/mTOR pathway in chordomas and the potential of its molecules to be used as targeted therapy.

The second aim was to analyse the status of the FGFR-RAS/RAF/MEK/ERK-ETS2-brachyury pathway in chordomas and to investigate the role of *brachyury* in chordoma pathogenesis by targeting its expression in a chordoma cell line U-CH1 by shRNA.

The final aim was to investigate the expression pattern and genetic alterations of *EGFR* and to test the effect of one of the EGFR inhibitors on the U-CH1 chordoma cell line in an attempt to find a basis for using EGFR inhibitors for treating chordomas.

2. MATERIALS AND METHODS

2.1 Clinical samples

The tissues and clinical data used in this study were retrieved from the archives of The Royal National Orthopaedic Hospital, Stanmore, UK and from the Institute of Neurology, University College London (UCL), London, UK. The selection was restricted to paraffin-embedded tissues and snap-frozen tissues available within the last 10 years. The study complied with standards laid down by the Central Office for Research Ethics Committees (COREC) and approved by the relevant ethics committees under the study number **07/Q0506/8.**

2.2 Tissue microarrays (TMAs)

Two tissue microarrays of 50 non skull-based chordomas and 50 skull-based chordomas were constructed using a manual tissue arrayer (Beecher Instruments Inc, Sun Prairie, WI, USA). H&E sections were examined and two different representative areas from each case were marked on the paraffin blocks. Two 0.6 mm cores were taken for the array from all cases. Paraffin blocks from salivary gland, kidney, tonsil, lymph node, placenta, thyroid, renal cell carcinoma, breast carcinoma and thyroid carcinoma were also marked for representative areas and cores were taken as controls and orientation markers.

2.3 Immunohistochemical analyses

Sections of 3 µm thickness were cut from paraffin-embedded tissue, de-paraffinized in xylene for 5 min, rehydrated in ethanol and treated with the appropriate antigen retrieval method as described in Table 2.1. The iVIEW DAB detection kit and Ventana NexES Autostainer (Ventana Medical Systems, Inc. Tucson, AR, USA) were used according to the manufacturer's instructions.

The detailed conditions and the antibodies used are listed in Table 2.1. Immunohistochemistry was also performed manually for some antibodies using the iVIEW DAB kit (Ventana Medical Systems, Inc.) with overnight incubation at 4℃ in a humidified chamber. Diaminobenzidine (DAB) was used as a chromogen in all reactions. Incubation without a primary antibody, as well as incubation with the matching IgG isotype, under the same conditions for each antibody served as the negative controls.

Each antibody was scored with reference to cores of positive control tissue included in the TMA design. For each antibody, the labelling intensity and extent were scored. The intensity scores included; negative in the absence of immunoreactivity, 'low' when the immunoreactivity was unequivocal but less strong than the positive control and 'high' when the immunoreactivity was at least as strong as the positive control. The extent of staining was assessed as +, ++ and +++ indicating that less than 5%, between 6 and 49%, and at least 50%,

respectively, of the lesional cells were immunoreactive (Fasig et al., 2008). The presence of non-neoplastic cells (macrophages, lymphocytes, fibroblasts, endothelial cells) in the cores of neoplastic tissue was also used as internal negative control.

Table 2.1 Details of antibodies used for immunohistochemistry

	Antibody/clone	Source	Antigen retrieval	Dilution	Incubation time and temperature	Method
1	CK19 clone b170	Novocastra Laboratories Ltd, Newcastle upon Tyne, UK	Protease 20 min	1:100	30 min at 37℃	***Ventana NexES
2	Brachyury (H-210): sc-20109	Santa Cruz Biotechnology, Inc., Santa Cruz, CA, USA	*PC 2 min	1:50	30 min at 37℃	Ventana NexES
3	PTEN clone 28H6	Abcam, Cambridge, UK	PC 2 min	1:100	30 min at 37℃	Ventana NexES
4	p16 ^{INK4a} CINtec® clone E6H4TM	MTM laboratories AG, Heidelberg, Germany	PC 2 min	1:100	20 min at 37℃	Manual staining
5	p-AKT (ser 473) clone 736E11	Cell Signaling Technology, Danvers, MA, USA	PC 6 min	1:50	**O/N at 4℃	Manual staining
6	Harmatin/TSC1	Cell Signaling Technology	PC 2 min	1:25	30 min at 37℃	Ventana NexES
7	Tuberin/TSC2	Santa Cruz Biotechnology	PC 2 min	1:100	30 min at 37℃	Ventana NexES
8	p-tuberin/TSC2 (Thr^{1462})	Abcam	PC 4 min	1:25	O/N at 4℃	Manual staining
9	p-mTOR (ser ^{2448}) clone 49F9	Cell Signaling Technology	PC 3 min	1:100	30 min at 37℃	Ventana NexES
10	Total mTOR	Cell Signaling Technology	PC 4 min	1:50	O/N at 4℃	Manual staining
11	p-p70 S6K1 (Thr ^{389})	Cell Signaling Technology	PC 4 min	1:50	O/N at 4℃	Manual staining
12	S6K	Abcam	PC 6 min	1:100	O/N at 4℃	Manual staining
13	p-S6RP ($^{ser235/236)}$ clone 91B2	Cell Signaling Technology	PC 3 min	1:50	30 min at 37℃	Ventana NexES
14	Total S6RP	Cell Signaling Technology	PC 2 min	1:100	30 min at 37℃	Ventana NexES
15	p-4E-BP1 (Thr^{70})	Cell Signaling Technology	PC 2 min	1:50	O/N at 4℃	Manual staining
16	eIF4E	Cell Signaling Technology	PC 2 min	1:50	O/N at 4℃	Manual staining
17	FGFR1/Flg (C-15): sc-121	Santa Cruz Biotechnology	Protease 14 min	1:150	30 min at 37℃	Ventana NexES
18	FGFR2/Bek (C-17): sc-122	Santa Cruz Biotechnology	Protease 14 min	1:100	30 min at 37℃	Ventana NexES
19	FGFR-3 (C-15): sc-123	Santa Cruz Biotechnology	Protease 14 min	1:100	O/N at 4℃	Manual staining
20	FGFR-4 (C-16): sc-124	Santa Cruz Biotechnology	Protease 14 min	1:50	30 min at 37℃	Ventana NexES
21	EGFR	Dako UK Ltd., Ely, Cambridgeshire, UK	Protease 14 min	1:25	30 min at 37℃	Ventana NexES
22	p-EGFR (Tyr^{1173})	Cell Signaling Technology	PC 3 min	1:100	O/N at 4℃	Manual staining

*PC = pressure cooker: min= minute
**O/N = over night
***Ventana NexES = Ventana NexES Autostainer

2.4 Fluorescent *in situ* hybridisation (FISH) analysis

FISH was performed on TMAs using probes from the bacterial artificial chromosomes (BACs) from the RP-BACs library (BAC/PAC resources centre, Oakland, CA, USA). The details of the BACs used are shown in Table 2.2. Chromosome enumeration probes (CEP) were used as references and obtained from three different resources; ready-labelled for chromosomes 9 and 16 from Vysis (Vysis, Abbott Laboratories Inc, Des Plaines, IL, USA), alpha satellite DNA for chromosomes 1, 6 and 7 (Resources for Molecular Cytogenetics, Bari, Italy) labelled in green with Vysis reagents and telomeric BAC clones (BAC/PAC resources centre) for chromosomes 5 and 21 labelled in green with Vysis reagents. Details of chromosome enumeration markers are listed in Table 2.3.

TMA sections were cut at 4 µm thickness, de-paraffinized in xylene and rehydrated in ethanol. Sections were pre-treated using the Paraffin Pretreatment Reagent Kit II (Vysis). Briefly, the slides were placed in the pre-treatment solution at 80℃ for 50 -70 min, and in pepsin solution 0.05% at 37℃ 20 to 25 min. The probes wer e applied to the slides and co-denatured for 5 min at 73℃ and hybri dized for at least 16 h at 37℃ in a Thermo-Brite hybridizer (Iris, Westw ood, MA, USA). The slides were washed in formamide-free solutions: 2XSCC/0.3% Igepal CA-630 (Sigma-Aldrich Company Ltd, Gillingham, Dorset, UK) at room temperature for 5 min, at 73℃ for 2 min and at roo m temperature for 1

min, and then counter-stained with 4',6'-diamidino-2-phenylindole (DAPI) and analysed under a fluorescent microscope (Olympus, Watford, Hertfordshire, UK) using AnalySIS software (Olympus). The chromosome localisation of all BAC clones was confirmed on normal metaphase spread slides (Vysis).

Fifty non-overlapping nuclei that contained unequivocal signals were counted for each case. For all of the probes used apart from *EGFR probes*, amplification was defined by a ratio of more than 2 for the gene-specific probe compared to the chromosome-specific reference probe, and hemizygous deletion was defined as more than 20% of non-overlapping tumour nuclei containing one gene-specific probe signal (red) and two chromosome-specific probe signals (green).

FISH analysis for *EGFR* comprises two groups; FISH positive (*EGFR* genomic gain) and FISH negative (no or low *EGFR* genomic gain) according to the Colardo criteria developed or non small cell lung carcinoma, The former included high level polysomy (≥ 4 copies/cell in ≥ 40% of cells) and amplification (defined by the presence of tight gene clusters, or ratio *EGFR* gene signals/CEP7 signals ≥ 2, or ≥ 15 copies of the gene per cell in ≥ 10% of analysed cells). The latter included two subgroups; low level polysomy (> 2 copies/cell in ≤ 40% of cells or 3 copies/cell in ≥ 40% of cells) and diosomy (≤ 2 copies in > 90% of the cells) (Cappuzzo et al., 2005; Martin et al., 2009; Varella-Garcia et al., 2009).

Table 2.2 Details of BACs used to generate FISH probes

	BAC reference	Gene covered	Chromosome location	Type of aberration looked for	Labelling colour
1	RP11-235F13	*Brachyury*	6q27	Amplification	Orange
2	RP11-830D9	*ETS2*	21q22.2	Amplification	Orange
3	RP11-8N7	*ETS2*	21q22.2	Break-apart	Orange
4	RP11-42C22	*ETS2*	21q22.2	Break-apart	Orange
5	RP11-381G5	*EGFR*	7p11.2	Amplification	Orange
6	RP11-1008G19	*FGFR4*	5q35.2	Amplification	Orange
7	RP11- 81C14	*TSC1*	9q34.13	Deletion	Orange
8	RP11-846C9	*TSC2*	16p13.3	Deletion	Orange
9	RP11-1107P2	*mTOR (FRAP1)*	1p36.22	Deletion	Orange
10	RP11-624N8	*S6RP*	9p22.1	Deletion	Orange

Table 2.3 Details of probes used as chromosome enumeration markers

	Location	Company	Labelling colour
Chromosome enumeration probe 9 (CEP9)	Chromosome 9	Vysis, Abbott Laboratories Inc, Des Plaines, IL, USA	Green
Chromosome enumeration probe 16 (CEP16)	Chromosome16	Vysis	Green
D1Z5 (CEP1)	Chromosome 1	Resources for Molecular Cytogenetics, Bari, Italy	Green
Chromosome 6 alpha satellite DNA (CEP6)	Chromosome 6	Resources for Molecular Cytogenetics	Green
Chromosome 7 alpha satellite DNA (CEP7)	Chromosome 7	Resources for Molecular Cytogenetics	Green
RP1-240G13	Chromosome 5	BAC/PAC resources centre, Oakland, CA, USA	Green
RP11-159E6	Chromosome 21	BAC/PAC resources centre	Green

2.5 DNA isolation and mutational analysis by denaturing high performance chromatography (dHPLC) and direct sequencing

Genomic DNA was extracted using proteinase K (Qiagen, Crawley, West Sussex, UK) from 23 frozen chordoma samples according to the manufacturer's protocol. Briefly, the samples were

dissolved in 180 µl of lysis buffer ATL, and 20 µl of proteinase K was added and the sample was incubated at 56℃ for 3 h, after which, 200 µl of buffer AL was added and the sample was incubated at 70℃ for 10 min. After a brief centrifugation, 200 µl of 100% ethanol was added and each sample was applied to a QIAamp spin column and centrifuged at 8000 rpm for 1 min. The column was washed in Buffers AW1 and AW2 and centrifuged at 14000 rpm for 3 min; the DNA was eluted in 100 µl of buffer AE and kept at -20℃.

The tissue samples comprised at least 80% tumour. The PCR primers were designed to include the intron/exon boundaries to be analysed in addition to the coding sequence (Table 2.4).

2.5.1 Denaturing high performance liquid chromatography (dHPLC) analysis of KRAS and BRAF for the common mutations

Fifty nanograms of genomic DNA was amplified using the following touchdown PCR protocol which involved initial heating at 95℃ for 15 min. The annealing temperature was reduced by 1℃ per cycle, from 65℃ to 56℃, followed by 35 further cycles at 56℃. Each cycle was performed as follows: denaturation at 95℃ for 45 s, annealing at 65℃ down to 56℃ for 45 s, extension at 72℃ for 90 s, followed by a final extension step at 72℃ for 10 min. The PCR reaction was performed in a total volume of 25 µL containing 2.5 µL of 10X PCR buffer II, 0.2 µM of dNTP, 10pmol of each primer, 0.1 mM $MgCl_2$, 1.25 U of optimase enzymes (Transgenomic, Crewe, Cheshire, UK). Prior to

dHPLC analysis, the PCR products were run on an agarose gel to ensure that only the specific product was amplified and that no contaminating bands were present.

A Transgenomic Wave DNA Fragment Analysis System was used to perform dHPLC analysis (Transgenomic Inc, Omaha, NE, USA). Prior to dHPLC analysis, the un-purified PCR products were denatured at 95℃ for 5 min and cooled to 25℃ using a temperatu re ramp of 1℃ /min to produce heteroduplexes, and 6 µL of the PCR products were loaded onto a preheated DNASep® HT Cartridge column (Transgenomic Inc). DNA was eluted at a flow rate of 0.9 ml/min using a linear acetonitrile gradient that consisted of buffer A (0.1 M triethylammonium acetate; TEAA) and buffer B (0.1 M TEAA, 25% acetonitrile). The dHPLC melt software, available from *http://insertion.stanford.edu/melt.html* was used to select the optimal temperature to separate heteroduplexes.

2.5.2 Direct sequencing

Fifty nanograms of genomic DNA was amplified by the following touchdown PCR protocol which involved initial heating at 95℃ for 15 min. The annealing temperature being reduced by 1^{o}C per cycle, from 65℃ to 56^{o}C, followed by 35 further cycles at 56℃ as describ ed above. The PCR reaction was performed in a total volume of 50 µL containing 5 µL of 10X Hotstart buffer I, 0.2 µM dNTP, 10 pM of each primer, 1 U of Hotstart DNA polymerase (CLP, San Diego, CA, USA). PCR products

were purified using Qiagen PCR Purification kit (Qiagen) and sent for DNA sequencing at the Scientific Support Services at UCL Cancer Institute/Wolfson Institute for Biomedical Research (WIBR). Sequencing reactions were run using GenomeLab™ DTCS Quick Start chemistry (Beckman Coulter UK Ltd, High Wycombe, Bucks, UK) and were analysed on a CEQ™ 8000 Genetic Analysis System (Beckman Coulter).

Table 2.4 Primer sequences used for mutation analysis of the *FGFRs*, *Brachyury*, *KRAS, BRAF, RHEB, PI3KCA, and EGFR*

***FGFRs* primers**			
Gene (exon)	Primer sequence		Length bp
FGFR1 (exon 3)	F	5'- AGATGTGGAGCCTTGTCACC -3'	226
	R	5'- CCTGTTGACCACATCACCTG -3'	
FGFR1 (exon 6	F	5'- TGCCTGTCTCTCTTGGCTTT -3'	314
	R	5'- CCTCCCCTGTTCCCATTACT -3'	
FGFR1 (exon 11)	F	5'- TGGGAAGCCCTGACTAAGAA -3'	355
	R	5'- AAGCAAGGAATGCCTTCAAA -3'	
FGFR1 (exon 12)	F	5'- GTGGGGTTTCTTTGAGGTGA 3'	302
	R	5'- CACCGGCTGGAAGACTAGGG -3'	
FGFR1 (exon 14)	F	5'- CTCCCCTGTGCTGCTTTC -3'	368
	R	5'- CATCTGGAGCAGAGGGAATG -3'	
FGFR2 (exon 5)	F	5'- TTTACTCATGGAGGGGAAGC -3'	314
	R	5'- CGAGACTCCATCGCAAAAA -3'	
FGFR2 (exon 7)	F	5'- GCGTTTTCCTTGCAGCGGCTGG - 3'	321
	R	5' - GTAAGTCACAGGATTCCCGTC - 3'	
FGFR2 (exon 11)	F	5' - CTTTAGTAAGCCGCTGAAAGA -3'	
	R	5'- TTCACATGCCACAAAGGAA - 3'	302
FGFR2 (exon 12)	F	5'- CGGGAAACACAAAAACATCA - 3'	408
	R	5'- CTGAAGCCTCTCCACCTCTC -3'	
FGFR3 (exon 2)	F	5'- AGGCTTCCACTGCTGTGTCT -3'	389
	R	5'- GCACTCGGCTCCTTTCTGTA - 3'	
FGFR3 (exon 3)	F	5'- AGGAAGTGCTGCCCAAATG - 3'	258
	R	5'- TTAGTCCCTCAGCTGCCTGT - 3'	
FGFR3 (exons 4,5)	F	5'- GAAGGGGGTTGTTCAGAGG -3'	538
	R	5'- CTGTGGGGGCAGATGACGCTCA -3'	
FGFR3 (exon 6)	F	5'- GCGTCGTGGAGAACAAGTTT -3'	449
	R	5'- GAAGCTCCAACCCCTAGACC -3'	
FGFR3 (exon 7)	F	5'- GCCTATCGCTCTGCTCTCTC -3'	275
	R	5'- GGCCGTAAGTCACAGGATTC -3'	
FGFR3 (exon 8)	F	5'- GCTCCTTCTCTCCAGGGTCT -3'	340
	R	5'- TTCCACCAGCATTGAATGAA -3'	
FGFR3 (exon 9)	F	5'- TTCATTCAATGCTGGTGGAA -3'	430
	R	5'- CCTCTGACTGGTGGCTGTTT -3'	
FGFR3 (exon 15)	F	5'- CTGCAGAGCTCAGGCTTCA -3'	453
	R	5'- CGCCTTATTCGGGAACAG -3'	

FGFR3 (exon 17)	F	5'- CCCAGAGTGCTGAGGTGTG -3'	476
	R	5'- ACCCAGGGTACCTCTGCAC -3'	
FGFR4 (exon 7)	F	5'- GCAGGGTAAGCAGGAGACAG -3'	447
	R	5'- GACATGCTCTGGGGTCACA -3'	
FGFR4 (exon 9)	F	5'- GAGCTGGGAGGGACTGAGTT -3'	601
	R	5'- ATGGAGAAAGTCCAGCCTCA -3'	
FGFR4 (exon 16)	F	5'- CTGTGGTGGGTCATGTCTGT -3'	349
	R	5'- GGAGGAGGACGAGGAGTTCT -3'	
***Brachyury* primers**			
Gene (exon)	Primer sequence		Length bp
Brachyury (promoter)	F	5'- GCGCAAGACTCCTCTGAACT -3'	609
	R	5'- CTCTCACCATCTGGAAAAGGAA -3'	
Brachyury (exon 2)	F	5'- AGGGAAGGTGGATCTCAGGT -3'	380
	R	5'- CCTCCTCCAGGAGAAAAAGG -3'	
Brachyury (exon 3)	F	5'- CTCTGTGCCCCGAAATAACT -3'	502
	R	5'- GAGAAGGCTGTGGCAGTTTC -3'	
Brachyury (exon 4)	F	5'- TTCCCTCAACAGCAGAGACA 3'	368
	R	5'- CTTCCTCTCAGTGCGGGTTA -3'	
Brachyury (exons 5 and 6)	F	5'- ATTTAAAAGTGGTACTGGCATTT -3'	428
	R	5'- CTCCACTTCCCAGCTCTCAG -3'	
Brachyury (exon 7)	F	5'- GAGGGAGCACTAATGCAGGT -3'	398
	R	5'- AGTGGCGGAGACATAAAT -3'	
Brachyury (exon 8)	F	5'- GCAATAAATCTTGCCCCTGA - 3'	390
	R	5' - CCTATGGGAATGGAAACAGC - 3'	
Brachyury (exon 9)	F	5' - TTGGAGAAAATGACCTGTTTGA -3'	534
	R	5'- TGAGGCTGCATTTCCTTCTT - 3'	
***KRAS and BRAF* primers**			
Gene (exon)	Primer sequence		Length bp
KRAS (exon 2)	F	5'GATACACGTCTGCAGTCAACTG--3'	270
	R	5'-GGTCCTGCACAGTAATATGC-3'	
KRAS (exon 3)	F	5'-TGCACTGTAATAATCCAGACTGTG-3'	240
	R	5'-CTCCTTAATGTCAGCTTATTATATTCA-3'	
BRAF (exon 11)	F	5'- TCCCTCTCAGGCATAAGGTAA -3'	350
	R	5'- CGAACAGTGAATATTTCCTTTGAT -3'	
BRAF (exon 15)	F	5'- TCATAATGCTTGCTCTGATAGGA -3'	220
	R	5'-CTGATTTTTGTGAATACTGGGAAC TC-3'	
***RHEB* primers**			
Gene (exon)	Primer sequence		Length bp
RHEB (exon 2)	F	5'-TTTGTTGAAGGCCAATTTGTG-3'	180
	R	5'-TGGAGTATGTCTGAGGAAAGATAGAA-3'	
RHEB (exon 4)	F	5'-GGCCAATTTGTGGACTCCTA -3'	220
	R	5'-TCCCCACCATATCCAACAAT-3'	
***PI3KCA* primers**			
Gene (exon)	Primer sequence		Length bp
PI3KCA (exon 4)	F	5'-CGCCCCCTTAATCTCTTACA- 3'	386
	R	5'-TGGATGTTCTCCTAACCATCTG- 3'	
PI3KCA (exon 5)	F	5'-GGCAGCAACTAATTTTGGTGA -3'	392
	R	5'-ACTTTTTGTAGAAATGGGGTCT- 3'	
PI3KCA (exon 6)	F	5'-TTTCCAATCAATCTCTTTCCTG- 3'	396
	R	5'-TCCCAAGGTATTCTTCCATGAT-3'	
PI3KCA (exon 9)	F	5'-GCTTTTTCTGTAAATCATCTGTG -3'	286
	R	5'-CATGCTGAGATCAGCCAAATTC- 3'	
PI3KCA (exon 20)	F	5'-GTCTACGAAAGCCTCTCTAATTT- 3'	483
	R	5'-TAATGCTGTTCATGGATTGTGC- 3'	
***EGFR* primers**			
Gene (exon)	Primer sequence		Length bp
EGFR (exon 18)	F	5'-TTCCAAATGAGCTGGCAAGT- 3'	405

	R	5’-CTGAGTGTTTGGGAAACTCCA- 3’	
EGFR (exon 19)	F	5’-CCCCAGCAATATCAGCCTTA- 3’	455
	R	5’-TCTCCCATGCTGGTATCCAC- 3’	
EGFR (exon 20)	F	5’-CTTTTGCAGGCACAGCTTTT- 3’	431
	R	5’-GAGTTTGCCATGGGGATATG- 3’	
EGFR (exon 21)	F	5’-ACTAACGTTCGCCAGCCATA- 3’	412
	R	5’-ACATTCTGGGTGAGCTCG- 3’	

2.6 DNA Methylation studies

2.6.1 DNA extraction and bisulphite treatment of the DNA

Genomic DNA was extracted using proteinase K (Qiagen). In total, 500 µg DNA (concentration 100 ng/µl) was treated using EZ DNA Methylation-Gold^{TM} Kit (Zymo Research, Orange, CA, USA) according to the manufacturer's protocol. Briefly, 130 µl of CT Conversion Reagent was added to 20 µl of DNA sample and mixed, then heated to 98℃ for 10 min and then 64℃ for 2.5 h and kept at 4℃. M- Binding Buffer was added (600 µl) to a Zymo-Spin IC Column, then the sample was added and the column was centrifuged at full speed (>10,000 rpm) for 30 s. The flow-through was discarded and 100 µl of M-Wash Buffer was added to the column. The column was centrifuged for 30 s and 200 µl of M-Desulphonation buffer was added to the column and left for 15-20 min at room temperature. The column was then centrifuged at full speed for 30 s. A wash step was then performed by addition of 200 µl of M-Wash Buffer to the column after which the column was centrifuged for 30 s. This wash step was repeated twice. M-Elution buffer (10 µl) was added directly to the column matrix and the bisulfite-treated DNA was collected in 1.5 ml micro-tubes and stored at -20℃.

2.6.2 PCR and pyrosequencing

The primers described in Table 2.6 were designed using the PyroQ assay design software (Biotage, Uppsala, Sweden). All pyrosequencing assays for repetitive elements included at least one primer in a unique sequence outside of the repeat and followed by a unique nested primer pair for some amplicons to ensure specific amplification. A common tag was placed on either the forward or the reverse primer (depending on the strand to be sequenced), and a common universal biotinylated primer was used for all reactions as described previously (Tost and Gut, 2007). Two rounds of bisulphite-PCR cycling conditions included denaturation at 95°C for 4 min, followed by 10 cycles of 94℃ for 15 s, touchdown from 60–50℃ (reducing 1℃ per cycle) for 15 s and 72℃ for 20 s followed by a further 30 cycles at a 50℃ annealing temperature. The second PCR used 2 µl of a 1:10 dilution of the first PCR as template and the same cycling conditions. All products were confirmed to be single bands by agarose gel electrophoresis. Methylation values were calculated as an average of all CpG sites within each assay as determined by the Pyro Q-CpG Software (Biotage).

Table 2.5 Sequence of primers used for methylation-specific PCR and pyrosequencing

FRAP1 (mTOR gene) primers		
*FRAP1*_F1 *FRAP1*_R1	GAGGGGTGGGAGTTAAGGTT TTTTTCAATCCATCTTCTCCCTA	First round PCR (F1-R1) – 339 bp Second round PCR (F2-R2) – 192 bp
*FRAP1*_F2 *FRAP1*_R2	[BIOTEG]-TTGGTYGTGGGTTTGGATATTA TCAAAACTAAAAACCCTCCTTC	
*FRAP1*_S1 *FRAP1*_S2 *FRAP1*_S3	AAACCCTCCTTCCCT ATAAAACAAAAAACCTAAA CRACAACTAAAACCTT	
RPS6 primers		
RPS6_F1 RPS6_R1	GTATTTTAGGATTTTGGTTTTAGG CCTTTCATATTACCTCCACACA	First Round PCR (F1-R1) - 403 bp Second Round PCR (F2-R2)- 170 bp
*RPS6*_F2 *RPS6*_R2	TGGAGAAGGGTTTTAAGTAGGA [BIOTEG]-ACCTACCRCAAACTAAACAACA	
*RPS6*_S1	GGTATGGAGTTTTTTGGT	

2.7 Tandem duplication study of *BRAF*

For detection of tandem duplication at *BRAF* locus, a reverse transcription polymerase chain reaction was performed using previously published primers (Jones et al., 2008). cDNA was prepared as previously described in section 2.6, from 23 chordoma tumours and 2 µl of a 1:5 dilution of the reverse transcribed cDNAs were used in the PCR assays. The PCR was performed in 25 µl containing 2 µl of cDNA, 1X PCR buffer, 0.5 U GoTaq Flexi DNA Polymerase (Promega), 200 nmol of each dNTP, 5 pmol of each primer. cDNA from a positive control was kindly provided by Dr David Jones, Cambridge University, Cambridge, UK.

Table 2.6 Primers used for tandem duplication study of *BRAF*

Gene (exon)	Sequence
KIAA1549 (ex15 F)	5'-CGGAAACACCAGGTCAACGG-3'
KIAA1549 (ex16 F)	5'-AAACAGCACCCCTTCCCAGG-3'
BRAF (ex9 R)	5'-CTCCATCACCACGAAATCCTTG-3'
BRAF (ex11 R)	5'-GTTCCAAATGATCCAGATCCAATTC-3'
BRAF (ex7 R)	5'-AAGGGGATGATCCAGATGTTAGG-3'
BRAF (ex6 F)	5'-TTGTGACTTTTGTCGAAAGCTGC-3'
Primer combinations for breakpoint detection:	
KIAA1549:BRAF (16_9):	KIAA1549 (ex16 F) / BRAF (ex9 R), 124bp
KIAA1549:BRAF (16_11):	KIAA1549 (ex16 F) / BRAF (ex11 R), 182bp
KIAA1549:BRAF (15_9):	KIAA1549 (ex15 F) / BRAF (ex9 R), 159bp

2.8 Protein isolation and Western blot analysis

Ten 10 μm sections were cut from snap-frozen tumours and placed into micro-tubes. A tumour lysate was produced with Radio-Immunoprecipitation Assay (RIPA) lysis buffer (150 mM NaCl, 1% Igepal CA-630, 0.5% sodium deoxycholate, 0.1% sodium dodecyl sulfate, 50 mM Tris [pH 8.0]) containing both phosphatase and protease inhibitor cocktails (Sigma-Aldrich). Lysates were incubated on ice for 15 min and then centrifuged at 13,000 rpm and 4℃ for 10 min to remove debris. Proteins were quantified with BCA protein assay kit (Fisher Scientific UK Ltd, Loughborough, Leicestershire, UK). Thirty micrograms of protein lysate were resolved by SDS-8% polyacrylamide gel electrophoresis (SDS-8% PAGE) and transferred to a polyvinylidene fluoride (PVDF) Immobilion-P transfer membrane (Millipore Corporation, Bedford, MA, USA) by standard semi-dry electro-transfer methods (Kurien and Scofield 2003). The membrane was blocked with PBS,

0.1% Tween 20, 5% BSA for a minimum of 30 min and probed with the appropriate primary antibody overnight at 4℃. Blot s were washed three times (10 min each) in 1X PBS with 0.1% Tween 20 (PBS-T) and incubated for 1 h at room temperature with the appropriate secondary horseradish peroxidise (HRP)-conjugated antibody, followed by further washing and enhanced using chemiluminescence (ECL) detection (GE Healthcare Ltd, Amersham, Buckinghamshire, UK). The details of antibodies used for Western blotting are shown in Table 2.7

Table 2.7 Details of antibodies used in Western blot analysis

	Antibody/clone	**Source**	**Dilution**	**Incubation time and temperature**
1	p-AKT (ser ^{473})	Cell Signaling Technology	1:250	O/N incubation at 4℃
2	Total AKT	Cell Signaling Technology	1:1000	O/N incubation at 4℃
3	p-p70S6K (Thr ^{389})	Cell Signaling Technology	1:1000	O/N incubation at 4℃
4	Total p70S6K (isoforms 1 and 2)	kindly provided by Prof. Ivan Gout (UCL, UK)	1:1000	O/N incubation at 4℃
5	p-4E-BP1 (Thr ^{70})	Cell Signaling Technology	1:1000	O/N incubation at 4℃
6	p-RPS6 (ser$^{235/236}$)	Cell Signaling Technology	1:1000	O/N incubation at 4℃
7	Total RPS6 (clone 54D2)	Cell Signaling Technology	1:1000	O/N incubation at 4℃
8	p-mTOR (Ser ^{2448})	Cell Signaling Technology	1:1000	O/N incubation at 4℃
9	mTOR (clone 7C10)	Cell Signaling Technology	1:1000	O/N incubation at 4℃
10	p-FRS2α (Tyr^{196})	Cell Signaling Technology	1:1000	O/N incubation at 4℃
11	p-ERK1/2	Cell Signaling Technology	1:1000	O/N incubation at 4℃
12	total ERK1/2	Millipore Ltd, Watford, Hertfordshire, UK	1:1000	O/N incubation at 4℃
13	Brachyury (H-210): sc-20109	Santa Cruz, CA, USA	1:10.000	O/N incubation at 4℃
14	GAPDH (Mab 6C5)	Advanced Immunochemical Inc, Long beach, CA, USA	1:5000	60 min at room temperature

Protein lysates from HeLa cells (a cervical carcinoma cell line, SKOV3 cells (an ovarian carcinoma cell line) and A431 cells (an epidermoid carcinoma cell line) were used as a positive control when

assessing activation of PI3K/AKT/TSC1/TSC2/mTOR molecules, FGFR pathway molecules and EGFR phosphorylation respectively (Shahbazian et al, 2006; Doukas et al, 1999; Meuillet et al, 2000).

2.9 Proteomic profiling of receptor tyrosine kinase activity

The activity of receptor tyrosine kinases was assessed using Human Phospho-Receptor Tyrosine Kinase (phospho-RTK) array membranes (R&D Systems, Minneapolis, MN, USA) using the manufacturer's instructions. These are nitrocellulose membranes with 42 receptor tyrosine kinase antibodies spotted in duplicates with control antibodies spotted at the corners.The protein lysates were added to the membranes and the levels of RTK phosphorylation were assessed using HRP-conjugated pan phospho-tyrosine antibody followed by chemiluminescence detection. Briefly, the membrane was blocked for 1 h in array buffer 1 and the protein lysate, extracted as described above in section 2.9, was diluted in array buffer 1 to a concentration of 100 µg/ml and incubated with the membrane overnight at 4℃. The membrane was then washed in wash buffer 1, and anti-phosphotyrosine-HRP detection antibody was added for 2 h at room temperature and subsequently washed in wash buffer. The reaction was detected by adding chemiluminescence (ECL) detection reagents (GE Healthcare Ltd) and exposed to X-ray film (GE Healthcare Ltd.) for 1-10 min. Scion image soft ware available from the following link

http://www.scioncorp.com/pages/download_now.asp was used to analyse the data.

2.10 Analysis of EGFR tyrosine phosphorylation using Human EGFR Phosphorylation Antibody Array membranes

The phosphorylation of various sites of EGFR was assessed using Human EGFR Phosphorylation Antibody Array 1 detecting the relative levels of phosphorylation of EGFR family at 17 different phosphorylation sites (RayBiotech, Inc, Norcross, GA, USA) according to the manufacturer's instructions.

Briefly, the membrane was blocked for 1 hour in blocking buffer and the protein lysate, extracted as described above in section 2.9, was diluted in the blocking buffer to a concentration of 100 µg/ml and incubated with the membrane overnight at 4℃. The membrane was then washed in wash buffer 1 and wash buffer 2 three times for 5 min each, and a diluted cocktail of biotin-conjugated anti-EGFR was added and incubated at 4℃ overnight followed by washing as described above. HRP-conjugated streptavidin was then added to the membrane and incubated at room temperature for 2 h followed by washes. To detect the reaction, equal volumes of detection buffer C and detection buffer D were mixed together and applied to the membrane for 2 min followed by exposure to X-ray film (GE Healthcare Ltd.) for 1-10 min.

2.11 Mammalian cell culture

2.11.1 The U-CH1 chordoma cell line

The U-CH1 chordoma cell line was generously provided by Dr David Alcorta (Duke University, Durham, NC, USA) through the Chordoma Foundation. The cell line was established from a recurrent sacral chordoma by Dr Silke Bruederlein at the University of Ulm, Germany (Scheil et al., 2001). U-CH1 cells have abundant vacuolated cytoplasm with physaliphorous appearance. The cells show positive immunoreactivity for CK19, brachyury and S100. The CGH analysis of U-CH1 cells showed nearly identical pattern to that of the parental tumour tissue (Scheil et al., 2001).

Cells were maintained as monolayers in 75 cm^2 flasks (Corning Glass works, Corning, NY, USA) coated with 0.1% gelatine (Sigma-Aldrich). The U-CH1 culture medium was formed from a four to one ratio (4:1) of Iscove's Modified Dulbecco's Medium (IMDM)/Roswell Park Memorial Institute medium 1640 (RPMI-1640). The medium was supplemented with 10% fetal bovine serum (FBS) (Invitogen), 100 U/ml penicillin G, and 100 µg/ml streptomycin (Invitrogen) and incubated at 37°C in 5% CO_2 incubator. When cultures had attained 80-90% confluence, the cells were split 1:3 using 0.05 mM trypsin/EDTA (Invitrogen).

2.11.2 Cell count calculations

Cells were counted using a Neubauer haemocytometer (Weber Scientific International Ltd., Middlesex, UK). Trypan blue solution (Sigma-Aldrich) was added to the cell suspension to identify dead cells.

2.11.3 HeLa human cervix carcinoma cells and HEK293T (Human Embryonic Kidney 293T) cells

HeLa and HEK293T cells and were obtained from the American Type Culture Collection (ATCC, Middlesex, UK). Cells were maintained in Dulbecco's Modified Eagle's Medium (DMEM) (Invitrogen) supplemented with fetal bovine serum (FBS) (Invitrogen), 100 U/ml pencillin and 100 µg/ml stereptomycin (Invitrogen).

2.12 Knockdown of *brachyury* gene using shRNA

Two green fluorescent protein (GFP)-labelled brachyury shRNA clones were selected from the GIPZ Lentiviral shRNAmir library from Open Biosystems (Huntsville, AL, USA). The referenced names are V2LHS_153725 and V2LHS_153729. A non-silencing sequence in the same vector was chosen as the non-silencing control to determine off-target effects. Detailed sequence information for each shRNA used is shown in Table 2.8 and a diagrammatic structure of the vector is shown in figure 2.1

Table 2.8 Sequences of shRNA

	Sense sequence	Loop sequence	Antisense sequence
V2LHS_153725	CCGAGGAGATCACAGCTCTTAA	TAGTGAAGCCACAGATGTA	TTAAGAGCTGTGATCTCCTCGT
V2LHS_153729,	CGCTAATCTCTTGTGTTGTTAA	TAGTGAAGCCACAGATGTA	TTAACAACACAAGAGATTAGCT
Non Silencing (NS)		TCTCGCTTGGGCGAGAGTAAG	
Empty vector	ATTACTCCGTCTCGTGTCTTGTTGCATATGTCTGCTGGTTTGTTTGATGTTGTTTGCGGGC		

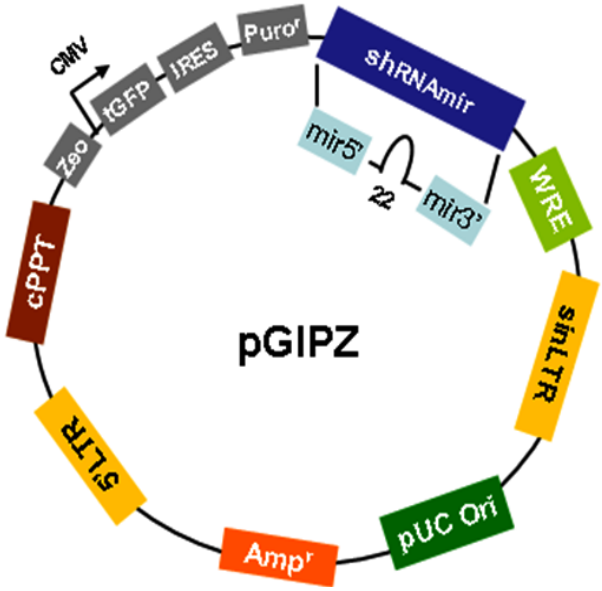

Vector element	Utility
CMV promoter	RNA polymerase II promoter
cPPT	Central Polypurine tract helps translation into the nucleus of non dividing cells
WRE	Enhances the stability and translation of transcripts
tGFP	Marker to track shRNAmir expression
IRES-puro	Mammalian selectable marker
AMPr	Ampicillin bacterial selectable marker
5'LTR	5' long terminal repeat
pUC Ori	High copy replication and maintenance of plasmid in E.coli
Sin-LTR	3'self inactivating long terminal repeat
RRE	Rev response element
ZEOr	Bacterial selectable marker

Figure 2.1 Schematic diagram of pGIPZ lentivirus structure.

2.12.1 Propagation of bacteria containing pGIPZ hairpin constructs and preparation of plasmid DNA

Bacteria containing pGIPZ hairpin constructs were streaked on to solid agar stab cultures containing 100 µg/ml ampicillin and the cultures were grown overnight at 37℃. On the following day, the bacteria were streaked on LB agar plates and kept overnight at 37℃. Single colonies were picked and grown in 5 ml LB broth containing 100 µg/ml ampicillin for 1 h at 37℃ with vigorous shaking and then diluted in 500 ml of LB broth and incubated overnight under shaking. The cell pellets were formed and DNA was extracted using Qiagen Plasmid Purification kit (Qiagen) following the manufacturer's instructions.

The pellet was re-suspended in 10 ml of buffer P1 and 10 ml of buffer P2 was added and incubated for 5 min at room temperature. Then, 10 ml of P3 buffer was added and incubated on ice for 20 min. The sample was then centrifuged at 15.000 rpm at 4°C and the supernatant containing the plasmid was removed and re-centrifuged for 15 min at 4℃. The columns were prepared by adding 10 ml of buffer QBT and allowed to empty by gravity. The supernatant was applied and allowed to enter the resin by gravity and then washed twice in 30 ml buffer QC. The DNA was eluted in 15 ml buffer QF and precipitated by adding 10.5 ml isopropanol with centrifugation at 13,000 rpm for 30 min at 4℃. The pellet was washed in 5 ml of 70% ethanol at room temperature, air-dried for 10 min and re-suspended in 500 µl of TE

buffer pH 8. The quality of DNA extracted was assessed using a nanodrop (Thermo Scientific, NanoDrop products, Wilmington, DE, USA). The sequence of DNA was confirmed by direct sequencing at the Scientific Support Services at UCL Cancer Institute/WIBR. Sequencing reactions were run using GenomeLab™ DTCS Quick Start chemistry (Beckman Coulter UK Ltd.) and were analysed on a CEQ™ 8000 Genetic Analysis System (Beckman Coulter).

2.12.2 Lentivirus production

HEK293T cells were maintained in DMEM media supplemented with 10% FBS and 1% penicillin and streptomycin. They were split 3 times a week at a ratio of 4:1 using 0.05 mM trypsin/EDTA. HEK293T cells were seeded one day before the transfection by splitting a confluent plate 1/4 in 10 cm2 plates with 8 ml complete media and incubated at 37℃, 5% CO_2. On the day of transfection, the following mixture was prepared in 1.5 ml micro-tube; 1µg p8.91 (gag-pol expressor), 1 µg pMDG.2 (VSV-G expressor), 1.5 µg pGIPZ DNA (for each construct) and sterile TE for 15 µl final volume. In a second micro-tube, 10 µl Fugene (Roche Diagnostics Ltd., Burgess Hill, West Sussex, UK) was added to 200 µl Optimem (Invitrogen) for each of the transfection mixtures. The DNA mix was added to the Optimem-Fugene mix and left at room temperature for 15 min. The medium was changed with fresh complete medium and the Optimem/DNA/Fugene mix was added to the cells and incubated overnight at 37℃, 5% CO_2. The

medium was changed to fresh complete medium after 24 h. At 48 h, the lentivirus-containing supernatant was collected in a 10 ml syringe (Fisher) and filtered through a 0.45 µm filter (VWR International Ltd., Lutterworth, Leicestershire, UK) into a 50 ml tube. The supernatant was aliquoted and stored at -80℃.

2.12.3 Lentivirus titration and infection of the U-CH1 cells

The day before titration, 293T cells were seeded at $0.5x10^5$ cells per well in 6 well plates in 2 ml of complete medium and incubated overnight at 37C, 5% CO_2. Different concentrations of the virus stock to be titrated were added together with 8ug/ml polybrene (Sigma-Aldrich) to different wells and incubated for two days. The cells were detached with trypsin/EDTA (Invitrogen) and analysed by fluorescence activated cell sorting (FACS) for the ratio of the GFP expressing cells. The concentrations of viral stock that gave ratios of less than 20% were selected and used to transfect U-CH1 cells. Stable transfected U-CH1 cells were selected in 5 µg/ml puromycin (Sigma-Aldrich) after performing a puromycin-kill curve to determine the optimal concentration needed for selection. After 5 days, all non-infected cells were killed, and the remaining cells had GFP expression.

2.12.4 Semi-quantitative real time RT-PCR for *brachyury* expression

2.12.4.1 RNA extraction from cultured cells

Total RNA was extracted from the cultured cells using QIAzol lysis reagent (Qiagen). Briefly, the cells were washed with PBS and 700 µl of QIAzol was added and cells were scraped with a cell scraper and

kept in a micro-tube for 5 min at room temperature. Then 200 µl of chloroform were added and left for 3 min at room temperature followed by centrifugation at 13,000 rpm for 15 min at 4℃. The top clear supernatant was transferred to a new tube and 350 µl of isopropanol were added and left for 10 min at room temperature. The sample was then centrifuged at 10,000 rpm at 4℃ for 10 min and 400 µl of 100% ethanol was added and centrifuged at 10,000 rpm for 5 min at 4℃. The supernatant was removed and the pellet allowed to dry for 10 min and then re-suspended in 100 µl of nuclease free water. The RNA was purified using the RNeasy Mini Kit (Qiagen) following the manufacturer's protocol.

2.12.4.2 Synthesis of cDNA using gene-specific primers

Two hundred nanograms of total RNA were used to synthesise cDNA using Superscript III First-Strand Synthesis kit (Invitrogen) and gene specific primers. All primers used for reverse transcription and reverse transcription PCR are shown in Table 2.10. Briefly, 1 µl of primer mix and 1 µl of dNTP mix, were added to 200 ng total RNA, and the volume was made to 10 µl with RNase free water (Invitrogen). The mixture was incubated for 5 min at 65℃ and briefly chilled on ice before the addition of 2 µl of 10X first strand buffer (Invitrogen), 2µl of 0.1M DTT, 4 µl of 25 mM $MgCl_2$, 1 µl of RNaseOUT, and 1 µl (200 U/µl) of SuperScript III. The resulting mix was incubated at 50℃ for 50 min. The reaction was terminated at 85℃ for 15 min and then chilled on ice. For

each reaction, 1 µl (2 U) of RNase H was added and incubated at 37℃ for 20 min.

2.12.4.3 Real time semi-quantitative RT-PCR

The real time PCR reaction was performed in 25 µl and included 1µl of cDNA, 5 pmol of each primer, and 12.5 µl of SYBR® Green PCR Master Mix (Applied Biosystems, Birchwood, Warrington, UK). The cycles included initial heating at 95℃ for 3 min f ollowed by 50 cycles of heating to 95℃ for 15 s and 60℃ for 1 min. *GAPDH* was used as a control house keeping gene. The comparative threshold cycle (Ct) method with the calculation of $2^{-[delta][delta]Ct}$ was used to assess the relative level of expression of brachyury.

Table 2.9 Sequences of the primers used for real time RT-PCR

	Primer sequence	Product length
Brachyury	5'-GTGGCTTCTTCCTGGAACC-3'	67 bp
	5'-ACAATGCCAGCCCACCTAC-3'	
GAPDH	5'-GGAGTCAACGGATTTGGTCGTA-3'	78 bp
	5'-GGCAACAATATCCACTTTACCAGAGT-3'	

2.13 Senescence-associated beta-Galactosidase staining (SA-β Gal)

For detection of cell senescence, beta-Galactosidase staining was performed. The U-CH1 cells with *brachyury* knockdown and controls were plated in 6-well plates in triplicates for 3 d and then washed twice with PBS. The cells were then fixed in 4% formaldehyde for 5 min and then washed with PBS supplemented with 1 mM MgCl2. The staining solution (X-Gal solution) formed of 1 mg/ml of X-Gal, 0.12 mM K3Fe[CN]6, 0.12 mM K4Fe[CN]6 and 1 mM MgCl2 in PBS at pH

6.0 was added and the cells were incubated overnight at 37°C. Cells were examined under phase-contrast microscope and 100 cells were counted at different field. The result of the staining was expressed as stained cells/100 cells.

2.14 Treatment of U-CH1 cells with EGFR inhibitor tyrphostin (AG1478)

2.14.1 Morphologic changes

For morphologic analysis of the effect of EGFR inhibition on U-CH1 cells, the EGFR inhibitor tyrophostin (AG1478) from Cell Signalling Technology was applied to the cells. The cells were seeded in 6 well plates at a density of $1x10^5$ per well and incubated in complete U-CH1 media for 2 d after which the medium was replaced with complete medium containing different concentrations of the drug at 0, 5, 10, 20, 50, 100, 200 nmol/L with DMSO 0.05% as a vehicle. The cells were grown for two days after which the medium was replaced with fresh medium containing the drug and grown for another two days. In parallel a subset of cells for which the medium containing the drug was removed after 4 d and replaced with complete medium for another 4 d was grown to assess the reversibility.

To test for the effect of tyrphostin (AG1478) on phosphorylation of EGFR, the cells were starved for 24 h in a serum-free medium.The drug was diluted in a serum-free medium and added to the cells for 48 h and before harvesting the cells for protein extraction, EGF (50 ng/ml) was

added for 15 min to stimulate the cells. The cells were harvested using 0.05 mM trypsin/EDTA and protein was extracted as previously described in section 2.9. The experiments were performed at three separate times and in triplicates each time.

2.14.2 MTS assay

The U-CH1 cells were cultured in a density of 2500 cells/well in 96 well plates in 100 µl of complete U-CH1 medium and maintained in a 37℃ in an incubator with 5% CO2 for 48 h after whi ch tyrphostin was added in different concentrations (0, 5, 10, 20, 50, 100, 200 nmol/L) with 0.05% DMSO as a vehicle. Cell proliferation was assessed at days 0, 3, 4, 5 and 7 after addition of the drug using the MTS [3-(4,5-dimethylthiazol-2-yl)-5-(3-carboxymethoxyphenyl)-2-(4-sulfophenyl)-2H-tetrazolium, inner salt) assay (CellTiter 96® AQueous Non-Radioactive Cell Proliferation Assay, Promega). Briefly, 20 µl of MTS and phenazine methosulfate (MTS-PMS) solution was added to each well. Plates were incubated at 37℃ for 2 h, after which the absorban ce at 490 nm was measured using a microplate-reader (Thermo Scientific Varioskan Flash microplate-reader). For assessment of cell recovery after withdrawal of the tyrphostin (AG1478), the cells were plated as described above in 96-well plates and treated with the drug for 4 d after which, the drug-containing medium was removed and replaced with full medium, and cells were allowed to grow for another 4 d. The cells were examined by the MTS assay as described above.

2.15 Statistical Analysis

All experiments were performed in independent replicates. Error bars correspond to the standard deviation from the calculated mean. SPSS (Version 18.0, Chicago, IL) was used for all statistical analyses. Mean value and standard deviation were calculated using descriptive statistics. Comparison of means was performed by one-way analysis of variance. Chi-square tests, Student T test or Fisher exact tests were used, where applicable, to analyze differences between independent variants. Differences were considered significant if $p<0.05$.

3. ANALYSIS of PI3K/AKT/TSC/mTOR PATHWAY IN CHORDOMA

3.1 INTRODUCTION

The majority of chordomas occur as a sporadic disease, however a few families have been reported to have multiple affected members denoting that inherited genetic changes can predispose to these tumours (Larizza et al., 2005). There is no reported association between chordomas and any of the inherited tumour predisposition syndromes apart from six reported cases of tuberous sclerosis complex with chordomas (Dutton and Singleton, 1975; Schroeder et al., 1987; Borgel et al., 2001; Lee-Jones et al., 2004; Lountzis et al., 2006). One of these reports identified somatic inactivation of tuberous sclerosis genes within the chordoma tumours suggesting the possible aetiological role of these genes in chordoma (Lee-Jones et al., 2004). Somatic mutations of *TSC1* and *TSC2* were also identified in other tumours such as sporadic lymphangioleiomyomatosis (Sato et al., 2002).

Tuberous sclerosis complex syndrome (TSC) is a rare tumour suppressor gene-related syndrome characterised by abnormal tissue growth known as hamartoma affecting many organs including brain, kidney, heart, eyes, lung and skin. It is caused by inactivating mutations in *TSC1* and *TSC2* tumour suppressor genes encoding TSC1 (hamartin) and TSC2 (tuberin) respectively (van Slegtenhorst et al., 1997).

Hamartin and tuberin form a complex heterodimer and function by linking the PI3K/AKT signalling pathway to mTOR (mammalian target of

rapamycin) where they function to inhibit mTOR activation and subsequent transcription and cell proliferation (Hengstschlager et al., 2001).

The PI3K/AKT/TSC/mTOR pathway is found to be activated in a variety of solid cancers and haematological malignancies, including malignant gliomas, ovarian, endometrial, breast, renal, prostate, colon and lung carcinomas, mantle cell lymphoma, and in post-transplant lymphoproliferative disorders (Vivanco and Sawyers, 2002; Vignot et al., 2005; Vega et al., 2006; El-Salem et al., 2007). The mTOR protein kinase, is an essential regulator of protein synthesis, and controls entry into G1 phase of the cell cycle through phosphorylation of the substrates p70S6K and 4E-BP1, molecules that cooperate in translational initiation and ribosomal biogenesis. It is for these reasons that mTOR inhibitors are considered potential therapeutic agents in tumours where mTOR signalling is activated. Therefore, screening of tumour specimens for activated molecules in this pathway may provide a rational basis for identification of the patients who might benefit from therapy with mTOR inhibitors (Vega et al., 2006). Based on the previous reports of chordoma occurrence in the context of TSC syndrome, looking for this pathway activation is considered reasonable.

3.1.1 PI3K/AKT/TSC/mTOR pathway

The PI3K/AKT/TSC/mTOR pathway regulates several normal cellular functions including cellular proliferation, growth, survival and

mobility. Components of this pathway are frequently abnormal in various types of tumors (Vivanco and Sawyers, 2002). The PI3K/AKT/TSC/mTOR signalling pathway can be activated via over-expressed or mutated receptor tyrosine kinases (Bose et al., 2006). The pathway components are schematically represented in Figure 3.1.

3.1.1.1 Phosphoinositide 3 kinase (PI3K)

Phosphoinositide 3 kinase (PI3 kinase or PI3K) is a heterodimer lipid kinase consisting of p85 and p110 catalytic subunits. It becomes activated by signals transmitted through many receptor tyrosine kinases resulting in phosphorylation of phosphatidylinositol-4,5-bis phosphate (PIP2) to phosphatidylinositol-3,4,5-tris phosphate (PIP3) at the cell membrane (Franke et al., 1997).

3.1.1.2 Protein Kinase B (PKB or AKT)

Protein Kinase B (PKB or AKT) is a cytosolic protein kinase recruited by PIP3 and in the presence of the activated membrane threonine kinase called phosphoinositide-dependent kinase 1 (PDK-1), AKT becomes phosphorylated at threonine^{308} (Thr^{308}). The full activation of AKT requires phosphorylation at serine^{473} (Ser^{473}) caused by reaction with phosphoinositide-dependent kinase 2 (PDK-2) proved to be the mammalian target of rapamycine complex 2 (mTORC2) (Toker and Newton 2000; Sarbassov et al., 2004). Phosphorylated AKT in turn phosphorylates many highly significant substrates involved in cell growth, proliferation and apoptosis (Bose et al., 2006; Stephens et al.,

1998). AKT phosphorylation of TSC2 leads to inhibition of the TSC1/TSC2 complex function thereby releasing its inhibitory effect on Rheb, which in turn leads to activation of mTOR (Inoki et al., 2002).

3.1.1.3 Tuberous sclerosis complex 1/ Tuberous sclerosis complex 2 (TSC1/TSC2)

Directly upstream of mTOR is a protein complex composed of *TSC1* and *TSC2*, and the presence of both proteins is required for the function of the heterodimer. TSC2 is the main reactive protein while TSC1 serves to stabilize the complex. The main function of TSC2 is to increase the intrinsic rate of GTP hydrolysis on RAS homologue enriched in brain (Rheb) resulting in its inactivation. TSC1/2 complex can be inactivated by mutation of either *TSC1* or *TSC2* genes as occurs in TSC syndrome (Inoki et al., 2005). TSC2 can be also inactivated by being phosphorylated at its GAP (guanosine triphosphatase activating protein) domain by activated AKT in response to activated membrane receptors (Manning et al, 2002; Han et al, 2004). Phosphorylation of TSC2 is thought to accelerate its degradation through ubiquitin-mediated mechanism (Plas and Thompson, 2003).

3.1.1.4 Phosphatase and tensin homologue deleted on chromosome 10 (PTEN)

Phosphatase and tensin homologue deleted on chromosome 10 (PTEN) is a phosphatase enzyme. It dephosphorylates PIP3 to PIP2

and so considered to be a tumour suppressor gene by negatively regulating the PI3K/AKT pathway (Radu et al., 2003).

3.1.1.5 RAS homologue enriched in brain (Rheb)

RAS homologue enriched in brain (*Rheb*) is a member of Ras family of oncogenes and is considered a potent mTOR activator. It is negatively regulated by TSC1/2 complex that converts Rheb guanosine triphosphate (GTP) to Rheb guanosine diphosphate (GDP), so inactivates the Rheb and accordingly inhibits mTOR (Brendan et al, 2003).

3.1.1.6 Mammalian target of rapamycin

Mammalian target of rapamycin (mTOR) is a 289-kDa seine/threonine kinase originally identified in 1994 shortly after its orthologues TOR1 and TOR2 were identified in yeast as the target protein for the drug rapamycin. It represents an integration point linking numerous upstream signals to the translation system (Heitman et al., 1991; Sabatini et al., 1994). It exists in two distinct complexes, each consists of mTOR, G protein β subunit-like (GβL, also known as mLST8) and either regulatory-associated protein of mTOR (raptor) in mTOR complex 1 (mTORC1) or rapamycin-insensitive companion of mTOR (rictor) in mTOR complex 2 (mTORC2). The mTORC1 is rapamycin sensitive and its activation regulates protein synthesis, cell growth, and proliferation through its downstream targets, eukaryotic initiation factor 4E (elF-4E), binding protein 1 (4E-BP1) and p70S6

kinase (p70S6K). mTORC2 is rapamycin resistant and its main function is to phosphorylate AKT at the Ser^{473} position, leading to full activation of AKT and organization of the cytoskeletal structure. It acts as a positive feedback loop (Sarbassov et al., 2004; Sarbassov et al., 2005).

3.1.1.7 p70S6 Kinase

p70S6 Kinase (S6K) is a serine/threonine kinase, the activity of which leads to an increase in protein synthesis and cell proliferation via phosphorylation of S6 ribosomal protein (RPS6) leading to increased translation of mRNAs (Nojima et al., 2003). There are two similar S6K proteins (S6K1 and S6K2) encoded by two different genes, with S6K1 showing rapamycine sensitivity. The S6Ks are activated at different sites of which Thr^{389} is the most important one (Lee-Fruman et al., 1999).

3.1.1.8 Ribosomal protein S6 (RPS6)

S6 protein of the 40S ribosomal subunit becomes phosphorylated by the active S6K at several sites, including $Ser^{235,236}$, leading to initiation of protein synthesis (Dufner et al., 1999).

3.1.1.9 Euokaryotic Initiation factor 4E -Binding Protein 1 (4E-BP1)

Euokaryotic Initiation factor 4E-Binding Protein 1 (4E-BP1) is a cytoplasmic protein that binds to and inhibits the function of the cap-dependent euokaryotic initiation factor 4E (eIF-4E). Phosphorylation of 4E-BP1 releases its inhibitory effect on resulting in increased translation of mRNAs (Rojo et al., 2007).

3.1.1.10 Euokaryotic initiation factor 4E (eIF-4E)

Euokaryotic Initiation factor 4E (eIF-4E) is a translation initiation factor involved in cap-dependent translation of mRNAs and is considered as the rate-limiting component of the eukaryotic translation apparatus (Mamane et al., 2004).

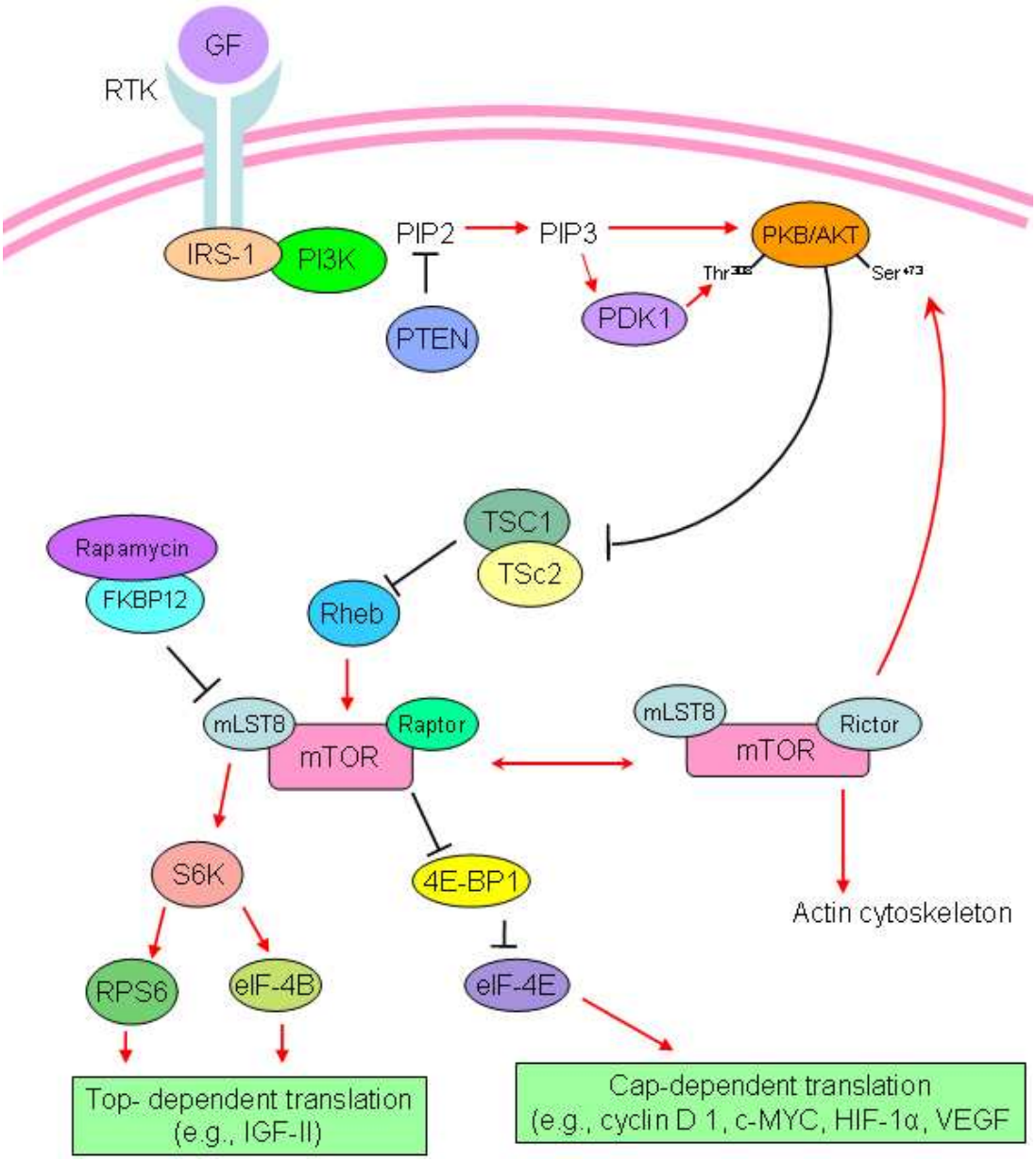

Figure 3.1 A schematic diagram of PI3K/AKT/mTOR pathway

3.1.2 Aim

The aim of this part of the project was to investigate the activation status of PI3K/AKT/TSC/mTOR signalling pathway in a cohort of 50 sacro-coccygeal chordomas, 50 skull-based chordomas and a chordoma-derived cell line, U-CH1.

3.1.3 Objectives

- Analysis of PI3K/AKT/TSC/mTOR pathway activation in sacro-coccygeal chordomas as follow
- Study the expression of active phosphorylated molecules using immunohistochemistry on TMAs and confirm the results by Western blot analysis of selected cases.
- Study the genetic status of molecules in the PI3K/AKT/TSC/mTOR pathway through mutational analysis of genes in the pathway with previously reported activating mutations including PI3KCA and Rheb and analysis of the copy number changes in some of the pathway genes using interphase fluorescent *in situ* hybridisation (FISH).
- Analysis of PI3K/AKT/TSC/mTOR pathway activation in skull-based chordomas and the U-CH1 chordoma-derived cell line using immunohistochemistry.

3.2 RESULTS

3.2.1 Immunohistochemistry

Immunohistochemistry was performed on TMA slides from 50 sacro-ccocygeal chordomas using phospho-specifc antibodies. More than 90% were immunoreactive for p-AKT (Ser^{473}), p-TSC2 (Thr^{1462}), p-4E-BP1 (Thr^{70}) and eIF-4E (Figure 3.2, Table 3.1). The labelling pattern of these antibodies was largely similar and consisted of diffuse granular cytoplasmic immunoreactivity, although nuclear positivity for p-AKT and p-4E-BP1 was noted in less than 10% of cases (Figure 3.2). The immunoreactivity for p-mTOR (Ser^{2448}), p-S6K (Thr^{389}), p-RPS6 ($Ser^{235/236}$) was found in 13 of 48 (27%), 29 of 46 (62%) and 11 of 49 (22%) cases respectively (Table 3.1, Figure 3.2). Immunohistochemistry results for the total proteins mTOR, S6K, RPS6 showed positive labelling for 33 of 44 (75%), 50 of 50 (100%) and 22 of 45 (49%) respectively.

As shown in table 3.2, immunohistochemistry results for the skull-based chordoma TMA containing 50 tumours showed immunoreactivity for p-AKT (62.5%), p-TSC2 (68.7%), p-mTOR (54%), p-p70S6K (52%), p-4E-BP1 (95.8%), p-RPS6 (62.5%), eIF-4E (91.6%).

Immunoreactivity for PTEN was absent in 16% (7/43) of sacro-coccygeal and skull-based (8/50) chordomas (Figure 3.2, Table 3.1, Table 3.2).

A summary of the immunohistochemistry results in skull-based chordoma versus sacro-coccygeal chordoma is shown in Table 3.3.

Formalin fixed U-CH1 chordoma-derived cell line showed immunoreactivity for p-AKT, p-TSC2, p-mTOR, p-RPS6, p-S6K, p-4E-BP1, eIF-4E with no immunoreactivity for PTEN (Figure 3.3).

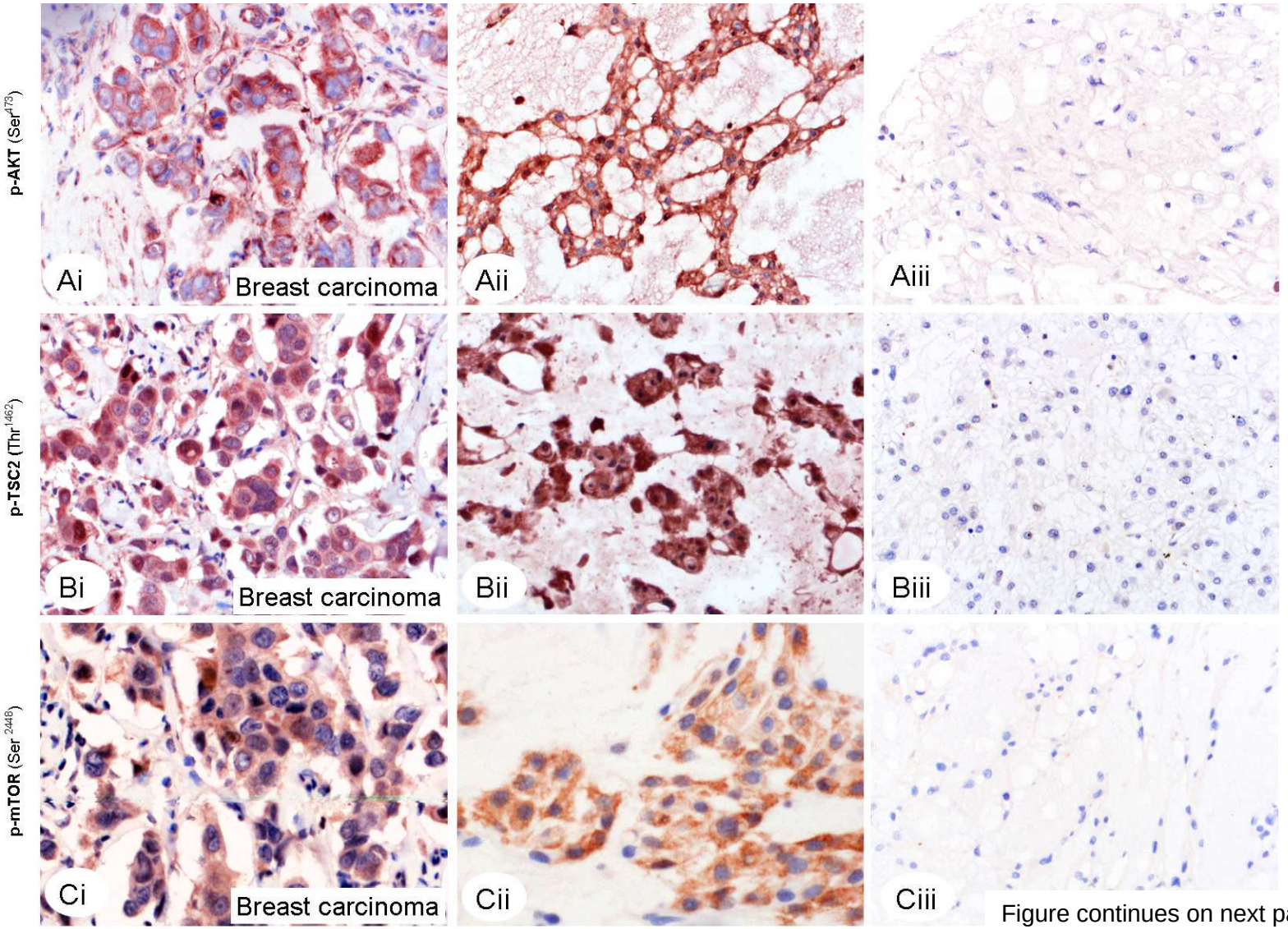

Figure continues on next page

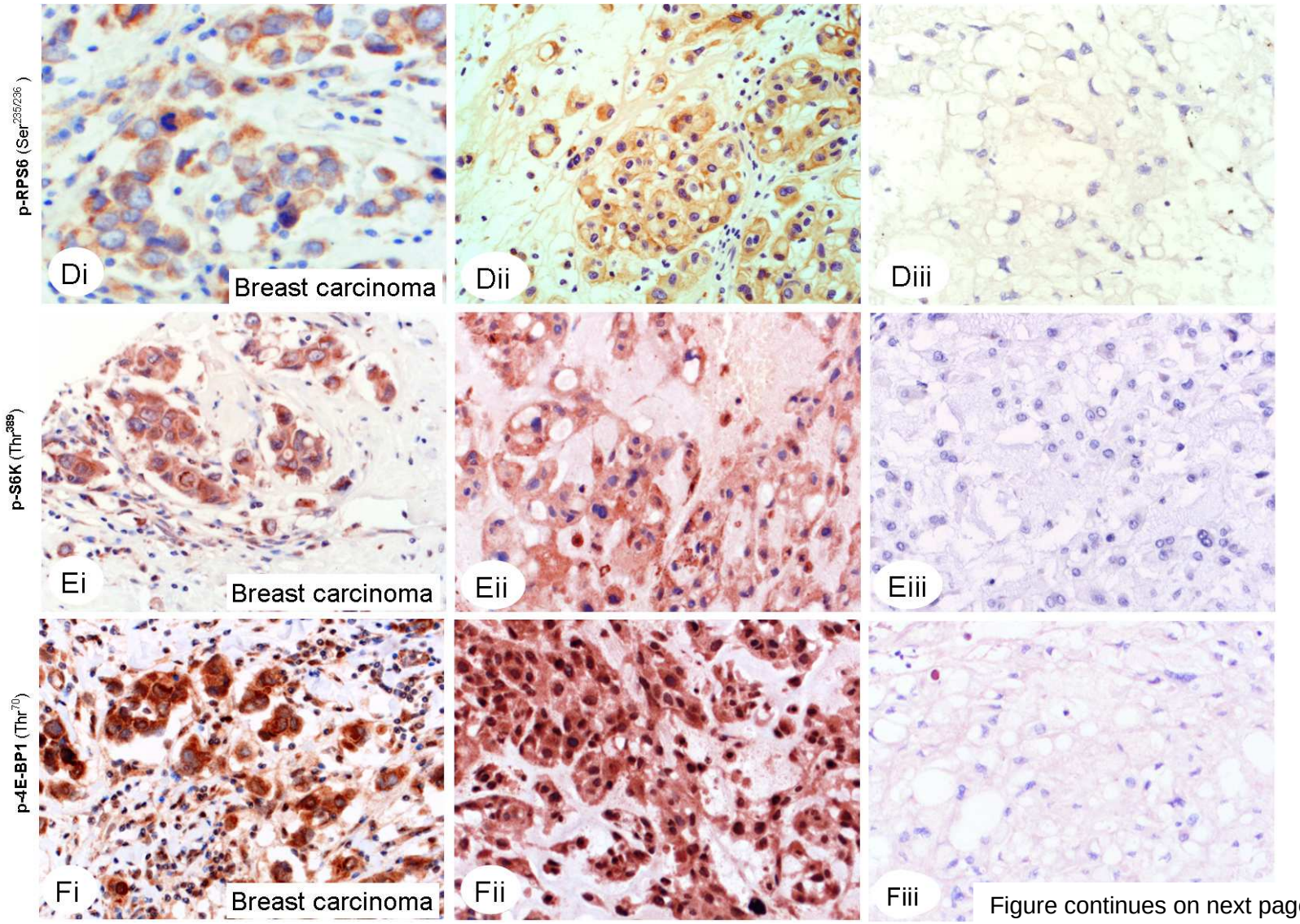

Figure continues on next page

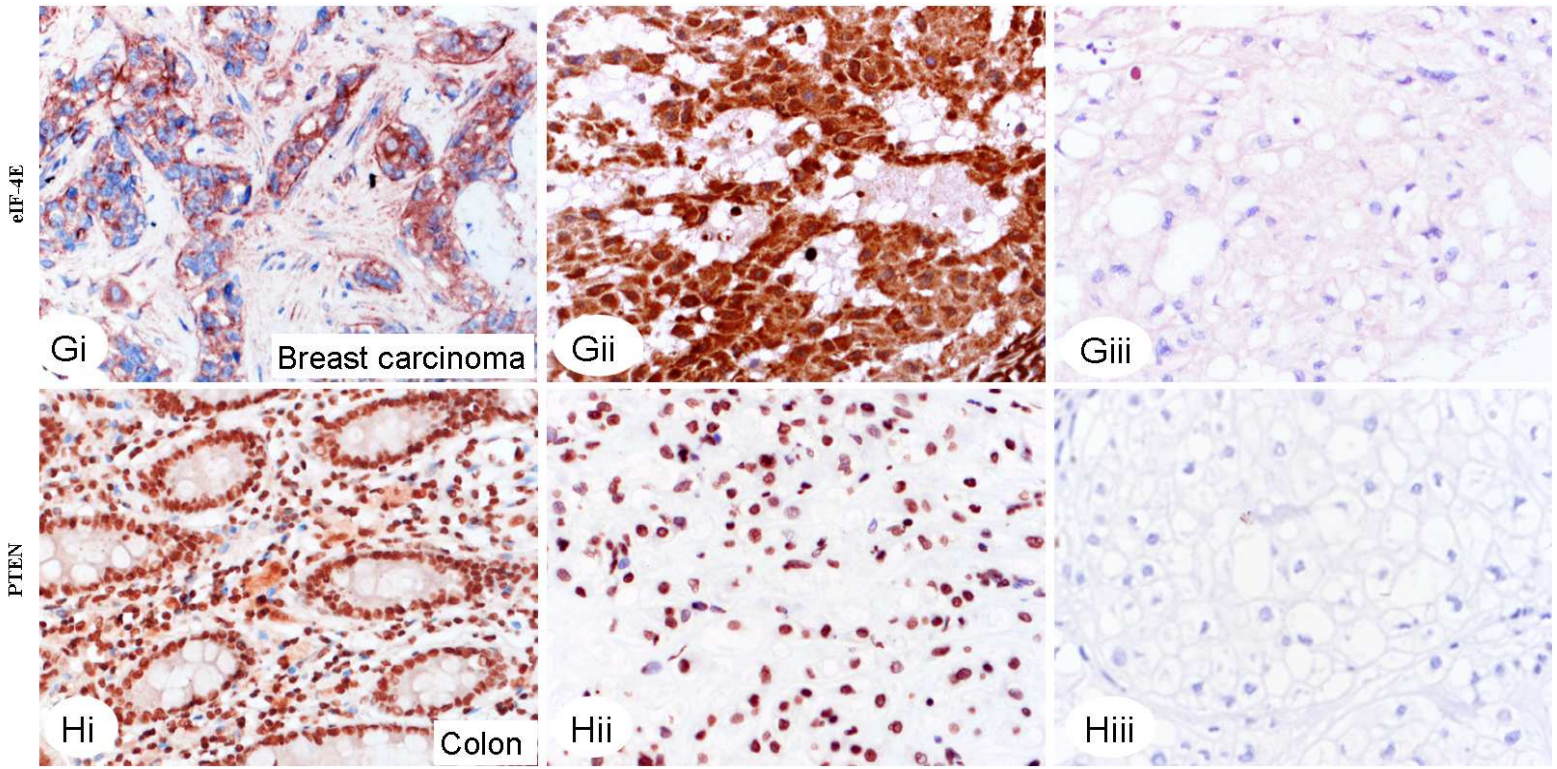

Figure 3.2 Immunohistochemistry results of PI3K/mTOR pathway active molecules in sacro-coccygeal chordomas; the photomicrographs on the left hand panel represent cores of positive control tissues (breast carcinoma Ai-Gi and colon, Hi) that are immunoreactive for the indicated antibodies. The middle panel shows representative chordomas which were scored as 'strong' for expression of the indicated antibodies indicating that the immunoreactivity is as strong as that in the positive control (Aii-Hii). The right hand panel includes representative chordomas that were not immunoreactive for the relevant antibodies (Aiii-Hiii). TMA slides incubated with the isotype IgG for each antibody served as negative controls.

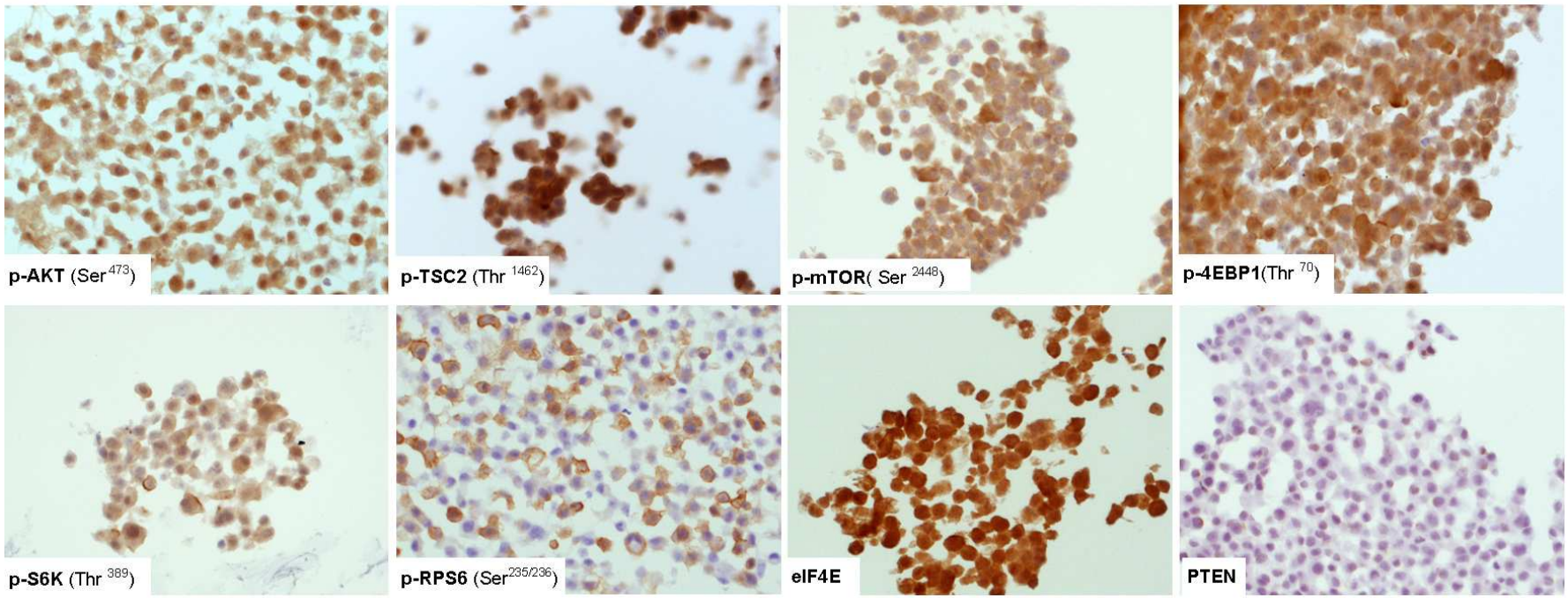

Figure 3.3 Immunohistochemistry of formalin-fixed, paraffin-embedded U-CH1 cell line for active molecules in the PI3K/AKT/TSC/mTOR pathway. Formalin-fixed, paraffin-embedded HeLa cells served as the positive control for various antibodies while slides incubated with IgG isotype served as negative controls for each of the antibodies used.

Table 3.1 Immunohistochemistry for AKT/TSC/mTOR pathway molecules in sacro-coccygeal chordoma

	p-AKT (Ser^{473})	TSC1	TSC2	p-TSC2 (Thr^{1462})	p-mTOR (Ser^{2448})	mTOR	p-p70S6K (Thr^{389})	S6K	p-RPS6 ($Ser^{235/236}$)	RPS6	p-4E-BP1 (Thr^{70})	eIF-4E	PTEN	CDKN2A
No immunoreactivity	4	26	0	2	35	11	18	0	41	23	2	1	7	46
Low immunoreactivity	31	14	40	47	5	33	11	50	8	21	25	35	28	2
High immunoreactivity	14	8	9	0	8	0	18	0	3	1	21	12	9	0
Positive cases/total cases (%)	45/49 (92)	22/48 (46)	49/49 (100)	47/49 (96)	13/48 (27)	33/44 (75)	29/47 (62)	50/50 (100)	11/49 (22)	22/45 (49)	46/48 (96)	47/48 (98)	37/43 (86)	2/48 (4)

Table 3.2 Immunohistochemistry for AKT/TSC/mTOR pathway molecules in skull-based chordoma

	p-AKT (Ser^{473})	p-TSC2 (Thr^{1462})	p-mTOR (Ser^{2448})	p-p70S6K (Thr^{389})	p-RPS6 ($Ser^{235/236}$	p-4E-BP1 (Thr^{70})	eIF-4E	PTEN
No immunoreactivity	18	15	20	23	18	2	4	8
Low immunoreactivity	21	24	9	24	13	25	19	42
High immunoreactivity	9	9	17	1	17	21	25	0
Positive cases/total cases (%)	30/48 (62.5)	33/48 (68.7)	26/48 (54)	25/48 (52)	30/48 (62.5)	46/48 (95.8)	44/48 (91.6)	42/50 (84)

Table 3.3 Percentage of sacro-coccygeal versus skull-based chordomas showing immunoreactivity for active molecules in PI3K/AKT/TSC/mTOR pathway

	Sacro-coccygeal chordoma TMA	Skull-based chordoma TMA
p-AKT	92%	62.5%
p-TSC2	96%	68.7%
p-mTOR	27%	54%
p-S6K	62%	52%
p-RPS6	22%	62.5%
p-4E-BP1	96%	95.8%
eIF-4E	98%	91.6%
PTEN	86%	84%

Although the TMAs were composed of 50 non skull-based and 50 skull-based chordomas, the total numbers in the tables represent the number which could be interpreted. The scoring system employed was as follows: negative in the absence of immunoreactivity, 'low' when the immunoreactivity was unequivocal but less strong than the positive control, and 'high' when the immunoreactivity was at least as strong as the positive control. In all of the positive cases, the staining was diffuse and in more than 95% of the neoplastic cells

3.2.2 Western blot analysis

Western blot analysis of p-AKT, p-4E-BP1 and p-p70S6K on six selected chordomas was largely in agreement with the results of immunohistochemistry (Figure 3.4). In addition, the Western blot result for total p70S6K showed positive reactivity for the rapamycin-sensitive p70S6K isoform 1 in the six examined cases (Figure 3.4). Specifically, Western blot analysis of p-mTOR confirmed the results of immunohistochemistry in four out of six studied cases by showing positive reactivity in one case and absence of activated protein in the other three cases. In two cases, Western blot analysis failed to detect the p-mTOR showed by immunohistochemistry. This can be explained by the technical difficulties to detect the phosphorylated high molecular weight proteins like mTOR (289 kDa) by Western blot analysis. The Western blot results for p-RPS6 confirmed the immunohistochemistry data in five out of six cases with one discrepant case showing p-RPS6 by immunohistochemistry but not by Western blotting. On the other hand, Western blot analysis detected total RPS6 protein in all the 6 cases although two of these were negative by immunohistochemistry. These two cases revealed loss of one allele of *RPS6* gene by FISH analysis (see below) and both were negative for p-RPS6 by Western blot analysis suggesting that the positive result for total RPS6 by Western blot may be explained by non-neoplastic contaminating stromal cells.

A Western Blotting

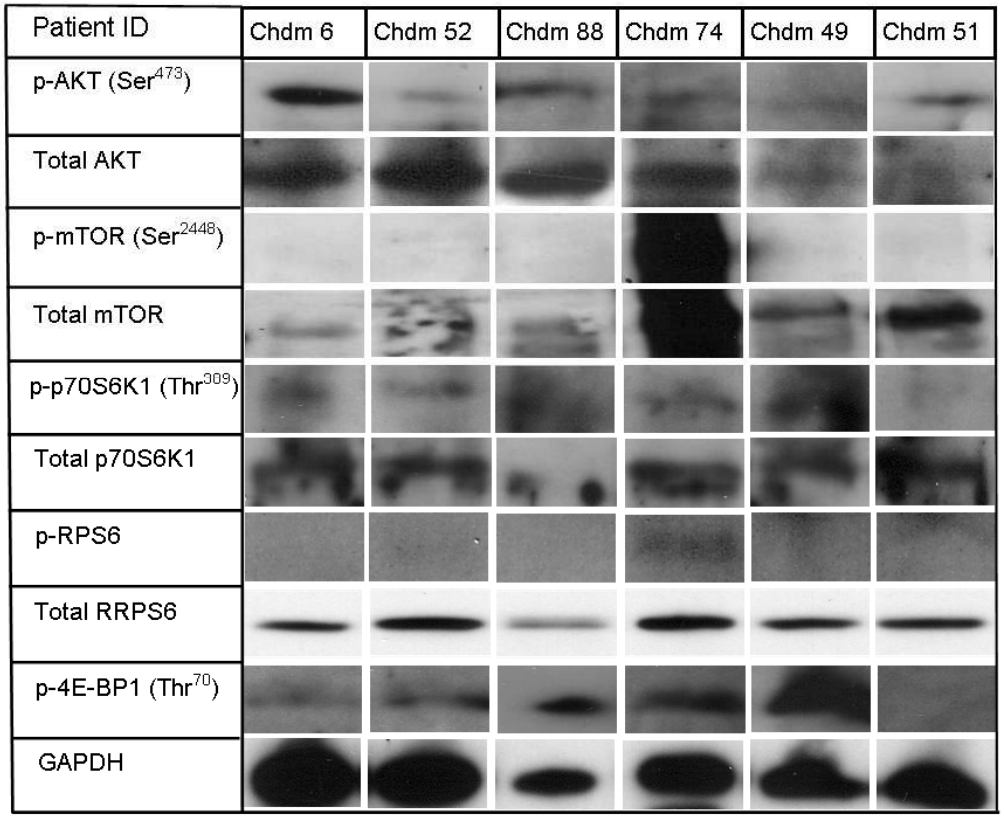

B Immunohistochemistry

Chdm 6	Chdm 52	Chdm 88	Chdm 74	Chdm 49	Chdm 51
low	high	high	high	high	low
ND	ND	ND	ND	ND	ND
0	0	high	high	0	high
low	low	low	low	0	low
low	high	high	high	low	0
low	low	low	low	low	low
0	0	high	high	0	0
0	low	high	low	0	low
low	high	high	high	high	low / equivocal
ND	ND	ND	ND	ND	ND

Figure 3.4 Western blot analysis of 6 selected chordomas (Chdm) for active molecules in the PI3K/AKT/TSC/mTOR pathway correlated with immunohistochemistry results. All cases showed a strong band for p-AKT at Ser^{473} (all 6 cases positive by immunohistochemistry). For p-mTOR, Western blotting confirmed the immunohistochemistry data in 4 of 6 cases showing the presence of the activated protein in one case

and the absence in 3 cases. Two cases were negative by Western blotting inspite p-mTOR can be detected by immunohistochemistry. Total mTOR protein was detected in all cases. Five cases showed a band for p-p70S6K expression and showed immunohistochemical reactivity while the last case showed no band with Western blotting was also negative by immunohistochemistry. Antibodies against isoform 1 and 2 of total p70S6K protein showed that p70S6K1 isoform was expressed in the 6 analysed chordomas. Western blot identified p-RPS6 expression in one case and this reflected the immunohistochemistry findings. All cases showed a band corresponding to total RPS6 expression despite the fact that two cases did not express total RPS6 by immunohistochemistry. Expression of p-4E-BP1 (Thr^{70}) was shown in five chordomas by both methods, however, Western blot failed to reveal a band for one case which was scored as equivocal on immunohistochemistry. The membranes were probed with the first antibody (p-AKT) and then with anti-GAPDH antibody as a loading control and then stripped with addition of each of the various antibodies used. The GAPDH images showed here represent GAPDH expression before stripping of the membranes.

3.2.3 FISH results for *mTOR* (*FRAP1*), *RPS6*, *TSC1* and *TSC2*

FISH analysis for *mTOR* (*FRAP1*) locus on chromosome 1 showed loss of one allele in 11 of 33 (33.3 %) and for *RPS6* showed loss of one allele in 21 of 45 (46.6%) cases (Figure 3.5). FISH for *TSC1* (28 of 28 cases) and *TSC2* (24 of 24 cases) showed two alleles.

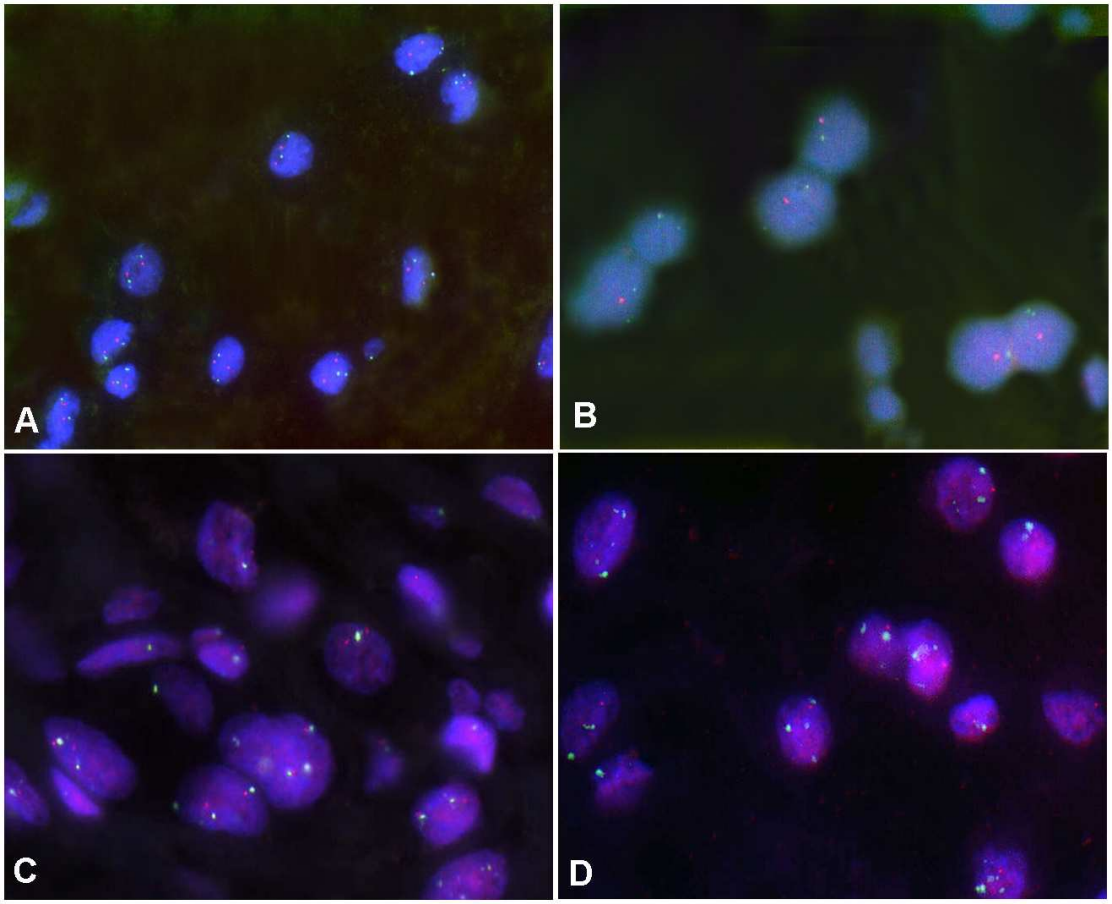

Figure 3.5 FISH analysis of *mTOR* (*FRAP1*) and *RPS6*. Chordoma with no allelic loss for *mTOR* (*FRAP1)* (A), chordoma with allelic loss for *mTOR* (*FRAP1)* (B), chordoma with no allelic loss for *RPS6* (C) and chordoma with allelic loss for RPS6 (D). The red signals identify *mTOR (FRAP1)* and *RPS6* respectively. The green signals represent chromosome enumeration probe 1 (CEP1) for *mTOR* and (CEP9) for *RPS6*. Fifty non-overlapping nuclei were counted for each case. Hemizygous deletion was defined by the presence of >30% of the tumour nuclei containing one *mTOR* (*FRAP1*) or *RPS6* signals with the presence of two signals of the correosponding chromosome enumeration probes.

3.2.4 Correlation of mTOR positive chordomas with other markers

Most of the chordomas (12/13) that showed immunoreactivity for p-mTOR were immunoreactive for total mTOR and showed two copies of mTOR locus by FISH, and all showed phosphorylation of 4E-BP1, and expressed eIF-4E. Activation of p70S6K was detected in 11 of the 13 cases reactive for p-mTOR, and 7 of these showed immunoreactivity for p-RPS6. The two cases negative for p70S6K activation were also negative for p-RPS6 (Figure 3.6).

3.2.5 Correlation of mTOR negative chordomas with other markers

Thirty-five of 48 chordomas were negative for p-mTOR; 30 of these could be analysed and 21 (70%) were immunoreactive for total mTOR. Out of these 21 total mTOR-immunoreactive cases, 15 were analysable by FISH and most of these (11 of 15) showed two mTOR alleles while the remaining 4 revealed loss of one allele (Figure 3.6). Seven of the 9 cases negative for total mTOR immunoreactivity as assessed by immunohistochemistry were analysable by FISH and most of these 5 of 7 showed loss of one allele. The remaining two cases showed 2 copies of the gene.

Approximately fifty percent of the p-mTOR negative chordomas showed activation of neither p70S6K nor RPS6. The remaining p-mTOR negative chordomas were positive for p-p70S6K (Figure 3.6).

3.2.6 Correlation of RPS6 negative chordomas with other markers

Thirty-eight of 49 (78%) chordomas were negative for p-RPS6, 35 of which were analysable for other markers. Twenty three of these 35 analysable cases showed no expression of the total protein RPS6. Most of these cases 21 of 23 (91%) showed only one copy of the gene (Figure 3.6). In total 21 cases of 49 (42%) showed loss of one copy by FISH.

In view of *RPS6* being located in the same chromosomal region as *CDKN2A (p16^{INK4})*, a common tumour suppressor gene that is lost frequently in chordomas (Hallor et al., 2008), it was suspected that the allelic loss of *RPS6* correlated with the loss of *CDKN2A* and this was confirmed by showing that CDKN2A was detected by immunohistochemistry in only 5 of 48 chordomas (Table 3.1), and that these 5 cases showed no evidence of allelic loss for *RPS6* with immunoreactivity for total RPS6 protein. In contrast, ten CDKN2A negative cases showed p-RPS6 immunoreactivity with no *RPS6* allelic loss (no data for one case).

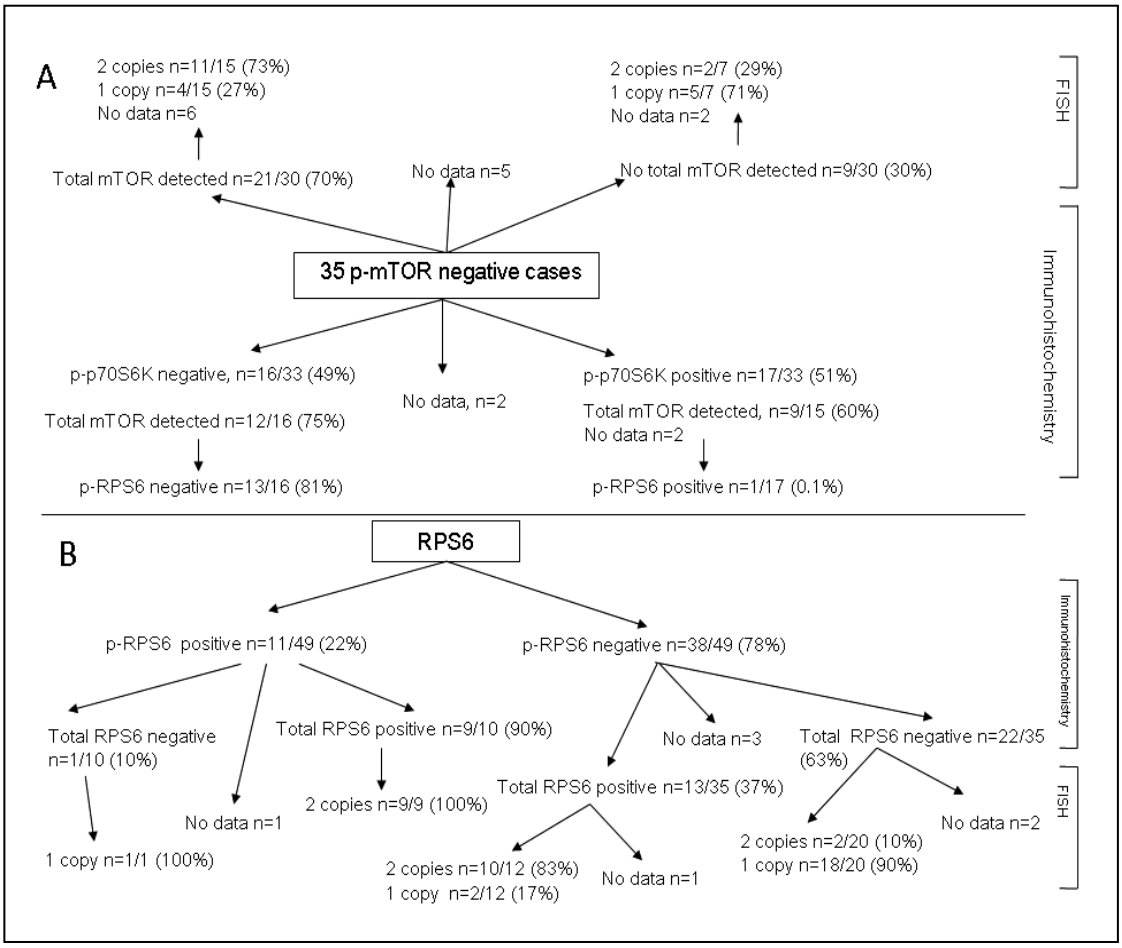

Figure 3.6 A schematic diagram for non skull-based chordomas analysed by immunohistochemistry (total and activated forms) and FISH for mTOR and p70S6K (A), and RPS6 (B).

3.2.7 Methylation study of *RPS6*

To address the issue of *RPS6* loss of expression in the presence of two alleles of *RPS6*, the methylation status of the promoter of *RPS6* was examined in cases negative for RPS6 protein which have two *RPS6* gene alleles. Paired genomic DNA was available from 10 cases, and the results showed that there was no hypermethylation of the *RPS6* promoter region in tumour samples compared to matched normal DNA and to a positive control (Figure 3.7).

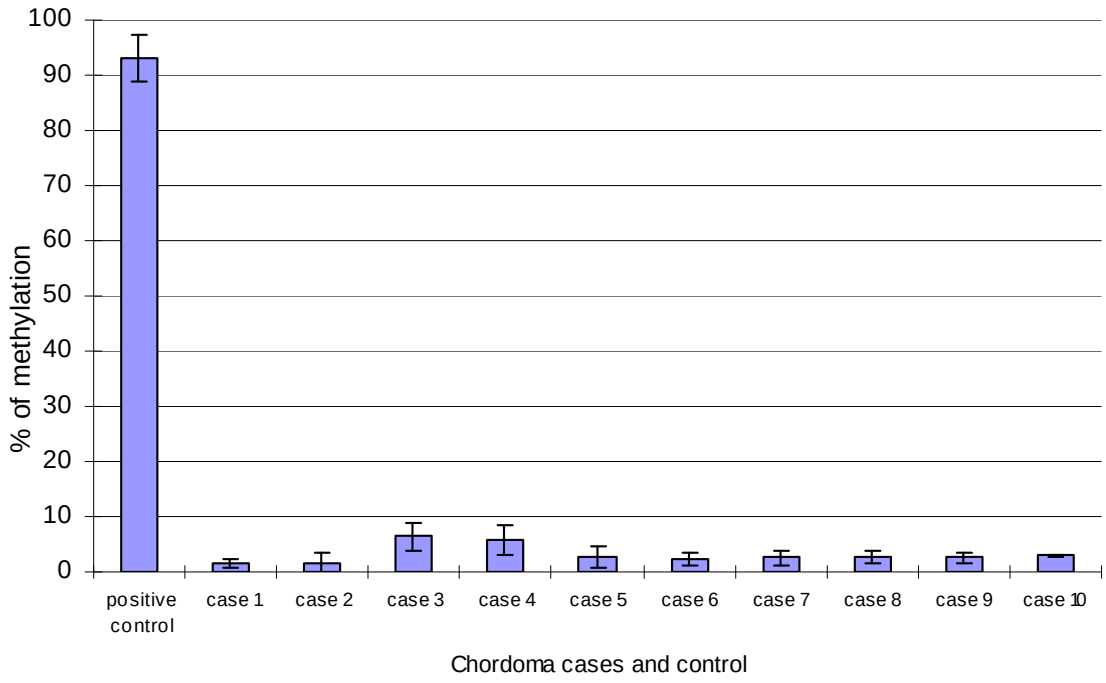

Figure 3.7 Pyro-sequencing of the *RPS6* promoter. There is no hypermethylation in the *RPS6* promoter region in any of the examined 10 chordoma cases. The experiment was performed two times, and each sample was analysed in triplicates. Error bars represent standard deviation from the mean. The positive control is bisulfite-treated mixed human DNA with more than 90% methylation.

3.2.8 Mutational analysis in *PI3KCA* and *Rheb*

Direct sequencing for commonly reported mutations in *PI3KCA* (exons 4, 5, 7, 9 and 20) (Samuels, 2004) and for predicted mutations in *Rheb* codons 15, 16 and 64 which are similar to *KRAS* codons 12,13 and 61 respectively (Li et al, 2004; Yan et al, 2006), failed to reveal mutations in the examined chordomas. All the sequence data is on the attached compact disc.

3.3 DISCUSSION

In this part of the project, 50 sacro-coccygeal, 50 skull-based chordomas and a chordoma-derived cell line U-CH1, showed strong evidence that the PI3K/AKT/TSC/mTOR pathway is activated in at least 65% of the tumours. This figure is based on the numbers of the chordomas that exhibit p-mTOR and/or p-p70S6K.

The phosphorylated form of p70S6K is generally considered as a biomarker for PI3K/AKT/TSC/mTOR pathway activation in preference to p-mTOR to assess the tumour response to mTOR antagonists and to predict which tumours may be responsive to such agents (Boulay et al., 2004; MacKenzie and von Mehren, 2007; Xu et al., 2004). Previous studies found p-mTOR to be expressed in relatively low numbers of tumours such as renal cell carcinoma, and many studies make no reference to tumour p-mTOR expression when assessing the effect of rapamycin and/or its analogues (El-Salem et al., 2007; Gao et al., 2003; Jaeschke et al., 2002; Scheper et al., 2008; Krishnan et al., 2006). Technical difficulties involved in detecting large phosphorylated proteins (mTOR 289 kDa) (Tkaczyk et al., 2002), in addition to the general transient expression of phosphorylated proteins may contribute to the difficulty in detecting p-mTOR (Riemenschneider et al., 2006). Phosphorylation of mTOR may also occur on a variety of residues that have not been tested in this study (Cheng et al., 2004). The difficulties to detect the phosphorylated form of molecules in the

PI3K/AKT/TSC/mTOR by either Western blot analysis or immunohistochemistry suggests that single test may not be enough to assess the activation status of the pathway and can not be used in the clinical settings.

It is considered that the 9 (20%) sacro-coccygeal chordomas that do not express mTOR (total and phosphorylated) protein as assessed by immunohistochemistry (5 of these 9 revealed only one mTOR allele (2 cases with both alleles, 2 cases with no data) are unlikely to respond to mTOR inhibitors. Furthermore, it is also speculated that the 10 cases which express total mTOR but are negative for p-mTOR, p-S6K and p-RPS6 would also be at high risk of not responding to mTOR antagonists. On the basis of this calculation 35% of the examined sacro-coccygeal chordomas would be unlikely to be responsive to mTOR antagonists.

The complete absence of mTOR expression in 9 chordomas raises the question as to how cells survive in the absence of ribosomal biogenesis. One explanation is that the immunohistochemistry for mTOR is not sufficiently sensitive and/or that only very low levels of mTOR are required for assembling the protein complex mTORC1. Alternatively, an mTOR-independent pathway, capable of bringing about ribosomal biogenesis and initiation of translation, may be activated. The report that RAS/MEK/ERK pathway activates RPS6 independently of mTOR *via* p90S6K (RSK1) supports this postulate (Roux et al., 2004).

In view of the importance of ribosomal synthesis in cell growth, the absence of RPS6 protein expression in 49% of chordomas is striking but seems to be robust because the immunohistochemistry data is supported by the finding of *RPS6* allelic loss in 21 of the 23 cases. Furthermore, the allelic loss of *RPS6* located at 9p22.1 correlates with the reported loss of the adjacent gene *CDKN2A* located at 9p21.3 as detected by aCGH study (Hallor et al., 2008). The lack of RPS6 protein expression in some cases, suggests that its role in protein synthesis may be undertaken by other less studied substrates of p70S6K, such as splicing factor SCAR, translation initiation factor eIF-4B, EF-2B kinase and pro-apoptotic protein Bad1 (Harada et al., 2001; Raught et al., 2004; Richardson et al., 2004; Ruvinsky and Meyuhas, 2006).

It is also not clear how loss of *RPS6* contributes to the development of neoplasia although its allelic loss also has been reported in chondrosarcomas, a tumour with similarities to chordomas (Rozeman et al., 2006). Interestingly, a causal relationship between RPS6 phosphorylation and protein synthesis has revealed conflicting results. In addition to reports of activation of this protein resulting in elevated cell growth, there is also evidence of increased global protein synthesis in embryonic fibroblasts derived from RPS6-/- mice compared to wild-type cells (Ruvinsky et al., 2005). Furthermore, germline mutations in the ribosomal protein RPS19, which occur in patients with Blackfan Diamond syndrome, a cancer susceptibility syndrome

associated with haematological malignancies, have already established a role for the loss of ribosomal protein in cancer. Mutations in this syndrome are directly related to loss of ribosomal proteins such as RPS19, RPL5 and RPL11 (Draptchinskaia et al., 1999). The possibility of methylation of *RPS6* promoter has been largely ruled out by the pyrosequencing study of methylation in 10 matched samples of tumours and normal tissue, suggesting that there is another mechanism for *RPS6* loss of expression in these cases.

The results of this study shows loss of expression of PTEN in 16% of chordomas and in U-CH1, the chordoma-derived cell line by immunohistochemistry which suggests that *PTEN*, a well known tumour suppressor gene, may play a role in the pathogenesis of chordomas and could be one of the mechanisms for activation of PI3K/AKT/TSC/mTOR signalling pathway in at least some chordomas. The results here are in agreement with the recent report by Han et al, where 6 out of 10 examined chordomas revealed no expression of PTEN by immunohistochemistry. The limited number of chordomas examined by Han et al., could be responsible for the relatively higher percentage of loss of *PTEN* expression (Han et al., 2009a). *PTEN* mutations are commonly reported in some carcinomas as prostatic, endometrial and hepatocellular carcinomas and in glioblastoms (Li and Sun, 1998; Risinger et al., 1997).

The previously reported loss of heterozygosity in chordomas from 2 individuals with tuberous sclerosis complex syndrome (Lee-Jones et al., 2004) was one of the main reasons that triggered the performance of this study. However, the finding that AKT is activated in over 90% of chordomas argues that the tumour suppressor genes, *TSC2* and *TSC1*, in sporadic chordoma are likely to be 'inactivated' not as a result of loss of heterozygosity but rather by phosphorylation of TSC2 by p-AKT (Inoki et al., 2002). Indeed, if the tumour suppressor genes were inactivated, absence of the TSC2 protein would be expected and this was not the case. Furthermore, the FISH results confirmed the absence of allelic loss in *TSC1* and *TSC2* loci. For these reasons, it was decided not to sequence both genes for the mutations reported in individuals with the tuberous sclerosis complex syndrome. The data suggest that inactivation of TSC1/2 complex in sporadic chordoma is most probably accounted for by phosphorylation of TSC2 by activated AKT and not as a consequence of a mutation or deletion of the *TSC1* and *TSC2* genes. The failure to detect *Rheb* and *PI3KCA* mutations in 23 chordomas provides evidence that these genetic events are unlikely to account for the chordoma tumourigenesis in most cases. Furthermore, the published aCGH data showing that neither *AKT* nor *PI3KCA* loci are amplified in 21 cases, largely excludes activation of *AKT* through genetic events (Hallor et al., 2008).

The findings of this part of the project provide an evidence base for treating selected chordomas with mTOR, AKT inhibitors, and antisense molecules to the attractive cancer target, eIF-4E (Graff et al., 2008)(Graff, 2008). A combination of agents rather than individual drugs is more likely to offer therapeutic success particularly as there is evidence that AKT is activated at Ser^{473} by mTORC2, a rapamycin-insensitive molecule (Sarbassov et al., 2005). This view is supported by the recent report by Stacchiotti et al, where a response was seen using a combination of an inhibitor of mTOR (sirolimus) and imatinib, a receptor tyrosine kinase inhibitor in eight out of nine patients examined (Stacchiotti et al., 2009). The development of a new generation of mTOR blocking agents (TORKinibs) that interrupt the mTORC2 complex is under development and may provide therapeutic benefit over what is currently available (Feldman et al., 2009).

This part of the project provides a rationale for the use of PI3K/AKT/TSC/mTOR pathway inhibitors in the treatment of selected chordomas. However, a detailed study of the effect of inhibitors, using *in vitro* and *in vivo* models is required before embarking clinical trials and introducing these inhibitors as therapeutic options for chordoma management.

4. ANALYSIS OF THE FIBROBLASTIC GROWTH FACTOR RECEPTOR-RAS/RAF/MEK/ERK-ETS2/BRACHYURY SIGNALLING PATHWAY IN CHORDOMAS

4.1 INTRODUCTION

Chordomas are tumours that express brachyury, a molecule involved in notochord development. This, in addition to their morphology, and the anatomical site in which they arise argues in favour of them showing notochordal differentiation (Bjornsson et al., 1993; Mirra et al., 2002; Vujovic et al., 2006). Little is known about the regulation of *brachyury* in mammals although in the ascidian, zebrafish and Xenopus embryos, it is well established that *brachyury* is regulated via fibroblastic growth factor receptors (FGFRs) through RAS/RAF/MEK/ERK/ETS2 pathway (Isaacs et al., 1994; Nakatani et al., 1996; Schulte-Merker and Smith, 1995). The expression of *brachyury* in these models has been shown to require signalling through basic fibroblastic growth factor (bFGF), embryonic fibroblastic growth factor (eFGF) and FGFR1 (Ciruna et al., 1997; Isaacs et al., 1994). ETS2, a transcription factor also has been found to be required for brachyury expression in ascidian (Kawachi et al., 2003).

4.1.1 FGFR-RAS/RAF/MEK/ERK pathway

FGFR-RAS/RAF/MEK/ERK pathway is a signal transduction pathway involved in embryonic development, cellular proliferation and

differentiation and plays a crucial role in bone growth, chondrogenesis and osteogenesis (Liu et al., 2002; Peyssonnaux and Eychene, 2001).

Activation of this pathway is initiated by binding of members of the fibroblastic growth factors (FGFs) to fibroblastic growth factor receptors (FGFRs) with subsequent phosphorylation of a lipid-anchored adaptor protein known as fibroblast growth factor receptor substrate 2 alpha (FRS2α) and binding of the growth factor receptor bound 2 (Grb2) and a guanine nucleotide exchange factor called son of sevenless (SOS) to form Grb2/SOS complex leading to the activation of RAS which in turn activates RAF kinase (Avruch et al., 2001). RAF phosphorylates and activates mitogen-activated protein kinase kinase (MEK) which phosphorylates and activates mitogen-activated protein kinase (MAPK) (Kouhara et al., 1997; Meakin et al., 1999). A schematic diagram representating this pathway is shown in Figure 4.1.

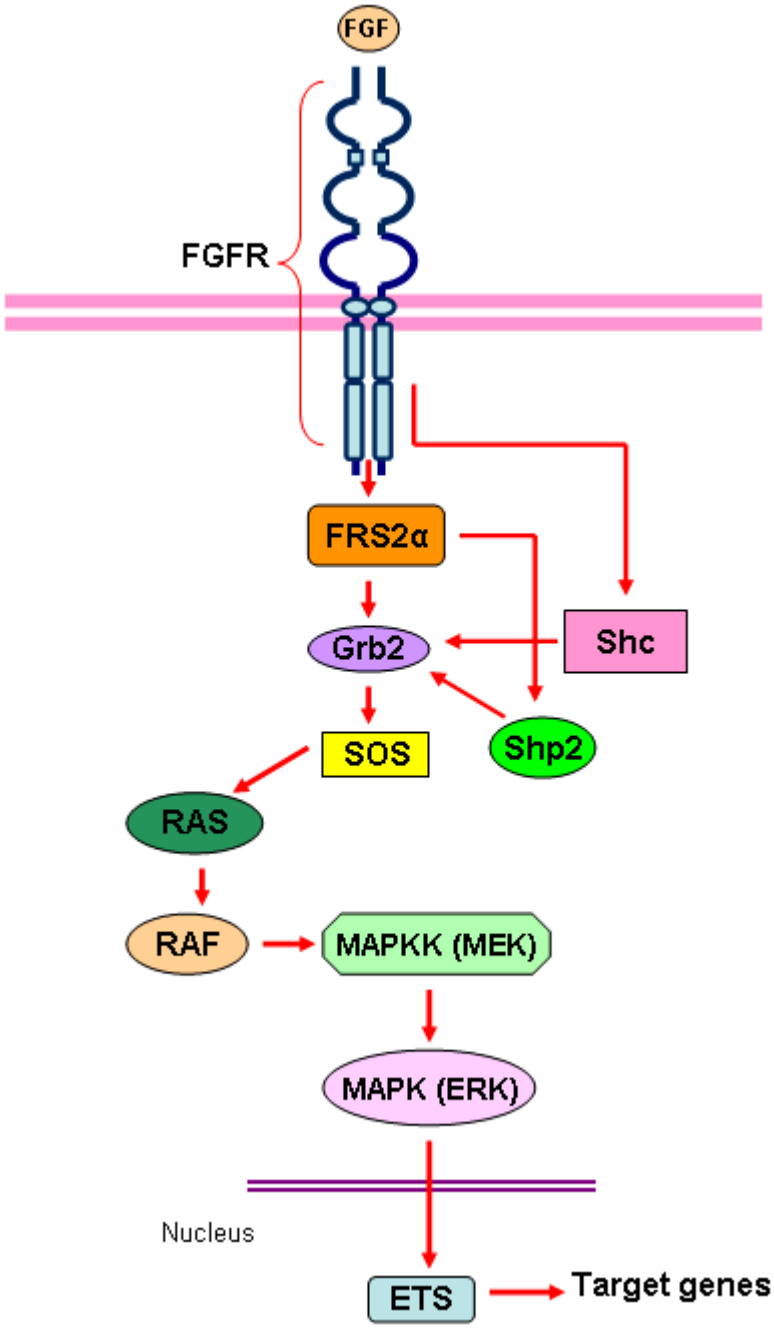

Figure 4.1 A schematic diagram of the signalling through the FGFR/ RAS/RAF/MEK/ERK-ETS2 pathway

4.1.2 Fibroblastic growth factors (FGFs)

Fibroblast growth factors (FGFs) are a family of structurally related growth factors of which 22 members have been identified in humans, 18 of which are associated with FGFRs activation (Ornitz and

Marie, 2002). Basic fibroblastic growth factor has been found to be expressed in chordoma using immunohistochemistry (Deniz et al, 2002).

4.1.3 Fibroblast growth factor receptors (FGFRs)

The fibroblast growth factor receptors are receptor tyrosine kinases which bind to FGFs and include 4 members, FGFR1, FGFR2, FGFR3, and FGFR4. Alternative splicing of *FGFR* transcripts gives a diversity of FGFR isoforms. The FGFRs consist of three extracellular immunoglobulin-type domains (I, II and III), a single trans-membrane helix domain, and an intracellular tyrosine kinase domain (Figure 4.2).

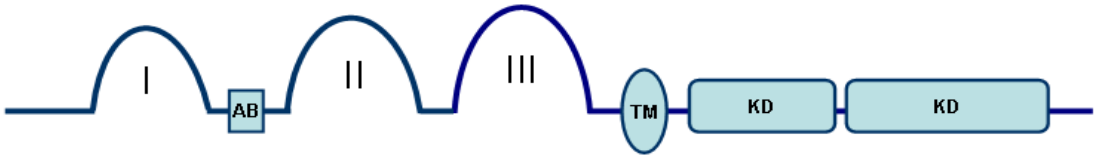

Figure 4.2 Diagrammatic representation of FGFR structure. I, II and III are D1, D2 and D3 immunoglobulin-like domains, AB, Acid box, TM, transmembrane domain, and KD, kinase domain

Several developmental bone diseases and syndromes are caused by gain of function germline mutations in various *FGFR* genes (Coutts and Gallagher, 1995; Ornitz and Marie, 2002). Mutations of different *FGFR* genes are also implicated in many types of cancers such as urothelial, endometrial, prostatic, and cervical carinomas (Dutt et al., 2008; Hernandez et al., 2009; Rosty et al., 2005; van Rhijn et al., 2002), while amplification of these genes has been reported in gastic carcinoma, ovarian carcinoma, squamous cell carcinoma and

rhabdomyosarcoma (Freier et al., 2007; Gorringe et al., 2007; Kunii et al., 2008; Missiaglia et al., 2009). An array comparative genomic hybridisation study of chordomas showed gain in the locus harbouring *FGFR4* (Hallor et al., 2008).

4.1.4 RAS, RAF, MEK and ERK

RAS, the prototypical member of GTPases is activated in close to 30% of all human cancers, most frequently in pancreatic cancer. The activation is caused mainly by point mutations in codons 12, 13 and 61 which all form part of the GTP-binding domain (Bos, 1989)

RAF is a serine/threonine kinase involved in signal transduction and in humans, there are three related genes; *ARAF*, *BRAF* and *CRAF*, of which *BRAF* is the key activator of mitogen activated protein kinase (MAPK) pathway in most tissues and cell types

BRAF is activated mainly through point mutations in about 7% of all human cancers, mainly in malignant melanoma (70%), sporadic colorectal tumours (15%), low grade ovarian serous carcinoma and thyroid papillary carcinoma (Davies et al., 2002)(Davis et al, 2002). The most common activating mutation is the missense thymine to adenine transversion at nucleotide 1799 resulting in valine-to-glutamate substitution at residue 600 (V600E) in exon 15 while the rest of mutations reside in the glycines of the G-loop in exon 11 (Davies et al., 2002; Nucera et al., 2009).

Tandem duplication at the *BRAF* locus (7q34) has been found to produce a novel oncogenic fusion gene incorporating a constitutively active *BRAF* kinase domain and has been demonstrated in 29 of 44 pilocytic astrocytomas (Jones et al., 2008). This is of interest because of the occurrence of pilocytic astrocytomas in two members of two different families with familial chordoma (Dalpra et al., 1999; Kelly et al., 2001; Miozzo et al., 2000). In pilocytic astrocytoma tandem duplication at 7q34 leads to a fusion between *KIAA1549* and *BRAF* (Jones et al., 2008).

Mitogen activated protein kinase kinase/Extracellular signal-regulated kinase kinase (MAPKK/MEK) and mitogen activated protein kinase/Extracellular signal-regulated kinase (MAPK/ERK) are serine/threonine protein kinases that form a part in the FGFR signal transduction pathway (Ahn, 1993). The activation of ERK results in activation of ribosomal S6 kinase (RSK, $p90^{RSK}$) and many transcription factors including c-MYC, CREB (cAMP response element binding) and c-FOS (Jones et al., 1988; Zhao et al., 1995).

4.1.5 *ETS2* and *brachyury*

ETS2 and *brachyury* are genes encoding for transcription factors. *ETS2* provides a link between the FGFR/RAS/RAF/MEK/ERK pathway and the induction of *brachyury* in Xenopus (Xbra) and thus in the development of the posterior mesoderm during early embryonic development (Kawachi et al., 2003; Foulds et al., 2004; Kawachi et al., 2003). *ETS2* is known to be translocated in leukaemia and prostatic

cancer (Sacchi et al., 1986; Yoshimura et al., 1998). Gibas et al, described a translocation at chromosome 21q22, involving either *ERG* or *ETS2*, in two sacral chordomas (Gibas et al., 1992).

Brachyury plays an important role in notochord development, as well as specification of posterior mesodermal elements (Edwards et al., 1996; Showell et al., 2004). *Brachyury* is expressed in chordomas and is largely specific for this disease (Vujovic et al., 2006; Tirabosco et al., 2008). Recently, duplication of *brachyury* has been found to be a major susceptibility factor in development of familial chordomas. The duplication has been found in four out of seven families studied (Yang et al., 2009b).

4.1.6 Hypothesis and Aim

The hypothesis of this work is that genetic alterations within the FGFR-RAS/RAF/MEK/ERK/ETS2-brachyury signalling pathway account for the development of chordoma.

The aim of this part of the project was to investigate the FGFR-RAS/RAF/MEK/ERK/ETS2-brachyury signalling pathway activation status in chordomas and to look for genetic abnormalities in this pathway with particular focus on candidate genes chosen on the evidence provided in the introduction of this chapter.

4.1.7 Objectives

- Study the expression of the four FGFRs in chordomas using immunohistochemistry on TMAs.
- Determination of the activity of the FGFR pathway by assessing the phosphorylation status of FRS2α and ERK1/2 by Western blot analysis of selected cases.
- Screening for previously reported mutations in the four FGFR genes, *KRAS*, and *BRAF* by direct DNA sequencing or dHLPC.
- Mutational analysis of the coding exons and promoter region of *brachyury* by direct DNA sequencing.
- Study the copy number variations and chromosomal rearrangements in *ETS2*, *brachyury* and *FGFR4* loci using FISH.
- Analysis of *BRAF* locus for the presence of tandem duplication using RT-PCR.

4.2 RESULTS

4.2.1 Expression of the four FGFR proteins in chordoma

Analysis of the expression of FGFRs on the non skull-based and skull-based chordomas in a tissue microarray revealed that 47 of 50 (94%) of the former and 45 of 49 (91.8%) of the latter showed immunoreactivity for at least one of the FGFRs (Table 4.1, Figure 4.3). In 39 non skull-based chordomas and 31 skull-based chordomas, more than one receptor was detected by immunohistochemistry and in 17 non skull-based chordomas and 13 skull-based chordomas the tumour cells were immunoreactive for all 4 receptors. In the majority of cases, more than 50% (+++) of the tumour cells showed immunoreactivity. The details of immunohistochemistry results are shown in Table 4.1.

Table 4.1 FGFR 1, 2, 3 and 4 immunoreactivity in chordomas

	Immunohistochemistry score	FGFR1	FGFR2	FGFR3	FGFR4
Non skull based-chordomas	3 +++	17	8	13	4
	++	0	0	0	1
	+	0	1	0	0
	2 +++	8	9	10	11
	++	1	1	1	2
	+	0	0	0	0
	1 +++	1	17	15	15
	++	0	1	0	2
	+	1	3	0	0
	0	22	10	11	15
	Total number of positive cases (%)	28/50 (56 %)	40/50 (80 %)	39/50 (78 %)	35/50 (70 %)
Skull-based chordomas	3 +++	11	4	13	5
	++	2	3	3	3
	+	0	1	1	0
	2 +++	7	3	7	9
	++	1	0	5	2
	+	1	0	1	1
	1 +++	2	17	8	15
	++	0	2	0	3
	+	0	1	2	0
	0	25	18	9	11
	Total number of positive cases (%)	24/49 (49%)	31/49 (63%)	40/49 (82%)	38/49 (77%)

The scoring system employed was as follows: Negative immunoreactivity (0). Positive immunoreactivity includes the following subgroups; (1) 'weak', the intensity of the staining is less than the positive control, (2) 'moderate' the intensity of the staining is as strong as the positive control, and (3) 'strong' the intensity of the staining is stronger than the positive control. In addition, +, ++ and +++ indicates that less than 5%, between 6% and 49%, and more than 50% respectively of the lesional cells were immunoreactive.

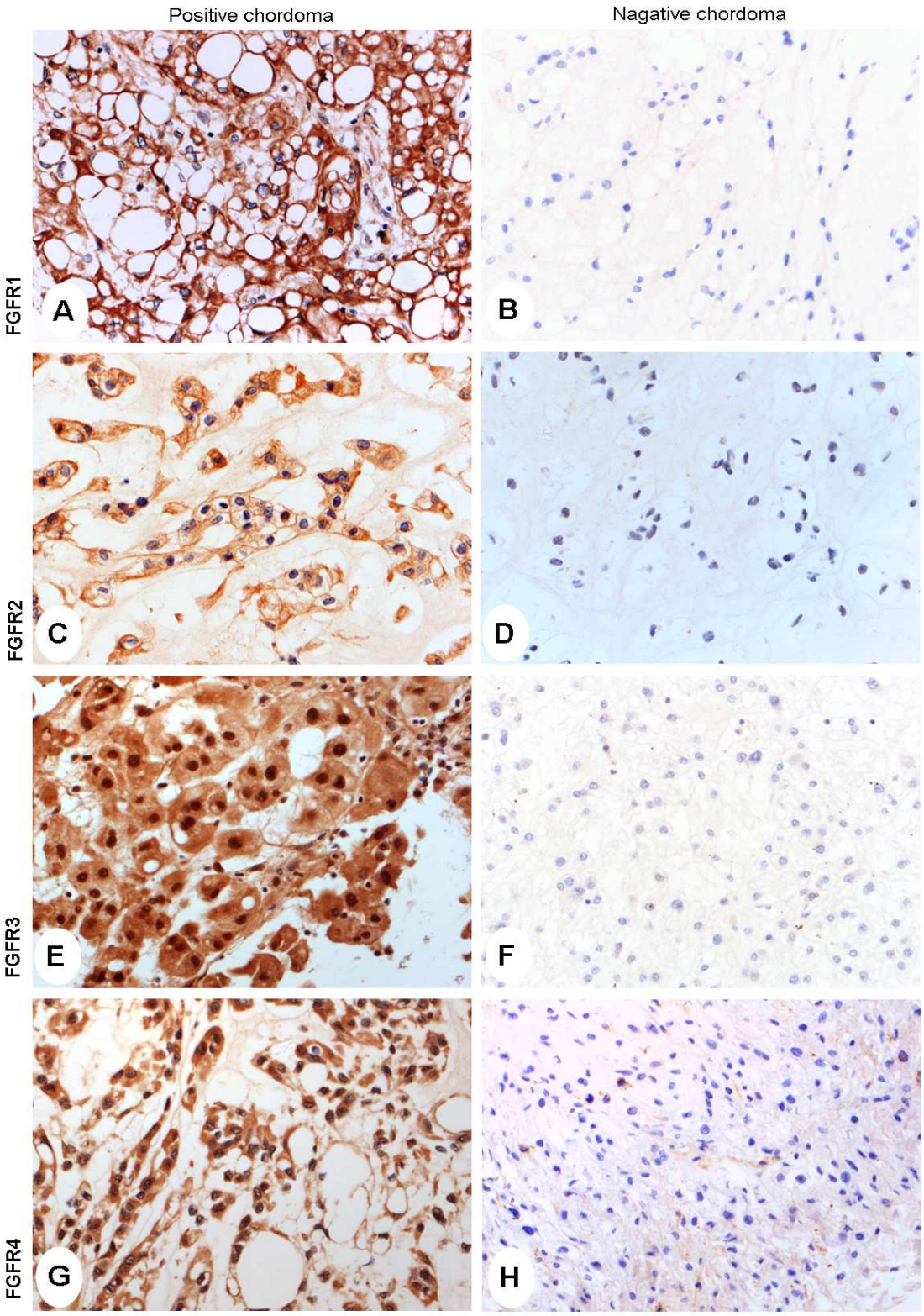

Figure 4.3 Immunohistochemistry results of FGFRs on chordoma TMAs Representative transmitted light photomicrographs of chordomas on TMA. The photomicrographs on the left panel represent positive immunoreactivity and the right panel includes representative chordomas that were not immunoreactive for each of the four FGFRs. Magnification 200X.

4.2.2 Western blot analysis for the active phosphorylated forms of FRS2α and ERK

To test whether the expressed FGFRs, detected by immunohistochemistry, were involved in signalling in chordomas, Western blotting was performed using antibodies against p-FRS2α (Tyr^{196}) and p-ERK1/2 (Thr^{202}/Tyr^{204}). FRS2α is a docking adaptor signalling protein that links FGFRs to the RAS/RAF/MEK/ERK signalling pathway and ERK1/2 represents a critical point in the pathway activation. Western blot analysis showed phosphorylation of FRS2α and ERK1/2 in 6 chordomas that were also reactive by immunohistochemistry for at least one of the FGFRs (Figure 4.4). Two chordomas with no reactivity by immunohistochemistry for any of the four FGFRs, were also negative by Western blot analysis for p-FRS2α, although these were positive for p-ERK1/2 (Figure 4.4).

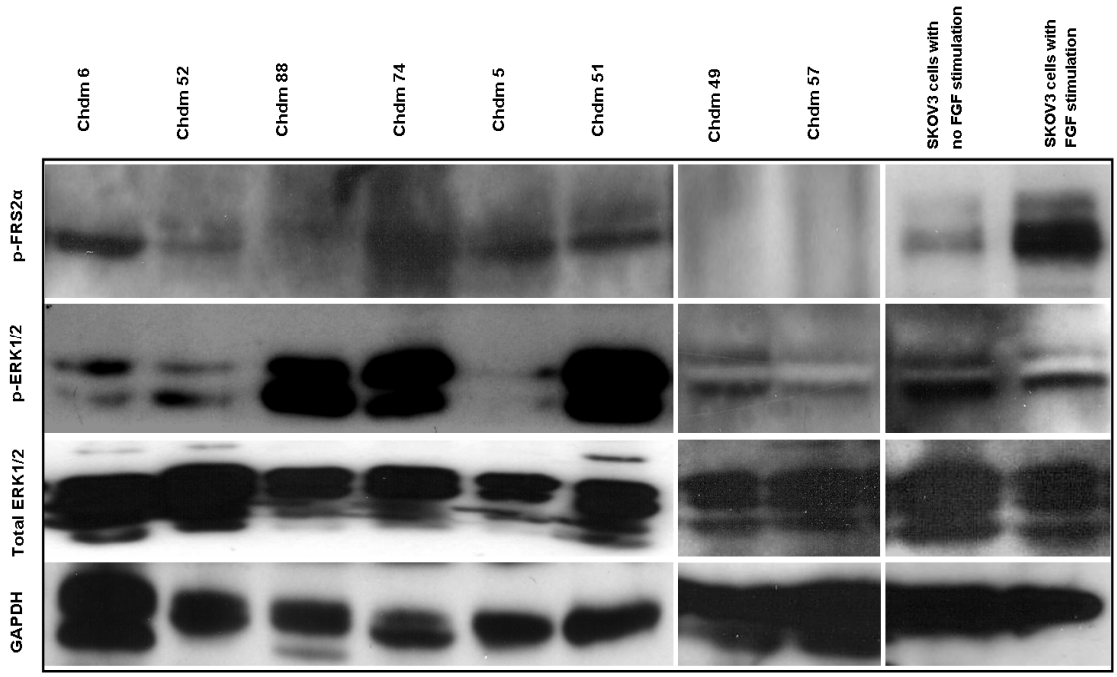

Figure 4.4 Western blotting analysis for p-FRS2α (Tyr^{196}) and p-ERK1/2 (Thr^{202}/Tyr^{204}) on 8 selected chordomas (CHD). The left hand panel with six chordomas were positive by immunohistochemistry for at least one of the FGFRs and showed a band corresponding to p-FRS2α and p-ERK1/2 by Western blotting. The middle panel of two chordomas, found to be negative for any FGFR by immunohistochemistry, did not display a band for p-FRS2α. Nonetheless, a band was detected by Western blotting for p-ERK1/2 in these 2 cases. In the right hand panel, SKOV3 cell line, non stimulated and stimulated with basic FGF, was used as a positive control. The membranes were stripped and re-probed with total ERK1/2 and anti-GAPDH antibody to assure even loading of proteins in each lane.

4.2.3 Mutational analysis of the four *FGFR* genes by direct sequencing for the previously reported mutations

In view of *FGFRs* being known to be involved in the regulation of *brachyury*, and the knowledge of mutations in these genes being implicated in tumourigenesis, direct sequencing of those exons in which activating germline and somatic mutations have been reported previously was performed: these included *FGFR1* (exons 3, 6, 11, 12,

14), *FGFR2* (exons 5, 7, 11, 12), *FGFR3* (exons 2, 4, 5, 6, 8, 9, 15) and *FGFR4* (exons 7, 9, 16). Sequencing failed to reveal any mutations in the 23 chordomas analysed. All the sequencing data are on the attached compact disc.

4.2.4 FISH investigation for *brachyury* copy number gain

FISH analysis of the *brachyury* locus in chordomas showed three patterns; amplification where the ratio between *brachyury* specific signals and chromosome 6 chromosome enumeration probe signals (CEP6) was more than 2, aneuploidy where there were more than two copies of both *brachyury* and CEP6 specific probes giving rise to a ratio of less than 2, and imbalance where two copies of CEP6 and more than two copies of *brachyury* locus were present (Table 4.2, Figure 4.5).

Table 4.2 Brachyury FISH results for skull-based and non skull-based chordomas

	Skull-based chordomas	Non skull-based chordomas	Total (%)
Amplification	1/47	2/48	3/95 (3.2)
Aneuploidy +6	23/47	17/48	40/95 (42)
Imbalance (rearrangement)	5/47	4/48	9/95 (9.5)
Disomic (normal pattern)	18/47	25/48	43/95 (45.3)

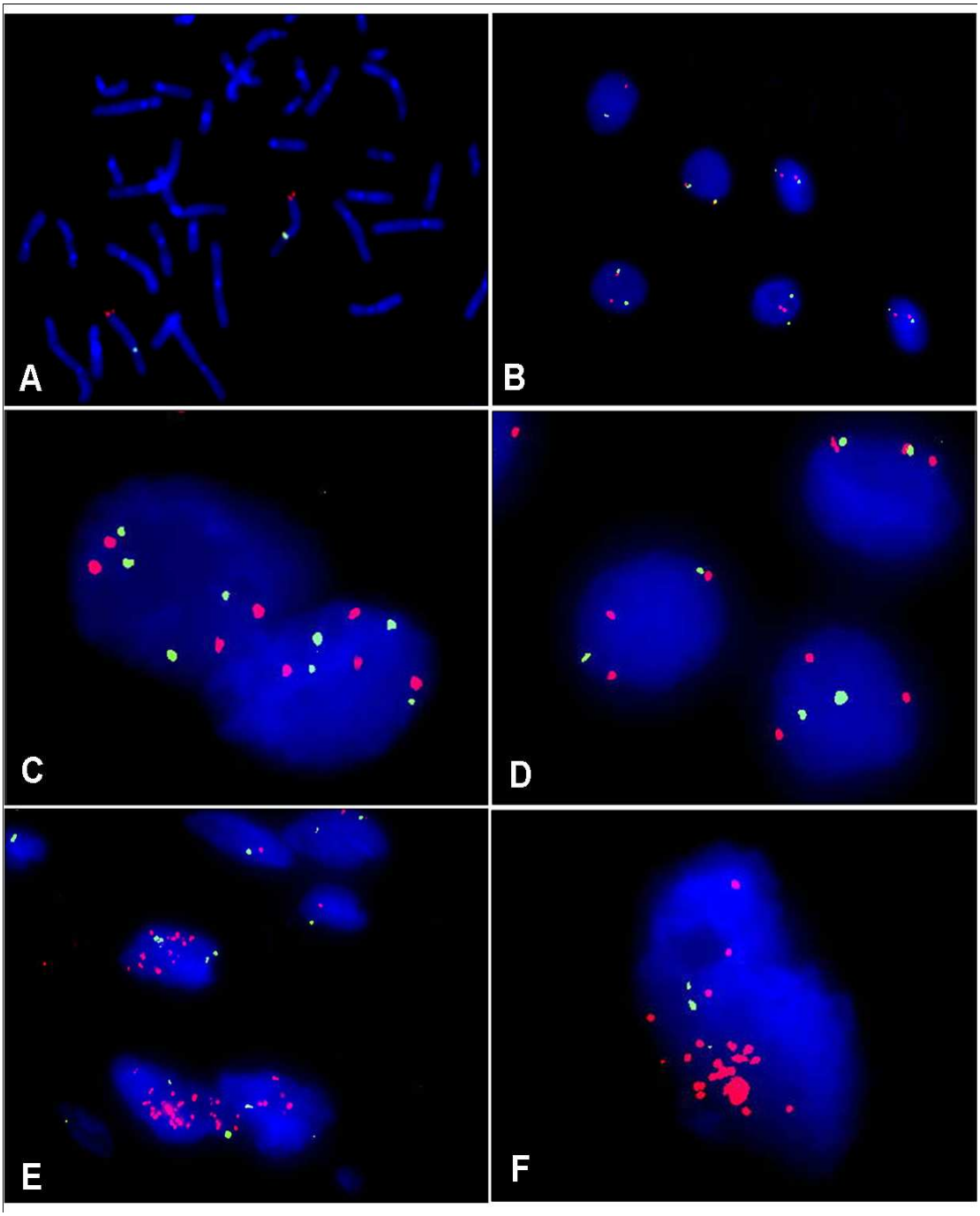

Figure 4.5 FISH analysis of *brachyury* gene on chordoma TMAs. Photomicrographs of interphase FISH showing a metaphase spread to validate the probe localisation (A), chordoma with a normal disomic pattern (2 *brachyury* and 2 CEP6 signals (B), aneuploidy (equal numbers of more than 2 signals for both *brachyury* and CEP6 (C), *brachyury* imbalance (more than 2 *brachyury* signals and 2 CEP6 with a ratio less than 2 (D), examples of *brachyury* amplification (more than 2 *brachyury* signals with a ration of *brachury*:CEP6 more than 2 (E and F). The red signals represent *brachyury* and the green signals represent CEP6 probes.

4.2.5 FISH screening for *ETS2* and *FGFR4* amplification, and *ETS2* and *ERG* gene rearrangement

The FISH analysis for *ETS2* amplification showed a normal pattern (disomy) with two green signals of chromosome 21 markers and two *ETS2* red signals. The 'in-house generated' break-apart probe designed to detect *ETS2* and *ERG* rearrangement showed no rearrangement at the loci of these genes as assessed in 27 informative cases (Figure 4.6 A). FISH was performed on the non skull-based TMA which included 50 chordomas to determine if there was amplification of *FGFR4* because an aCGH report previously showed that the locus harbouring *FGFR4* was found to be gained in more than 5 out of 21 cases (Hallor et al, 2008). However, FISH failed to reveal any amplification of *FGFR4* in the informative 43 cases (Figure 4.6 B).

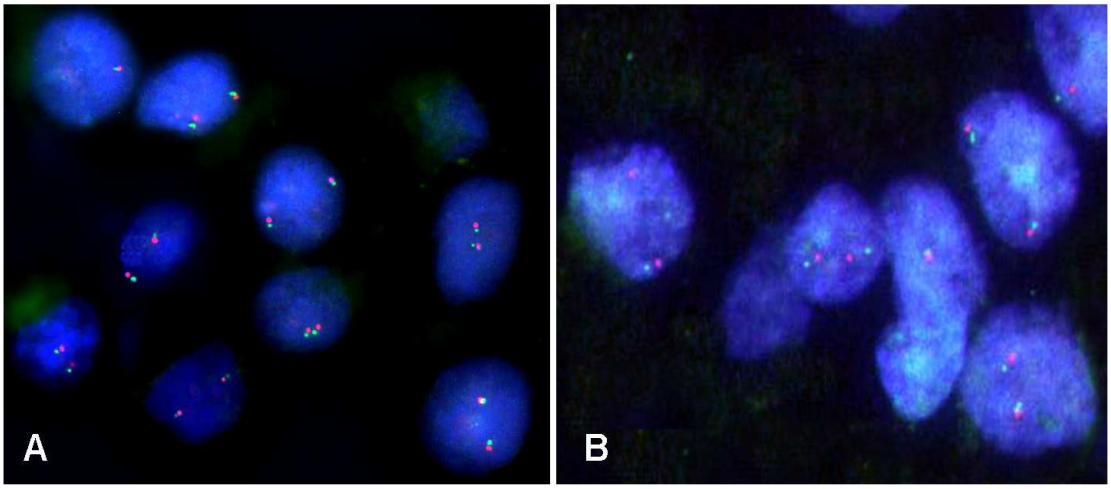

Figure 4.6 FISH results of ETS2/ERG rearrangement and FGFR4 amplification. (A) normal pattern 2 red and 2 green signals for *ETS2*/*ERG* breakapart probes (red and green). (B) normal disomic pattern with no amplification using *FGFR4* probe (red) compared to chromosome (5) enumeration probe (green).

4.2.6 Mutational analysis of *brachyury* using direct sequencing of promoter region and coding exons

Direct DNA sequencing of *brachyury* coding exons (2-9) and the promoter region showed that expression of *brachyury* is not accounted for by somatic mutations in 23 analysed chordomas. The sequencing data are on the attached compact disc.

4.2.7 Screening of *KRAS* and *BRAF* for the commonly reported mutations using denaturing high-performance liquid chromatography (dHLP)

As *KRAS* and *BRAF* are upstream molecules in the signalling pathway of *ETS2* and *brachyury*. Denaturing high-performance liquid chromatography (dHPLC) for detection of the common mutations in *KRAS* (exons 2 and 3; codons 12, 13, and 61) and *BRAF* (exons 11 and 15) in 23 chordomas failed to reveal any abnormalities.

4.2.8 Screening for tandem duplication at *BRAF* locus

A reverse transcription polymerase chain reaction (RT-PCR) with specific primers to detect the oncogenic fusion gene formed by tandem duplication at the locus of *BRAF* between *BRAF* and *KIAA1549* failed to detect the tandem duplication in any of the examined 23 cases (Figure 4.7).

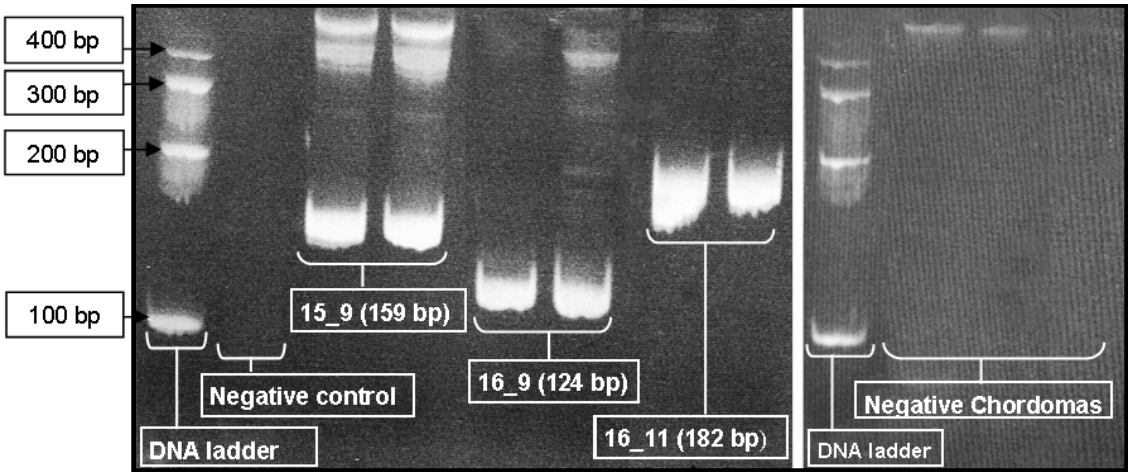

Figure 4.7 RT-PCR analysis for tandem duplication at *BRAF* locus and the resulting transcripts of the oncogenic fusion gene. The left hand panel shows negative control (no template control) and positive controls for the three possible fusion transcripts between *KIAA1549* exon 15 and *BRAF* exon 9 (15_9, 159 bp), *KIAA1549* exon 16 and *BRAF* exon 9 (16_9, 124 bp) and *KIAA1549* exon 16 and *BRAF* exon 11 (16_11, 182 bp). The right hand panel shows examples of chordoma cases lacking the presence of the oncogenic gene transcripts. The primer pairs used were described in chapter 2. Positive controls were cDNA with known fusion transcripts and negative control was formed of the PCR reaction mix without DNA template. The RT-PCR products were electrophoresed on 8% acrylamide gels.

4.3 DISCUSSION

The effects of FGFR signalling on tumours are numerous and include increased proliferation, resistance to apoptosis, enhanced motility and invasiveness, increased angiogenesis, metastasis, and resistance to chemotherapy and radiotherapy, all of which can result in tumour progression. As *brachyury* is known to be regulated by FGFR1 and FGFR3 in development (Hoffmann et al., 2002; Yamaguchi et al., 2004b), it was hypothesized that the FGFR signalling pathway is involved in the development of this tumour. Therefore interruption of the FGF signalling system is an attractive therapy, particularly since such therapies can affect tumour cells directly in addition to tumour angiogenesis (Reis-Filho et al., 2006; Dutt et al., 2008; Knowles, 2008). Of importance is that some agents are currently already in clinical trials (Trudel et al., 2006).

The results of this study demonstrate for the first time that FGFR1 and FGFR3 are expressed in 52.5% and 80% of chordomas respectively. It is also of particular interest that over 90% of chordomas express at least one of the four FGFRs. The study also shows that the expression of FGFRs is accompanied by activation of the downstream pathway as evidenced by Western blot analysis for p-FRS2α (Tyr^{196}) and p-ERK1/2 (Thr^{202}/Tyr^{204}). All 6 chordomas, which are immunoreactive for at least one of the FGFRs, were also reactive for the phosphorylated forms of both FRS2α and ERK1/2 by Western blot

analysis while 2 chordomas that were negative for all FGFRs by immunohistochemistry, were also negative for p-FRS2α although they showed p-ERK1/2 by Western blot analysis. This suggests that in the minority of cases, activation of the RAS/RAF/MEK/ERK signalling pathway in chordomas is not dependent only on FGFR signalling and therefore can be mediated by alternative receptors. As it is known that chordomas also express several other tyrosine kinase receptors including c-MET, PDGFR β, and KIT, EGFR, HER2, and TrKA which also activate the RAS/RAF/MEK/ERK pathway, these should be considered candidates for the regulation of brachyury (Weinberger et al., 2005; Tamborini et al., 2006; Park et al., 2007; Fasig et al., 2008; Naka et al., 2008).

Signalling through FGFRs can activate multiple signal transduction pathways that are known to be implicated in tumourigenesis, and include RAS/RAF/MEK/ERK, phospholipase C gamma (PLCγ), phosphatidyl inositol 3 kinase (PI3K), and signal transducers and activators of transcription (STAT) pathways (Chen et al., 2001; Chen et al., 2005; Hart et al., 2000). However, this part of the project focused on the RAS/RAF/MEK/ERK pathway as it represents the main downstream pathway in FGFR downstream signalling and analysis of the pathways was considered beyond the scope of this study.

The occurrence of *FGFR* mutations is well documented in the literature, and these are associated with both developmental syndromes and neoplasia. Gain of function germline mutations in *FGFR2* results in craniosynostosis syndromes, mutations in *FGFR1* are a cause of Pfeiffer syndrome, a rare craniosynostosis syndrome and *FGFR3* mutations are the cause of chondrodysplasia syndromes (Muenke et al., 1994; Muenke et al., 1997; Hart et al., 2000; Chen et al., 2001; Chen et al., 2005; Ornitz and Marie, 2002). The mutations implicated in neoplasia occur in urothelial, endometrial, gastric and prostatic cancers (Mehta et al., 2000; Shin et al., 2000; Kwabi-Addo et al., 2004; Forbes et al., 2006; Elbauomy et al., 2007; Pollock et al., 2007; Tomlinson et al., 2007; Kunii et al., 2008) and many of these mutations reported in neoplasia are identical to germ-line mutations known to cause developmental syndromes.

Apart from *FGFR1* being known to be involved in *brachyury* expression, *FGFR genes* were therefore considered strong candidates for the role of mutation-bearing genes that would be causative in the development/progression of chordomas. Nevertheless, despite the immunoreactivity of the majority of chordomas for FGFRs the results in this section showed absence of the previously reported mutations in the 23 analysed chordomas by direct sequencing. Based on the previously reported amplification of some *FGFR* genes in cancer like gastric cancer and rhabdomyosarcoma (Freier et al., 2007; Gorringe et al., 2007; Kunii

et al., 2008; Missiaglia et al., 2009) and on the reported allelic gain at the chromosomal area 5q35.2 which harbours *FGFR4* using array comparative genomic hybridisation (Hallor et al., 2008), it was worth investigating whether *FGFR4* is amplified that there is gain in chordomas but FISH failed to detect increased copy number of this gene in 43 chordomas. Amplification of the other *FGFR* genes was not studied because there is no evidence in the literature of allelic gain in the loci of these genes in chordomas.

The absence of activating mutations in *KRAS* and *BRAF* together with the absence of tandem duplication at the *BRAF* locus in 23 cases examined suggests that genetic abnormalities involving these genes are unlikely to be the direct cause of FGFR pathway activation in chordomas. However, some of the less common *BRAF* mutations not screened in this study may explain activation of this signalling pathway.

ETS2 has previously been implicated in pathogenesis of chordoma by karyotyping (Gibas et al., 1992) and it is a particularly interesting candidate because this gene lies upstream of *brachyury* and is known to be involved in its regulation and it is also phosphorylated through activation of the RAS/RAF/MEK/ERK pathway (Kawachi et al., 2003; Matsumoto et al., 2007). Furthermore, rearrangements involving *ETS2* have been detected in other neoplasms including acute megakaryocytic leukaemia, acute non-lymphoblastic leukaemia and prostatic cancer (Sacchi et al., 1986; Hsu et al., 2004; Mehra et al.,

2007). However, the ‘in-house’ breakapart BAC probe failed to reveal a rearrangement in this gene in 23 chordomas. Furthermore, *ETS2* was not amplified as assessed by FISH. Therefore it appears that re-arrangement and amplification in this gene are unlikely to represent a common tumourigenic event in chordomas.

A recent report has shown that duplication of *brachyury* gene increased the susceptibility to development of familial chordoma in four out of 7 studied families with familial chordomas (Yang et al., 2009b). The failure to detect point mutations in any of the coding regions, splice junctions and promoter region of this gene in 23 chordomas implies that the expression of *brachyury* mRNA and protein is likely to be driven by other mechanisms or by events in upstream molecules. Looking for mutations in *brachyury* was considered a reasonable approach despite no *brachyury* mutations being reported in tumours to date because tumourigenic mutations have been found in related T-box genes, *TBX2* and *TBX3* which has been reported to occur in pancreatic and breast cancers (Sinclair et al., 2002; Fan et al., 2004). Furthermore, although *brachyury* amplification was detected only in 3 cases, a finding which corresponds to the results of the array comparative genomic hybridisation data previously published which showed gain of the *brachyury* locus in 6 out of 21 cases (Hallor et al., 2008), it is considered that amplification of this gene is also unlikely to account for the driving force in the growth and development of this tumour in view of the small

percentage of identified cases. However, the possibility remains that the aneuploidy and chromosomal imbalance affecting *brachyury* in 40% of chordomas examined could be a mechanism implicating *brachyury* in chordoma pathogenesis.

Recently, Santarius et al., have developed a weight-of-evidence based classification to facilitate the identification of the key cancer genes. They classified the genes implicated in cancer into 4 classes (I-IV) based on the type of supportive data. According to their criteria, *brachyury* can be categorised as a class II gene with 3 points providing supporting evidence for its involvement in development of cancer (Santarius et al., 2010). The criteria implicating *brachyury* in chordoma development include (1) the reported duplication of *brachyury* gene in familial chordomas (Yang et al., 2009b); (2) the expression and activation of other genes in the same pathway such as FGFRs and FRS2α as detailed in the previous chapter; and (3) the biological effect resulting from targeting *brachyury* with shRNA in the chordoma cell line U-CH1 (see chapter 5).

This part of the project has provided evidence for the activity of FGFR-RAS/RAF/MEK/ERK signalling in chordomas and has demonstrated that oncogenic events involving *FGFRS, KRAS, BRAF, and ETS2* are rare events in these neoplasms. Although *brachyury* amplification was detected in a small percentage of chordomas, the detected aneuoploidy of chromosome 6 and the genetic imbalance at

brachyury locus 6q27 may be a possible mechanism by which *brachyury* is involved in the progression and pathogenesis of the sporadic form of this disease. Further investigations using a greater number of chordoma cases, and other genome-wide platforms are required to validate these findings.

5. KNOCKDOWN OF *BRACHYURY* GENE IN CHORDOMA-DERIVED CELL LINE U-CH1 USING LENTIVIRUS-DELIVERED SHORT HAIRPIN RNA (shRNA)

5.1 INTRODUCTION

The century old concept that chordomas show notochordal differentiation was firmly established after the gene expression microarray finding that *brachyury*, a gene essential for notochordal development, is specifically highly expressed in chordomas (Henderson et al., 2005). *Brachyury* expression has proved to be a specific and sensitive marker for chordomas whereas a wide range of other tumours and normal tissues failed to express *brachyury* (Tirabosco et al., 2008; Vujovic et al., 2006). The exceptions include hemangioblastomas (Glasker et al., 2006) and normal spermatogenic tissue (Tirabosco et al., 2008). In a very recent report, *brachyury* duplication has been detected in members from four out of seven families with familial chordoma and it was concluded that *brachyury* duplication increased the susceptibility to develop chordoma (Yang et al., 2009b). *Brachyury* expression by all chordomas and the duplication of *brachyury* in familial chordomas strongly suggest a pathogenic role for *brachyury* in this tumour type. One of the most effective experimental approaches to elucidate the function of a gene is to knockdown its transcripts using short hairpin RNA (shRNA) *in vitro* or *in vivo* models and look for the consequences (Abbas-Terki et al., 2002). The models available to study chordomas are very sparse and the only *in vitro* model currently is the

U-CH1 cell line developed in Ulm University, Germany from a recurrent sacral chordoma (Scheil et al., 2001).

5.1.1 *Brachyury*

Brachyury or *T* gene is the prototypic member of the T-box family of transcription factors and these are characterized by a conserved, sequence-specific DNA-binding domain known as T box (Muller and Herrmann, 1997; Scheil et al., 2001). *Brachyury* was originally identified in 1927 as a tail length mutation in mouse. Hermann et al., cloned the mouse *brachyury* gene in 1990, while Edwards et al, (1996) cloned the human *T* (*brachyury*) and described gene structure and the mRNA sequence (Edwards et al., 1996; Herrmann et al., 1990). The function of *brachyury* is conserved in all vertebrates and it is crucial for notochord development and differentiation and to direct the differentiation of the posterior mesoderm (Cunliffe and Smith, 1992). The open reading frame of human *brachyury* encodes a protein of 435 amino acids that shares 91% identity overall with mouse *brachyury*. In humans, the *brachyury* gene has been mapped to the region 6q27 (Edwards et al., 1996).

5.1.2 Short hairpin RNA (shRNA)

RNA interference (RNAi) is a phenomenon in which double-stranded RNA (dsRNA) suppresses expression of a target protein by stimulating the specific degradation of the target mRNA (Hannon et al, 2002). Short hairpin RNA (shRNA) is one of the methods of RNAi, and

is composed of a sequence of RNA that makes a tight hairpin turn and can be used to silence gene expression. shRNA uses a vector to be introduced into cells and this ensures its continuous stable expression so that it can be cleaved by the cellular machinery into small interfering RNA (siRNA). The resulting siRNA is then bound to the RNA-inducing silencing complex (RISC) and targets mRNA which leads to its degradation and silencing of the expression of the gene of choice (Paul et al., 2002; Sui et al., 2002; Cao et al, 2005). Lentivirus delivery of shRNA has been shown to be an efficient tool for delivery of shRNA into the cells (Abbas-Terki et al., 2002a).

5.1.3 Hypothesis and Aims

This part of the project was based on the hypothesis that *brachyury*, being highly expressed in all chordomas and showing copy number gain in a subset of familial chordomas, plays a central role in the formation of chordomas. It was also hypothesized that targeting the expression of this gene would affect the development and/or progression of the tumour. If this were the case, the genes which are transcriptionally regulated by brachyury could be identified and this would be a means of identifying therapeutic targets. The aim was to establish knockdown of the *brachyury* gene in the chordoma-derived cell line U-CH1 and to study the cellular and morphological changes induced by this knockdown.

5.1.4 Objectives

- Preparation of the lentivirus (pGIPZ) containing short hairpins targeting brachyury mRNA along with the use of appropriate controls including an empty vector and non-silencing scrambled shRNA.
- Infection of the U-CH1 cells with lentivirus particles containing the shRNA constructs.
- Confirm the knockdown of *brachyury* at the mRNA level using qRT-PCR and at the protein level by Western blot analysis.
- Study the morphologic changes induced in the U-CH1 cells resulting from *brachyury* knockdown.

5.2. RESULTS

5.2.1 Silencing of *brachyury* gene in U-CH1 cell line

The silencing of *brachyury* gene in U-CH1 cell line was achieved using two different clones directed against two different regions of the gene. The first clone, V2LHS_153725, was directed against the region encompassing the junction between exons 4 and 5, and the second clone, V2LHS_153729, was directed against the region located at exon 9, at the 3'UTR, of the gene (Figure 5.1).

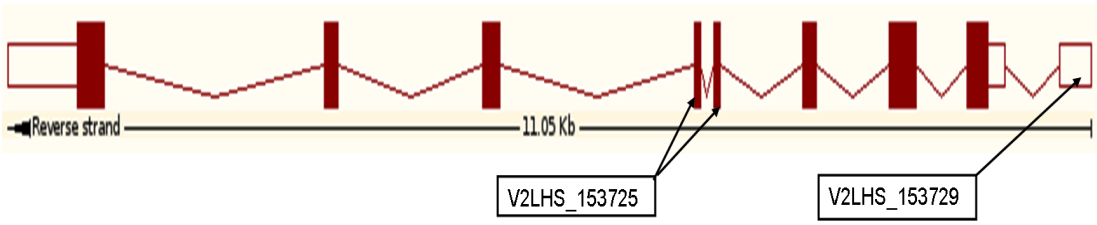

Figure 5.1 Structure of brachyury gene with mapping of the two shRNA constructs used for its silencing. The boxes represent exons and the lines represent introns. V2LHS_153725 is directed at the end of exon 4 and the start of exon 5. V2LHS_153729 targets 3'UTR of exon 9.

5.2.1.1 RT-PCR for *brachyury* expression

qRT-PCR was performed on mRNA obtained from the U-CH1 cell line and this revealed 97% silencing with construct V2LHS_153725 and 98.4% silencing with construct V2LHS_153729 (Figure 5.2).

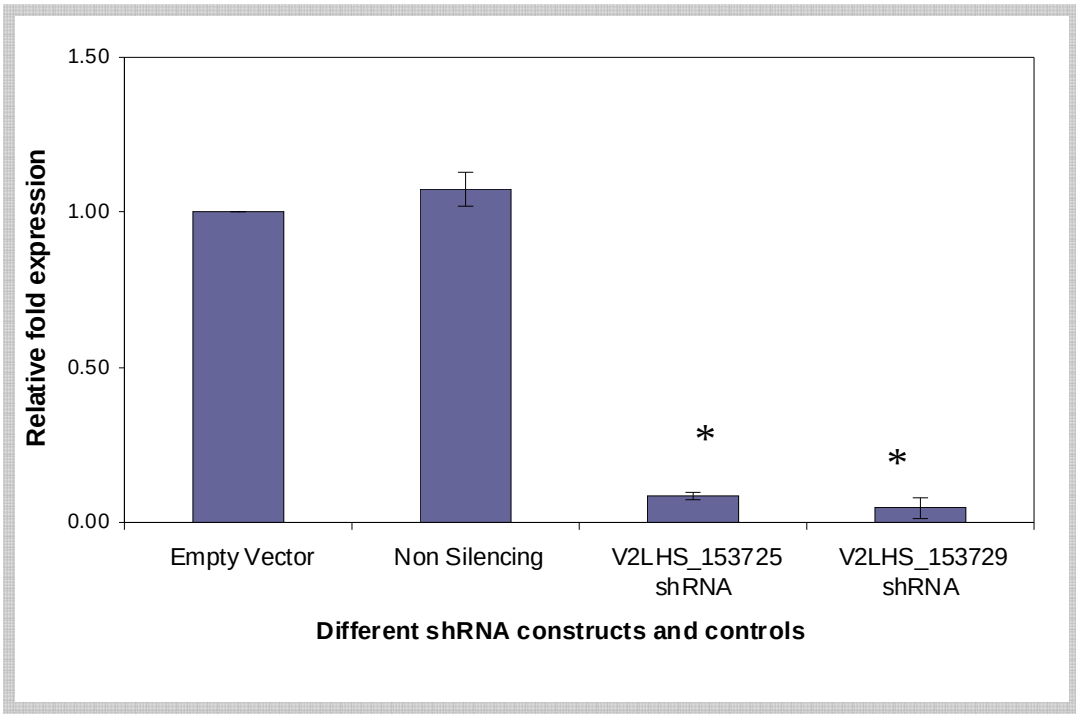

Figure 5.2 Results of RT-qPCR for *brachyury* knockdown in the U-CH1 cell line. The knockdown was performed using two different constructs (V2LHS_153725, V2LHS_153729) and an empty vector and non-silencing construct as controls. *Brachyury* expression is corrected to the PGK expression as a reference gene and normalised to the empty vector. The figure represents results from three different experiments, each performed in triplicate. Error bars represent standard deviation.

* $p < 0.05$ in comparison to non silencing vector control.

5.2.1.2 Western blot analysis of protein expression

Western blotting showed almost complete absence of brachyury protein in U-CH1-derived lysates, the cells of which had been targeted by the two shRNAs (V2LHS_153725, V2LHS_153729). Empty vector and non-sliencing constructs were used as controls (Figure 5.3 A&B).

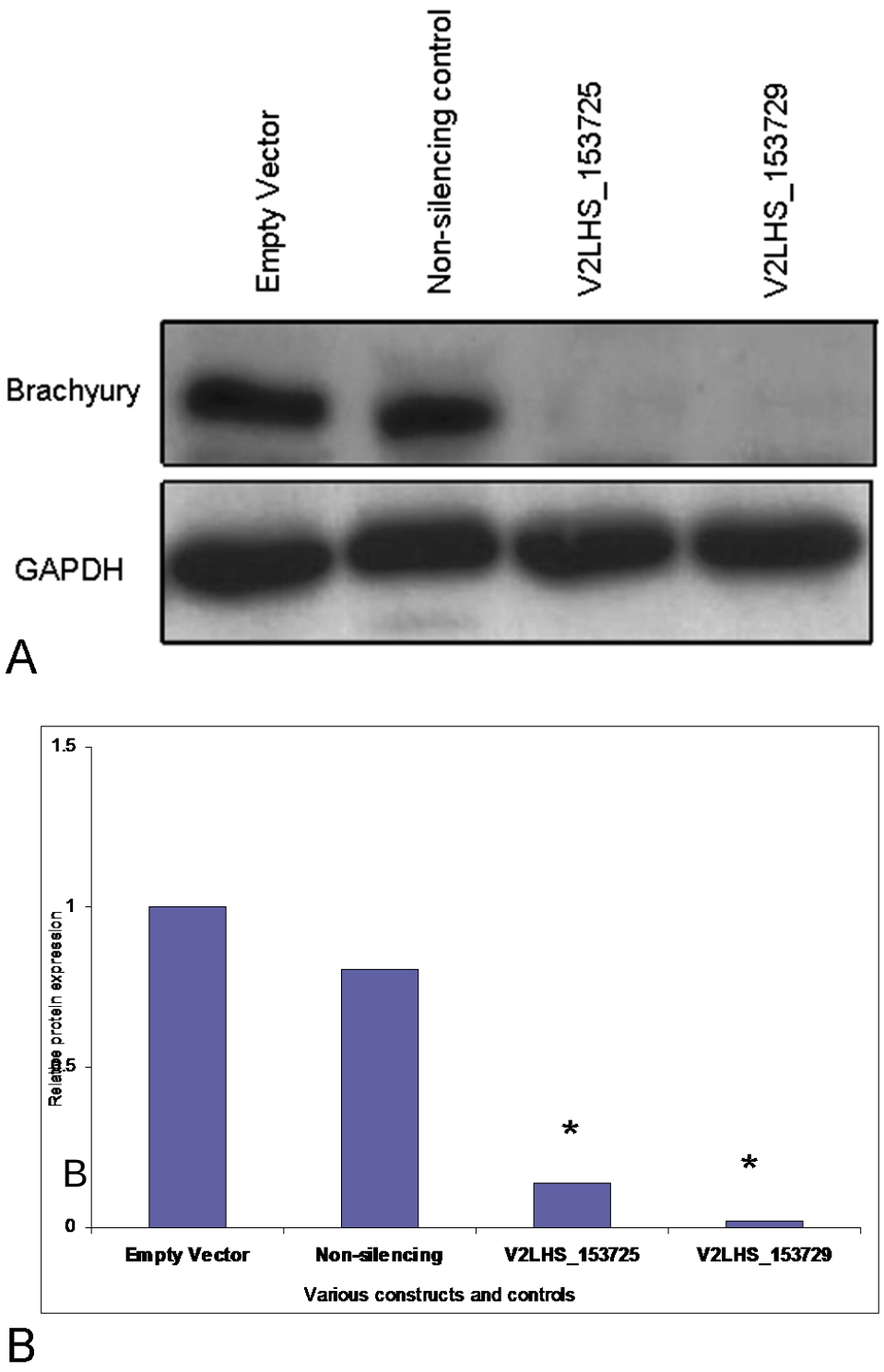

Figure 5.3 Western blot analysis of protein lysates from U-CH1 cells infected with lentiviral shRNA targeting *brachyury*. (A) represents the Western blot images and (B) represents densitometric measurement of relative *brachyury* expression corrected to GAPDH as a loading control and to the expression of the cells infected with empty vector construct. * $p<0.05$

5.2.2 Cellular changes in U-CH1 cells resulting from *brachyury* knockdown

5.2.2.1 Morphological changes

The U-CH1 cells with *brachyury* knocked down showed striking cellular morphological changes in the form of abnormal shapes, spindling, flattening and extensive branching (Figure 5.4). These changes started to appear on the fourth day after infection, were progressive in nature, and were associated with growth arrest as shown by the very low cell density in the 'knockdown' cells compared to the two controls after two weeks from the onset of infection. These changes are reminiscent of replicative senescence noticed in human tissue cultures after a large number of passages (Hayflick and Moorhead, 1961). Staining for detection of SA-β Gal. confirmed the presence of premature senescence; 65% of the cells in which *brachyury* had been knocked down stained for senescence-associated beta galactosidase while less than 2% of the cells in the control cultures showed positive staining (Figure 5.5).

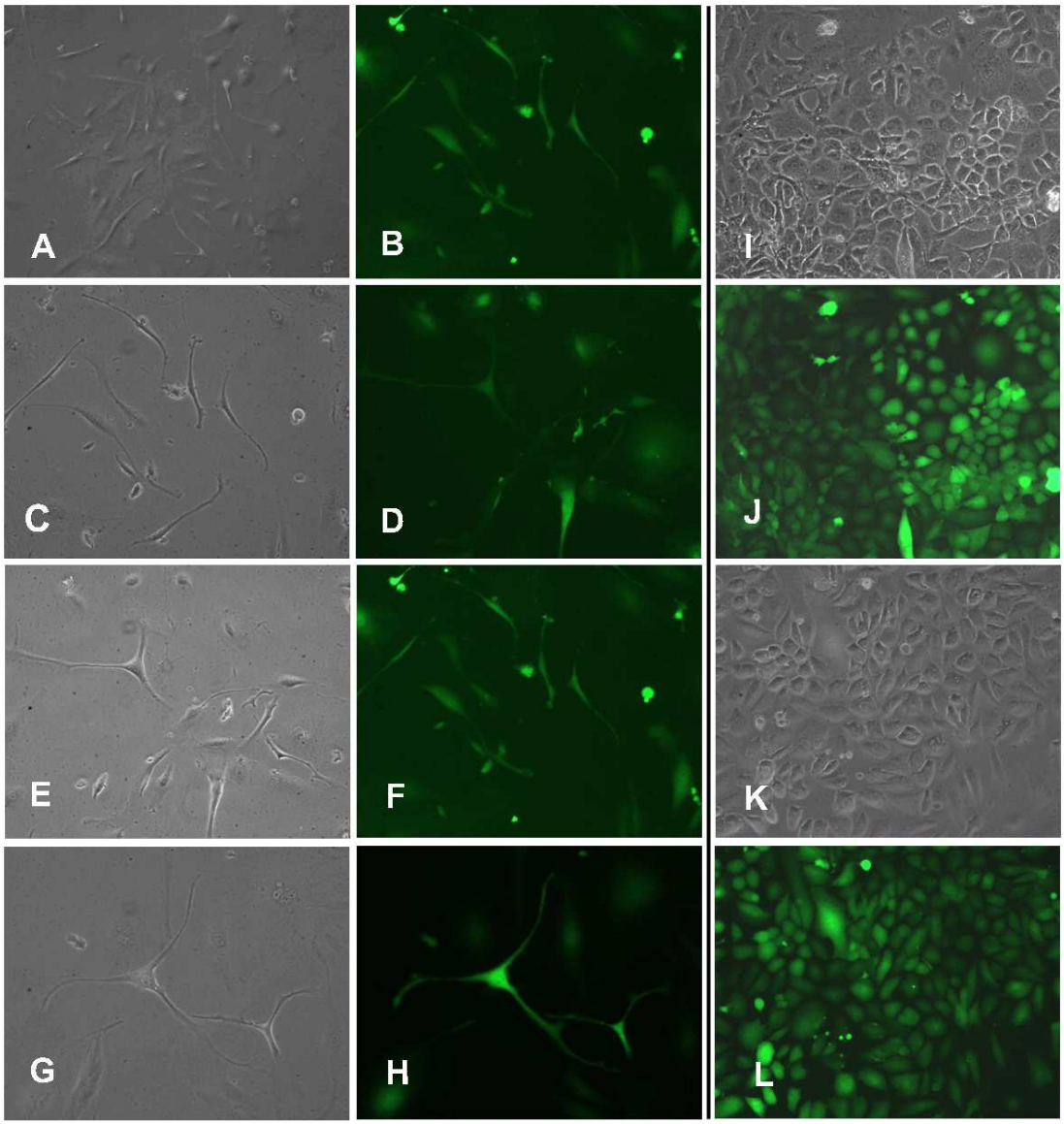

Figure 5.4 Morphological changes in U-CH1 cells as a result of *brachyury* silencing. Representative microscopic photomicrographs (phase contrast and fluorescent with GFP) of U-CH1 cells infected with lentivirus-delivered shRNA targeting *brachyury* showing various morphologic abnormalities ofcells in which *brachyury* was knocked down (A-H) compared to the control cultures (empty vector (I and J) and non-silencing/scrambled shRNA (K and L). The magnification in all images is 100X.

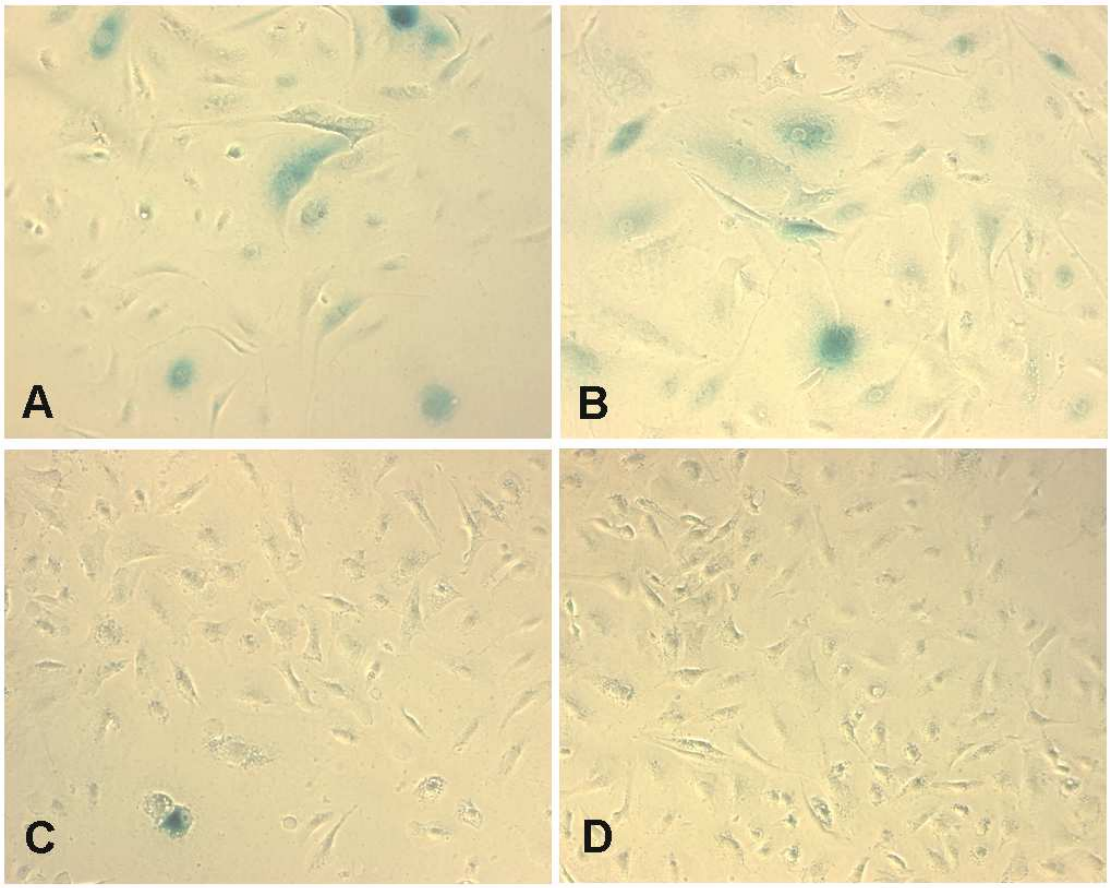

Figure 5.5 Senescence-associated beta galactosidase staining of U-CH1 cells with silencing of *brachyury*. Transmitted light microscopic images showing positive staining of a large proportion (65%) of the cells in which *brachyury* was silenced (A&B) compared to (2%) of the cells with empty vector (C) and a non-silencing construct (D). Hundred cells from different fields were counted per slide. Magnification: 100X.

5.2.3 Silencing of *brachyury* gene in 293T cells and HeLa cells

In order to exclude the possibility that the introduction of the lentivirus shRNA targeting *brachyury* was toxic to the cells, a knockdown of *brachyury* gene was performed in two different cell lines, 293T and HeLa. In both these cell lines no change in the morphology or proliferative capacity was induced when compared to the controls (Figure 5.6).

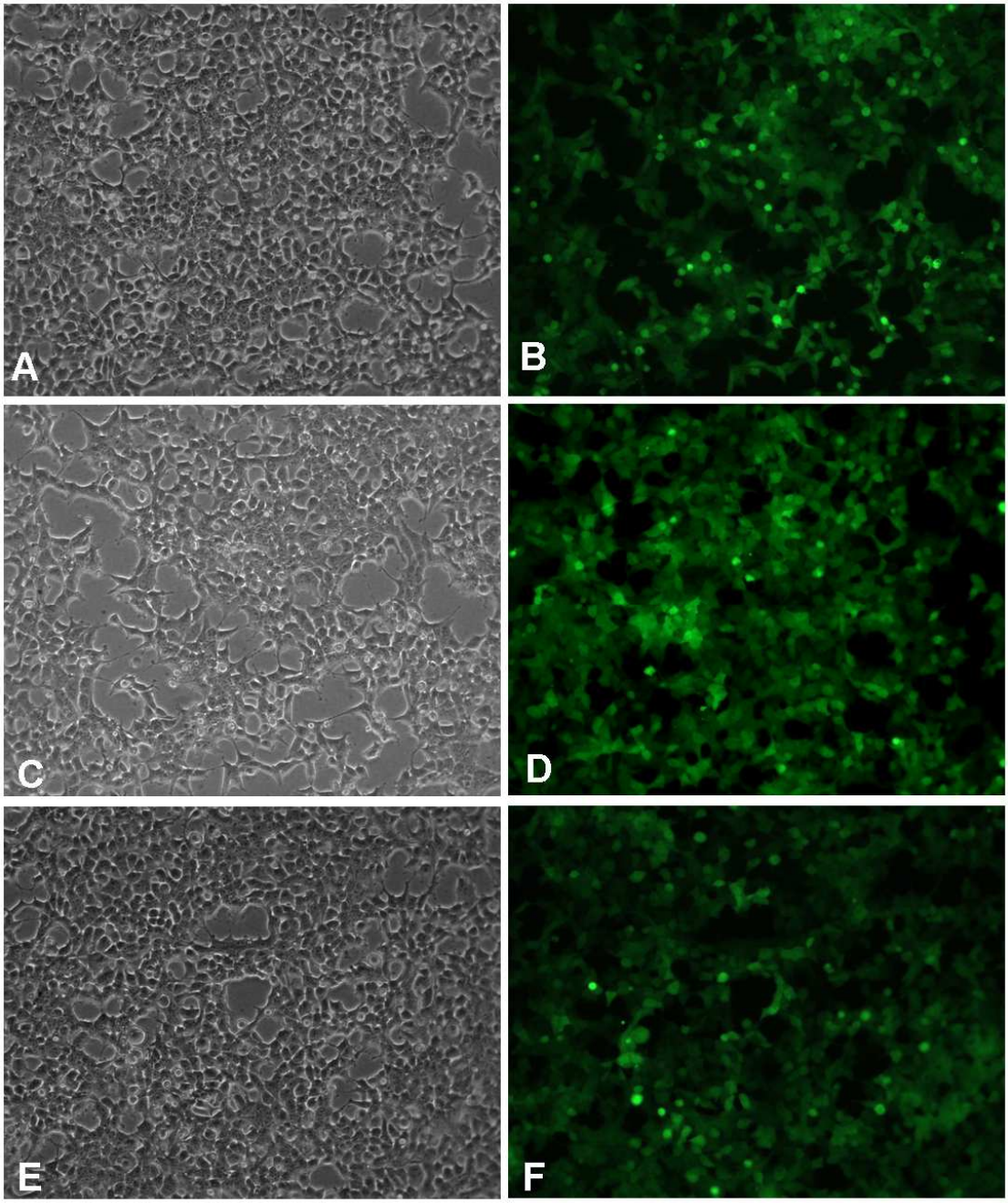

Figure 5.6 Morphology of 293T cells with *brachyury* knocked down. 293T cells were infected with lentivirus-delivered shRNA targeting *brachyury*. These cells showed no morphologic abnormalities when *brachyury* was silenced (A & B) compared to empty vector (C and D) and non-silencing scramble shRNA (E and F). For each construct, a transmitted light microscopic and a fluorescent microscopic images with GFP are shown. Magnififcation: 100X

5.3 DISCUSSION

The work presented in this chapter has proved that *brachyury* can be efficiently silenced using lentiviral-delivered shRNA which targets *brachyury* mRNA. Gene knockdown is a very useful tool to study *brachyury* function; however, the major concern in a knockdown experiment is the specificity of the shRNA to the gene of interest. There are several ways to show this specificity as proposed by Cullen, (2006). The work presented here has shown multiple ways to prove the shRNA specificity towards *brachyury*. First, the knockdown was successful using two different silencing constructs; second, the knockdown using both constructs was confirmed on both mRNA and protein levels by qRT-PCR and Western blot analysis respectively; third, the use of non-silencing scrambled shRNA and an empty vector did not induce alteration in the level of *brachyury* expression (mRNA or protein); fourth, the same constructs had no effect on two different cell lines 293T and HeLa that did not express brachyury. Another means of proving the specificity of shRNA knockdown is to perform a rescue experiment. This involves introducing *brachyury* cDNA into the cells in which *brachyury* has been knocked down and inducing a reversal of the cellular and functional changes caused by knocking down *brachyury*. However, this has not been done due to limitation of time and is planned for future work. This knockdown model can now be used in a variety of ways to study the role of *brachyury* in the pathogenesis of chordoma.

The cellular effects of knocking down *brachyury* can lead to a better understanding of its biological functions. Very little is known about the effect of *brachyury* over-expression in cells and tissues. However, two members of the T-box family, *TBX2* and *TBX3,* have been shown to affect cellular proliferation and to be involved in the development of cancer (Jacobs et al., 2000). The evidence includes their ability to repress the promoter of $p14^{ARF}$, which affects the *TP53* tumour suppressor pathway (Jacobs et al., 2000; Brummelkamp et al., 2002; Yarosh et al., 2008) In addition, *TBX2* maps to 17q23 locus, which is frequently altered in ovarian and breast carcinomas (Campbell et al., 1995; Barlund et al., 2000). *TBX2* has been also found to be amplified in some breast-cancer cell lines, and in a subset of breast carcinomas, and melanomas, and to be highly expressed in more than 60% of pancreatic carcinomas (Sinclair et al., 2002; Sinclair et al., 2003; Chen et al., 2008).

$p19^{ARF}$ in mice or $p14^{ARF}$ in humans is the alternative transcript encoded by the $INK4a^{ARF}$ locus which also encodes $p16^{INK4a}$. Jacobs et al, showed that *TBX2* represses *CDKN2A* and that affected cells were able to bypass the senescence-like growth arrest induced by $p14^{ARF}$ (Hallor et al., 2008; Naka et al., 2005). Generally, the T box genes are transcriptional activators. However, *TBX2* and *TBX3* are exceptions as they repress the promoter of $p14^{ARF}$ and it is interesting to postulate that brachyury behaves in a similar way, and thereby regulates the cell cycle

or senescence checkpoint. The argument for this is that the morphological changes in the U-CH1 cells resulting from *brachyury* knockdown are very similar to the premature senescence noticed when *TBX2* is knocked down in breast carcinoma cell lines (Jacobs et al., 2000). This raises the possibility that *brachyury* may account for the proliferation of chordoma cells in a mechanism similar to *TBX2* regulation of the promoter area of *CDK2NA*. The positive staining for SA β-gal. supports this concept. It is also noteworthy that $p16^{INK4}$, a *CDKN2A* protein product, is down-regulated in chordomas and that the locus of *CDK2NA* is lost in more than 70% of cases in an array comparative genomic hybridisation study performed on 21 chordomas (Naka et al., 2005; Hallor et al., 2008).

6. ANALYSIS OF EPIDERMAL GROWTH FACTOR RECEPTOR IN CHORDOMAS

6.1 INTRODUCTION

The main treatment option of chordomas is surgical removal with or without post-operative radiotherapy. Radical excision is rarely achieved due to the infiltrative nature of the tumour and the presence of vital structures in the tumour vicinity of both the skull base and in the sacro-coccygeal area (Agrawal et al., 2006; Smolders et al., 2003).

Radiotherapy alone is the second line of treatment if surgery is not feasible in which is usually the case for the skull-based chordomas. Proton beam radiotherapy and the new modalities of photon radiotherapy such as intensity modulated radiation therapy (IMRT), stereotactic radiosurgery and carbon-ion radiotherapy offer a better control of the disease (Gabriele et al., 2003; Muthukumar et al., 1998; Schulz-Ertner et al., 2003a; Schulz-Ertner et al., 2003b). Chordomas are regarded as chemo-resistant and so there is no role for chemotherapy (Fleming et al., 1993)

Hence, molecular therapeutic strategies have become relevant for the management of chordomas. Some agents are already in clinical trials, such as imatinib mesylate, targeting the patelet-derived growth factor receptor β (PDGFR-β). In a preliminary study, Casali et al., treated six patients with imatinib mesylate (Casali et al., 2004). Subsequently a more organized phase II clinical trial has been started

using this drug in 55 patients with advanced chordomas and showed a clinical benefit rate (complete response plus partial response plus stable disease for at least 6 months) of 73% and 38% of patients were free from progression at 1 year (Stacchiotti et al., 2007; Ferraresi et al., 2010). Epidermal growth factor receptor (EGFR) represents another possible target as EGFR inhibitors are already in clinical use for some tumours such as non small cell lung cancer (NSCLC), colorectal and head and neck cancers (Dassonville et al., 2007; Roberts et al., 2002).

There are a few reports showing expression of EGFR in chordomas by immunohistochemistry (Tamayama et al., 1990; Weinberger et al., 2005; Fasig et al., 2008; Ptaszynski et al., 2009) and one study showed over expression of the EGFR ligand transforming growth factor-alpha (TGF-α) in 10 out of 14 chordomas (Deniz et al., 2002). Three reports showed chordoma response to the inhibitors of epidermal growth factor receptor (EGFR) in three patients with advanced chordoma, suggesting EGFR as a possible therapeutic target (Hof et al., 2006; Linden et al., 2009; Singhal et al., 2009).

6.1.1 Epidermal Growth Factor Receptor (EGFR)

Epidermal growth factor receptor is a member of HER (Human Epidermal Growth Factor Receptor) family of tyrosine kinase receptors. The family is composed of four closely related receptors including EGFR (HER1, ErbB1), HER2/neu (ErbB2), HER3 (ErbB3), and HER4 (ErbB4) (Ullrich et al., 1984; Ullrich and Schlessinger, 1990).

EGFR is a large (170kDa) trans-membrane glycoprotein with an extra-cellular ligand-binding domain and a cytoplasmic domain with intrinsic tyrosine kinase activity and multiple autophosphorylation sites (Yarden and Ullrich, 1988). Five autophosphorylation sites have been identified: three major (Tyr^{1068}, Tyr^{1148}, and Tyr^{1173}) and two minor (Tyr^{992} and Tyr^{1086}) sites (Biscardi et al, 1999). The Tyr^{1173} site represents the most important phosphorylation site in vivo (Lombardo et al., 1995; Chattopadhyay et al., 1999). In addition, EGFR activation results in phosphorylation of Tyr^{845} required for mitogenic responses and Tyr^{1101} that represents a binding site for SH2 domain-containing proteins including the adaptor protein Grb-2 (Mass, 2004).

Epidermal growth factor (EGF) and TGF-α represent the two major ligands of EGFR and their binding leads to receptor autophosphorylation and subsequent activation of downstream signal transduction pathways, mainly the RAS/RAF/MEK/ERK and the PI3K/AKT pathways (Figure 6.1). This activation leads to cell proliferation, tumour growth, metastasis, angiogenesis and inhibition of apoptosis (Schlessinger, 2000; Yarden and Sliwkowski, 2001; Buettner et al., 2002; Song et al., 2002)

The mechanisms of increased EGFR signalling include high expression levels as a consequence of mutations (point mutations, increased gene dosage), heterodimerization with other members of the

HER family such as HER2, and increased ligand expression (Arteaga, 2002) .

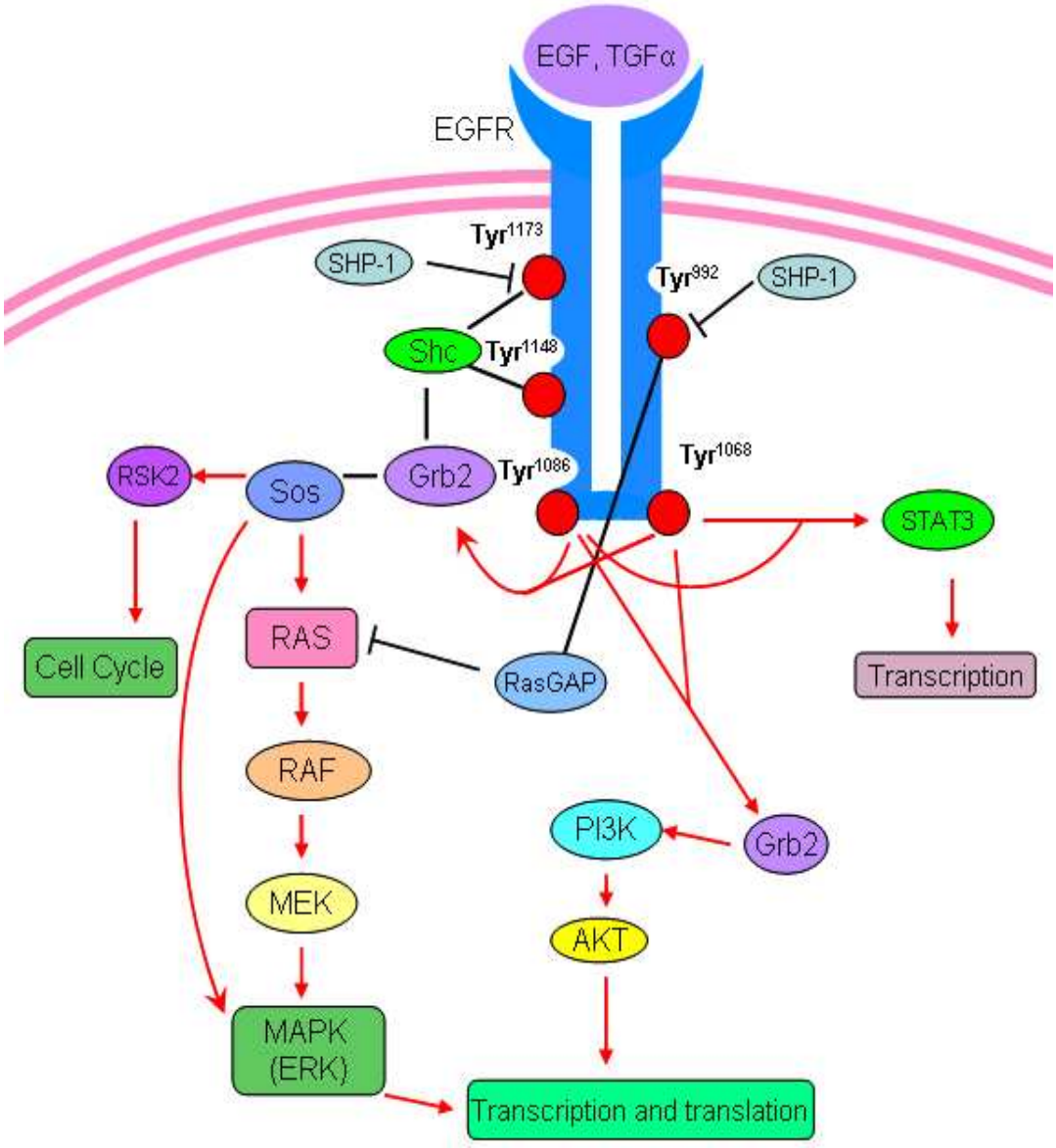

Figure 6.1 Schematic diagram of the EGFR signalling pathway

6.1.2 EGFR Inhibitors

The inhibitors of EGFR in clinical trials are classified mainly into two classes, anti-EGFR monoclonal antibodies such as mAb 528 and C225 (cetuximab) and small-molecule tyrosine kinase inhibitors (TKIs) as gefitinib (ZD1839), erlotinib (OSI-774) and tyrphostin (AG1478) (Ellis

et al, 2006). The tyrphostin (AG1478) is a reversible, highly potent and selective inhibitor of EGFR tyrosine kinase activity (Ellis et al., 2006; Zhang and Chang, 2008; Zhu et al., 2001).

Monoclonal antibodies against EGFR competitively inhibit ligand binding and thereby prevent receptor activation while TKIs competitively bind to the ATP binding domain of EGFR to inhibit autophosphorylation and activity (El-Rayes and LoRusso, 2004; Marshall, 2006). Food and Drug Administration (FDA) have approved only five EGFR inhibitors for clinical use. These include two monoclonal antibodies (cetuximab and panitumumab), two small-molecule TKI (erlotinib and gefitinib) and one that binds to both EGFR and HER2 (lapatinib). However, gefitinib was withdrawn in 2005 because of the results of phase 3 clinical trial that showed no survival benefit in patients with non-small cell lung cancer (NSCLC) (Raponi et al., 2008; Rocha-Lima et al., 2007; Thatcher et al., 2005).

Monoclonal antibodies exhibit greater specificity for the EGFR compared with some of the small-molecule compounds (Mendelsohn, 2001). In addition, receptor inhibition with monoclonal antibodies can be achieved with lower concentrations than those required for small-molecule inhibitors. However, monoclonal antibodies are administered intravenously, whereas the small-molecule tyrosine kinase inhibitors are orally active (Mendelsohn and Baselga, 2003).

6.1.3 Hypothesis and Aims

In this part of the project, it was hypothesised that EGFR activation as a consequence of over-expression due to increased gene dosage or activating mutations may result in chordoma progression. The main aim of this part of the project was to investigate if there were molecular evidence for offering EGFR inhibitors as a systemic treatment for a selective group of chordoma patients. To achieve this, a cohort of chordomas was screened for EGFR expression and for genetic changes (mutations and copy number variation). If evidence was found for either or both of these abnormalities in chordomas, the effect of an EGFR inhibitor, tyrphostin (AG1478) was to be tested on the only available chordoma-derived cell line, U-CH1.

6.1.4 Objectives

- Analysis of total and phosphorylated EGFR expression in chordomas using immunohistochemical technique on TMAs.
- Assessment of the p-EGFR status and other phospho-receptor tyrosine kinases (RTK) in the chordoma cell line and chordoma cases using a phospho-RTK antibody array membrane.
- Determination of EGFR gene dosage in chordomas and the U-CH1 cell line using interphase FISH on chordoma TMAs.
- Mutational analysis of (exons 18-21) encoding the tyrosine kinase domain of EGFR using direct sequencing of genomic

DNA, including the coding sequence and flanking intronic regions.

- Application of EGFR inhibitor tyrphostin (AG1478) to the chordoma-derived cell line U-CH1 *in vitro* and analysis of its cellular effects.

6.2 RESULTS

6.2.1 Immunohistochemical analysis of EGFR and p-EGFR expression in chordomas using TMAs

Thirty-two of 49 (65%) of the non skull-based chordomas and 30 of 48 (62.5%) of the skull-based chordomas expressed total EGFR as assessed by immunohistochemistry, whereas 24 of 49 (49%) of non skull-based chordomas and 22 of 48 (46%) of the skull-based chordomas showed p-EGFR immunoreactivity (Figure 6.2). The immunoreactivity was membranous and or cytoplasmic. A cut-off point of 10% of immunoreactive cells was required to classify the case positive for either EGFR or p-EGFR expression. In most cases, more than 90% of the neoplastic cells were immunoreactive (Table 6.1).

The non-neoplastic cells (macrophages, lymphocytes and fibroblasts) in the cores were used as internal negative controls.

Table 6.1 EGFR and pEGFR expression in chordomas by immunohistochemistry

TMA	Immunohistochemistry score	EGFR	p-EGFR
Non skull-based chordomas	3 +++	5	0
	++	1	0
	+	0	0
	2 +++	2	3
	++	1	0
	+	0	0
	1 +++	19	17
	++	3	4
	+	1	0
	0	17	25
	Total number of positive cases (%)	32/49 (65)	24/49 (49)
Skull-based chordomas	3 +++	3	1
	++	1	0
	+	0	0
	2 +++	7	3
	++	1	1
	+	1	0
	1 +++	11	13
	++	0	4
	+	6	0
	0	18	26
	Total number of positive cases (%)	30/48 (62.5)	22/48 (46)

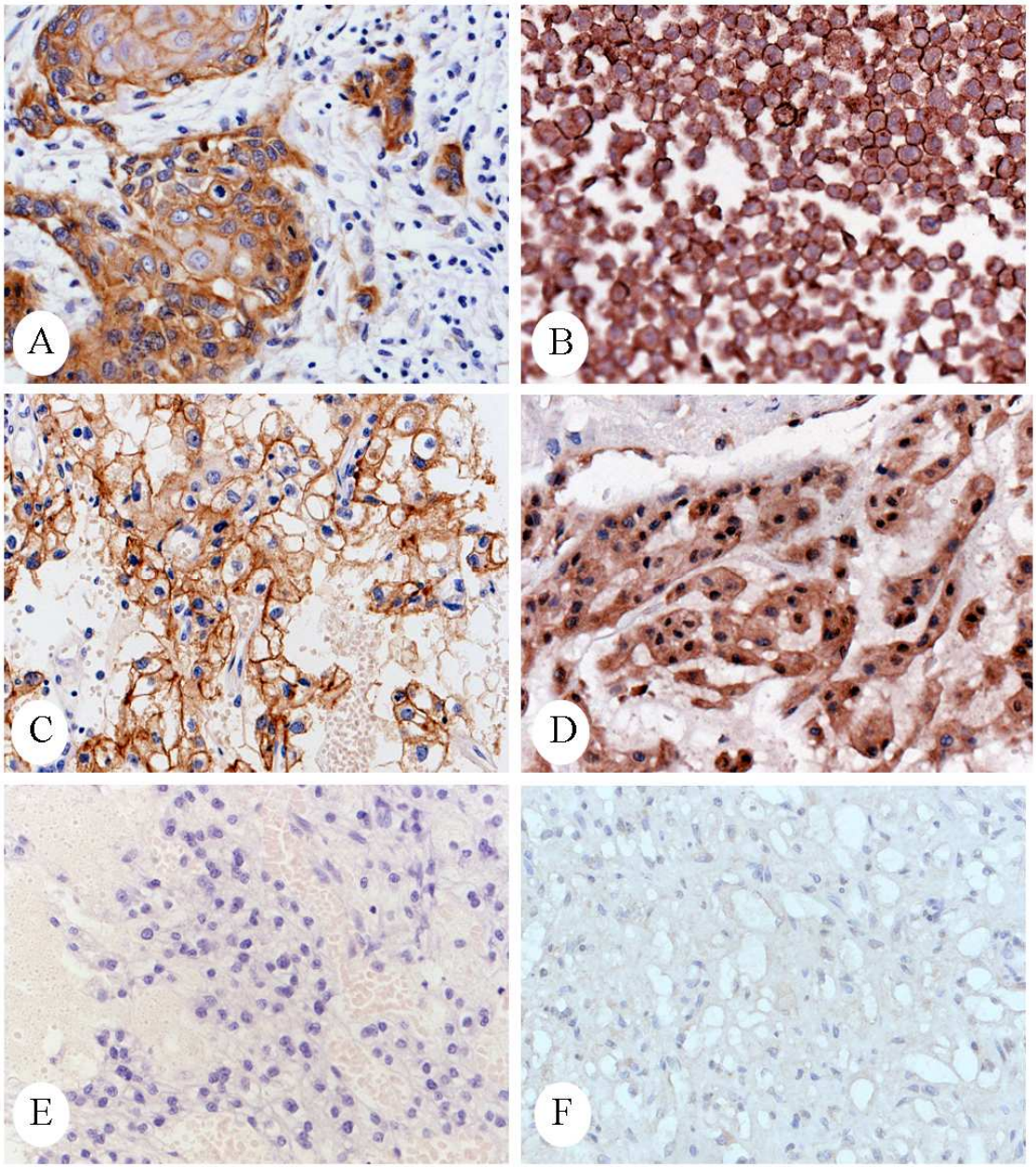

Figure 6.2 EGFR and p-EGFR immunohistchemistry. positive control for EGFR antibody (epidermal squamous cells) (A), positive control for p-EGFR antibody (formalin-fixed squamous cell carcinoma cell line, A431) (B), chordoma immunoreactive for EGFR (C), chordoma immunoreactive for p-EGFR (D), chordomas showing no immunoreactivity for EGFR (E) and p-EGFR (F).

6.2.2 Profiling of the receptor tyrosine kinases using receptor tyrosine kinase antibody array membranes

Protein lysates of the U-CH1 chordoma cell line and three primary tumours revealed high level expression of the active phosphorylated form of EGFR using the R&D p-RTK Antibody Proteome Profiler Array on which there were 42 different receptor tyrosine kinases in duplicates (Figure 6.3, 6.4). The membranes also showed high level expression of some other RTKs in the cell line and the three chordomas including macrophage-stimulating protein receptor (MSPR) and ephrin B2 (EphB2) (Figure 6.3).

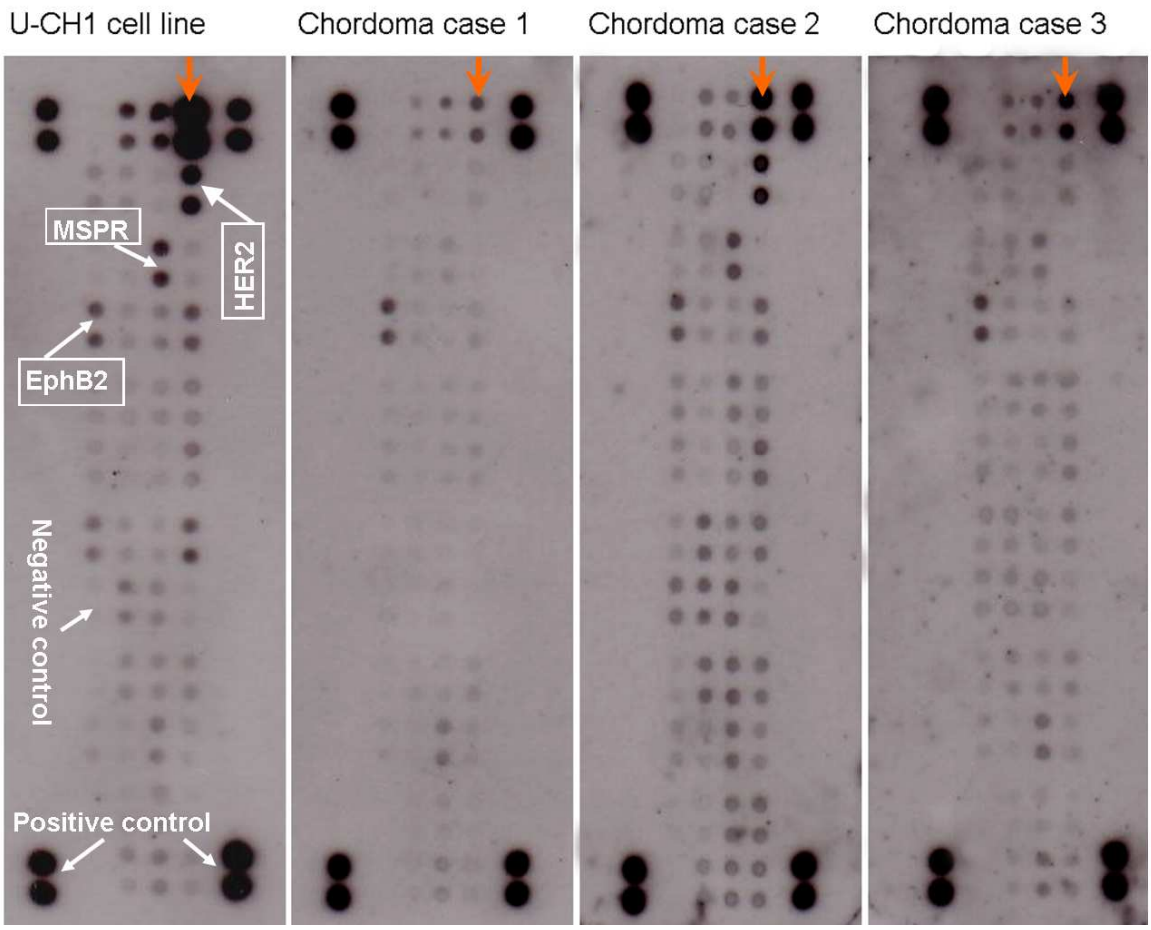

Figure 6.3 Human phopho-RTK antibody array membranes for U-CH1 cell line and 3 chordomas. The membranes show high expression level of p-EGFR (red arrows). The duplicate spots at the 4 corners of each membrane represent positive controls.

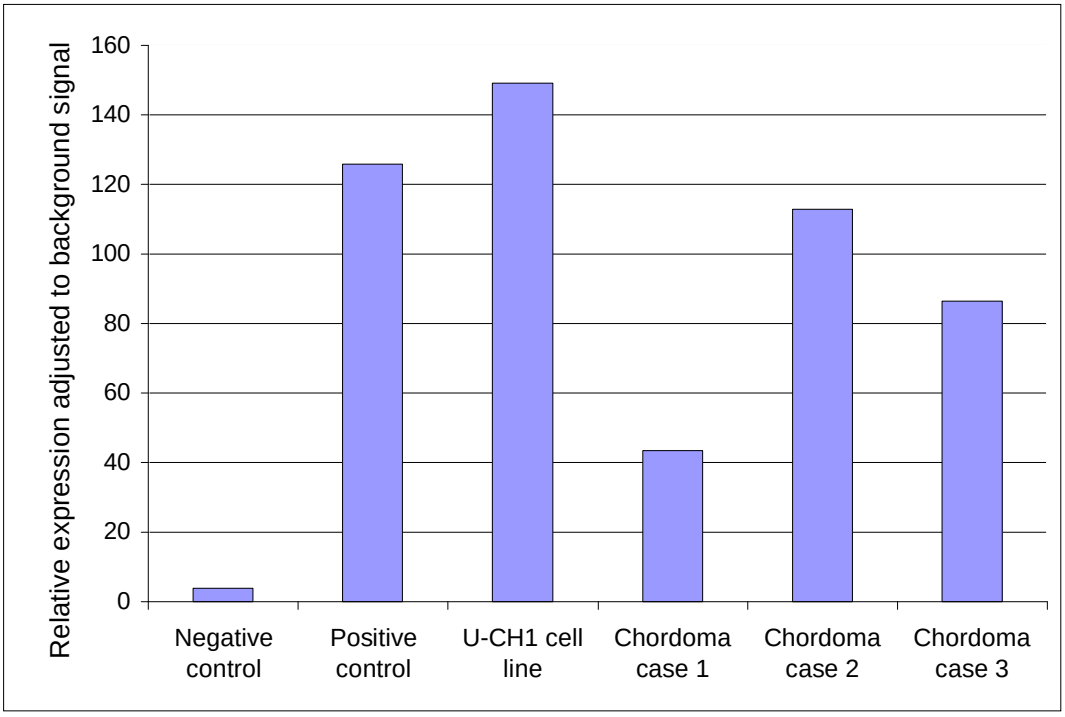

Figure 6.4 Densitometric analysis of p-EGFR expression in the U-CH1 cell line and three chordomas using RTK antibody array membranes. The cell line showed expression higher than the positive control, and the three chordoma cases showed high expression but slightly lower than the positive control. The background effect was substracted from each variable. The relative expression levels were adjusted to the background signals. The RTK antibodies included in the array membranes were spotted in duplicates. The mean densitometric values for these dfuplicates were used in this figure.

6.2.3 Fluorescent *in situ* hybridisation of EGFR probe and chromosome 7 chromosome enumeration probe (CEP7)

The results of the FISH assay for EGFR in 96 chordomas are shown in Table 6.3. The results were divided into FISH positive and FISH negative groups according to the Colorado criteria developed for lung carcinoma (Cappuzzo et al., 2005; Cappuzzo et al., 2008; Martin et al., 2009; Varella-Garcia et al., 2009). The former comprises two categories; high level polysomy (≥ 4 copies/cell in ≥ 40% of cells) and amplification, defined by

the presence of tight gene clusters, a ratio of EGFR gene signals:CEP7 signals ≥ 2, or ≥ 15 copies of the gene per cell in ≥ 10% of analysed cells. The second comprises low level polysomy, defined as > 2 copies/cell in ≤ 40% of cells or 3 copies/cell in ≥ 40% of cells, and diosomy (≤ 2 copies in > 90% of the cells) (Martin et al, 2009; Cappuzzo et al, 2005). Figure 3 shows examples of *EGFR* FISH.

Table 6.2. Results of EGFR FISH assay

	EGFR gene status	Non base of skull chordomas	Skull-based chordomas	Total
FISH positive	Amplification	5/50 (10%)	1/46 (2%)	43/96 (45%)
	High level polysomy	16/50 (32%)	21/46 (46%)	
FISH negative	Low level polysomy	10/50 (20%)	7/46 (15%)	53/96 (55%)
	Diosomy	19/50 (38%)	17/46 (37%)	

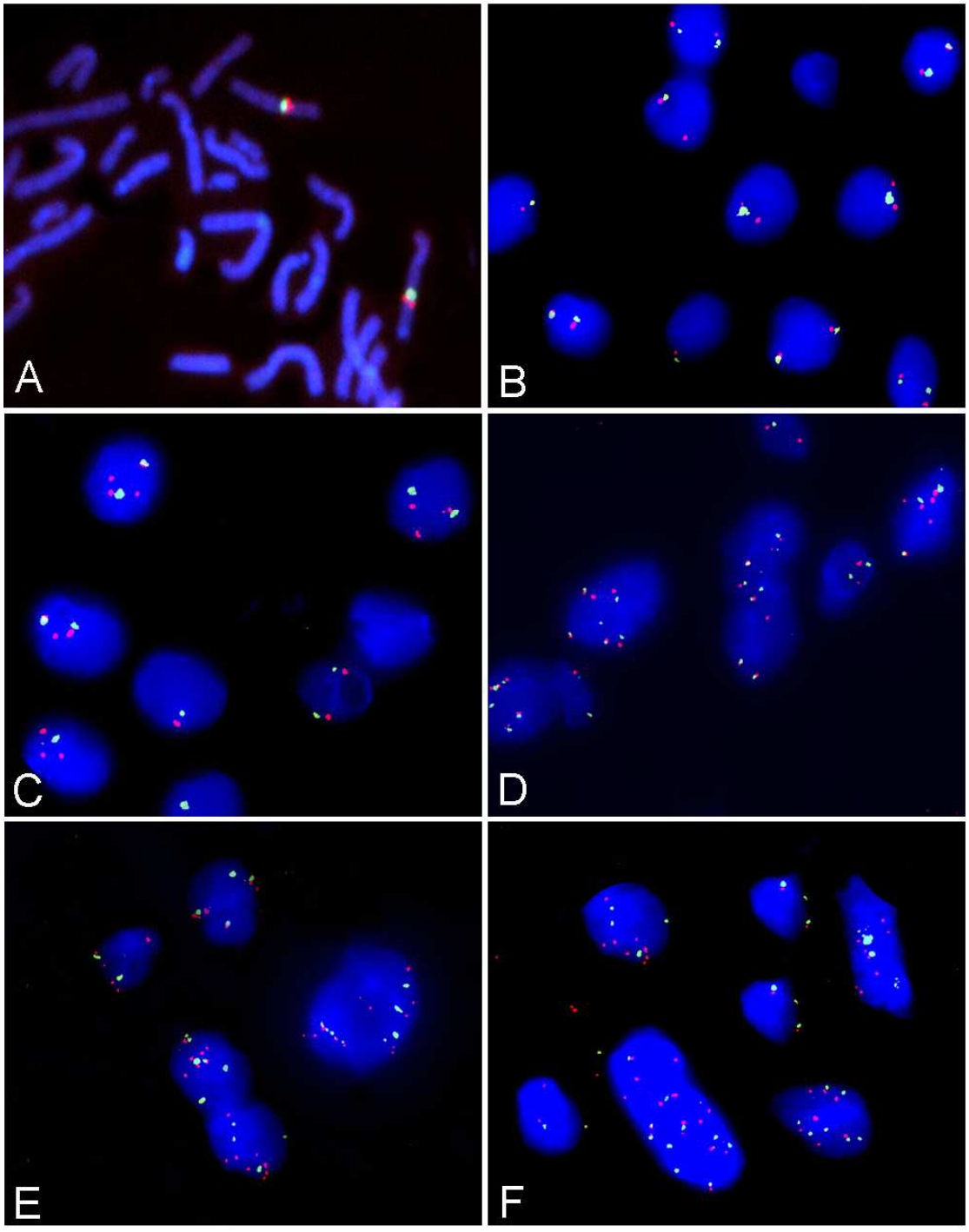

Figure 6.5 Representative images of FISH of *EGFR* on chordoma TMAs. metaphase spread showing mapping of the probes *EGFR* (red) and CEP7 (green) to the correct chromosomal regions (A), diosomy with 2 EGFR and 2 CEP7 signals in most of the

nuclei (B), low level polysomy (C), high level polysomy (D&E) and amplification (F). Fifty intact and non overlapping nuclei were counted for each case.

6.2.4 Mutational analysis of exons (18-21) of *EGFR* encoding the tyrosine kinase domain

Mutational analysis of the exons encoding the tyrosine kinase domain of *EGFR* by direct sequencing of genomic DNA failed to reveal any mutations in the 23 analysed cases. However, a recently reported single nucleotide polymorphism (SNP) (I.D rs1050171 and submission number ss52067157) in exon 20 was identified in 15 of 23 (65.2%) tumours. The SNP represents replacement of G to A in glutamine (number 787 and cDNA position 2607). To date there is no disease-association reported, and its prevalence in European population was found to be 58% whereas it was rare in the Asian and Sub-Saharan African populations (http://www.ncbi.nlm.nih.gov/snp). This SNP is synonymous and so has no functional effect.

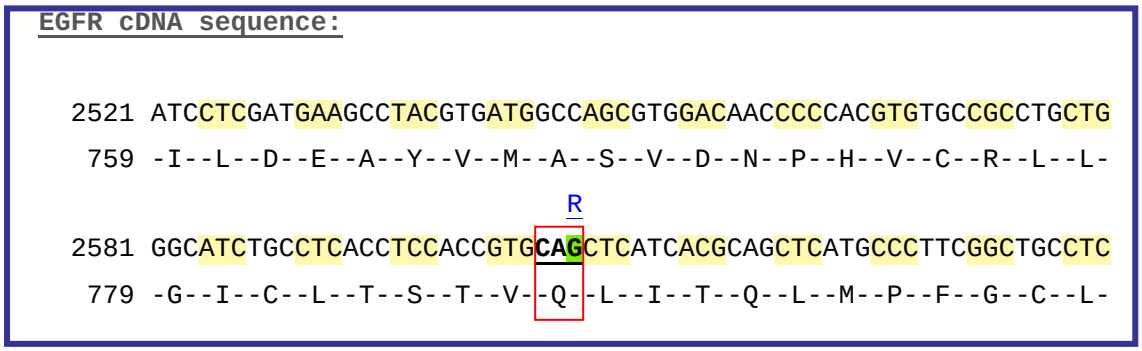

Figure 6.6 Mapping of the SNP reported in exon 20 of *EGFR*. The SNP represents replacement of G to A in glutamine (number 787 and cDNA position 2607). The normal pattern is CAG, which changed to CAA in the SNP pattern. This does not change the amino acid.

6.2.5 Effects of the selective EGFR inhibitor tyrphostin (AG1478) on the U-CH1 chordoma-derived cell line

6.2.5.1 Morphological changes of U-CH1 cells in response to tyrphostin (AG1478) treatment

The EGFR TKI tyrphostin (AG1478) was applied to the cells at various concentrations diluted in DMSO (0, 5, 10, 20, 50, 100 and 200 nmol/L). The cells showed morphological changes in response to the drug in the form of spindling and reduction in size together with decreased cell densities (Figure 6.7).

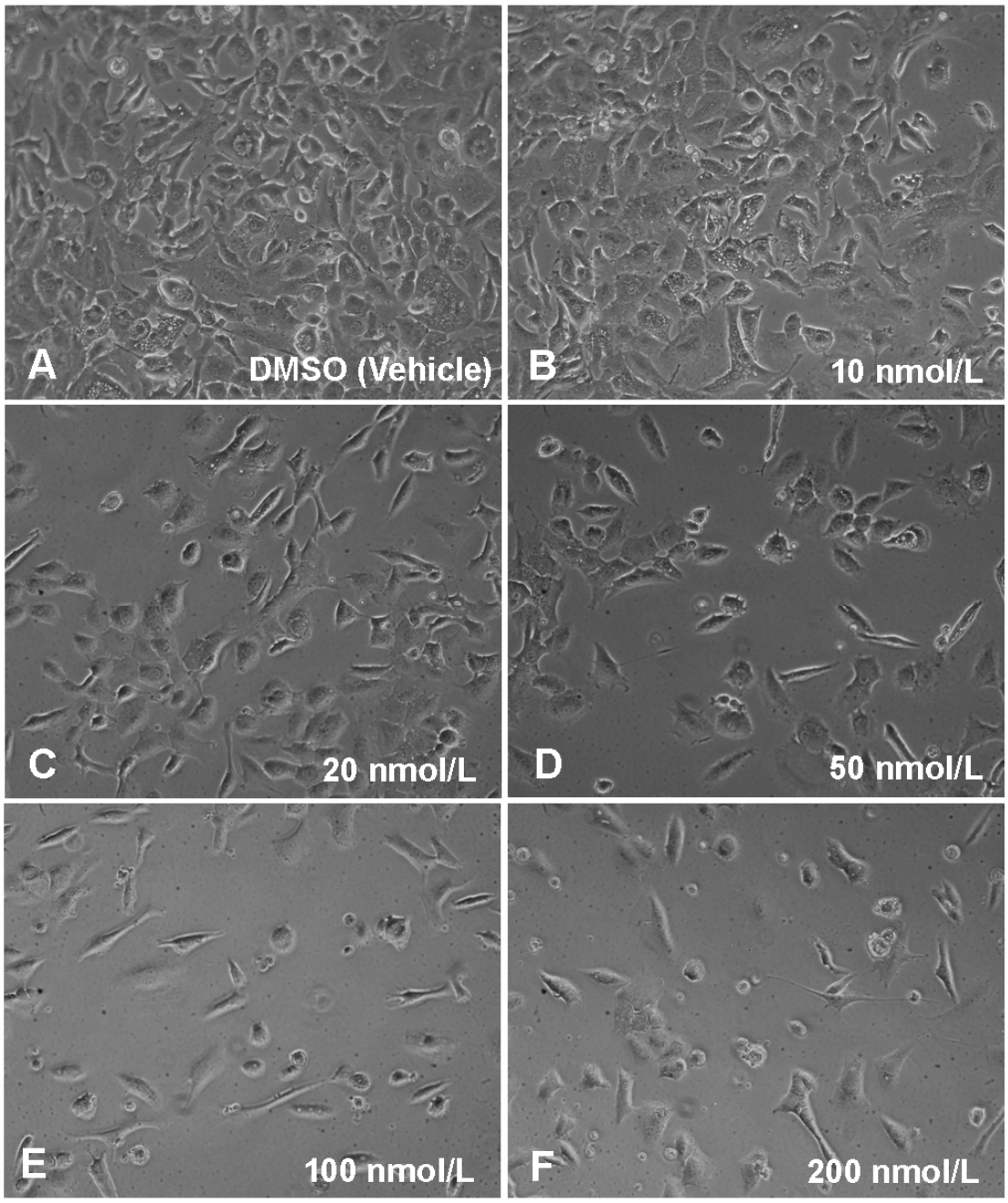

Figure 6.7 Morphological changes of U-CH1 cells in response to tyrphostin (AG1478). Phase contrast photomicrographs of the U-CH1 chordoma cell line in response to various drug concentrations. The drug was applied to the cells for 4 days in complete medium. The experiment was performed three separate times. Pictures represent examples of one experiment. Magnification is 100X.

6.2.5.2 Effect of tyrphostin (AG1478) on proliferation of U-CH1 cells as assessed indirectly by MTS assay

The MTS indirect proliferation assay (CellTiter 96® AQueous Non-Radioactive Cell Proliferation Assay (Promega) demonstrated that tyrphostin (AG1478) inhibited the growth of U-CH1 cells in a dose-responsive manner and resulted in a significant reduction in cell number being detected at a concentration as low as 20 nmol/L (Figure 6.8). The reduction in cell number was progressive with time over 7 days. Removal of tyrphostin (AG1478) from the cultures after 4 days revealed that the cell number recovered significantly apart from the cultures exposed to 100-200 nmol/L (Figures 6.9, 6.10). The experiments showed that there was more than 85% cell number recovery after 4 days growth following removal of the treatment in concentrations equal to or less than 50 nmol/L. At concentrations of 100 and 200 nmol/L, the cells showed only partial recovery of the cell number.

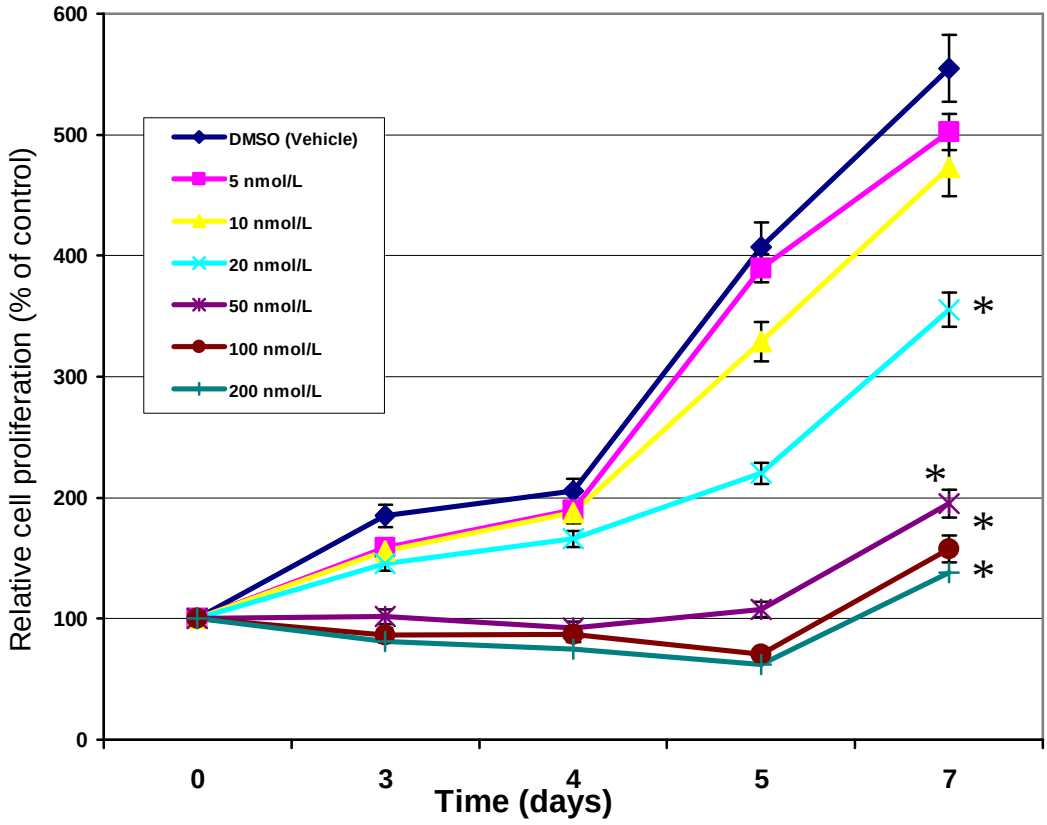

Figure 6.8 MTS assay of U-CH1 cells treated with tyrphostin (AG1478). The figure represents results from three separate experiments, with each variable being performed in triplicates. Error bars represent standard deviation of the calculated mean, * $p<0.05$ compared to vehicle (DMSO).

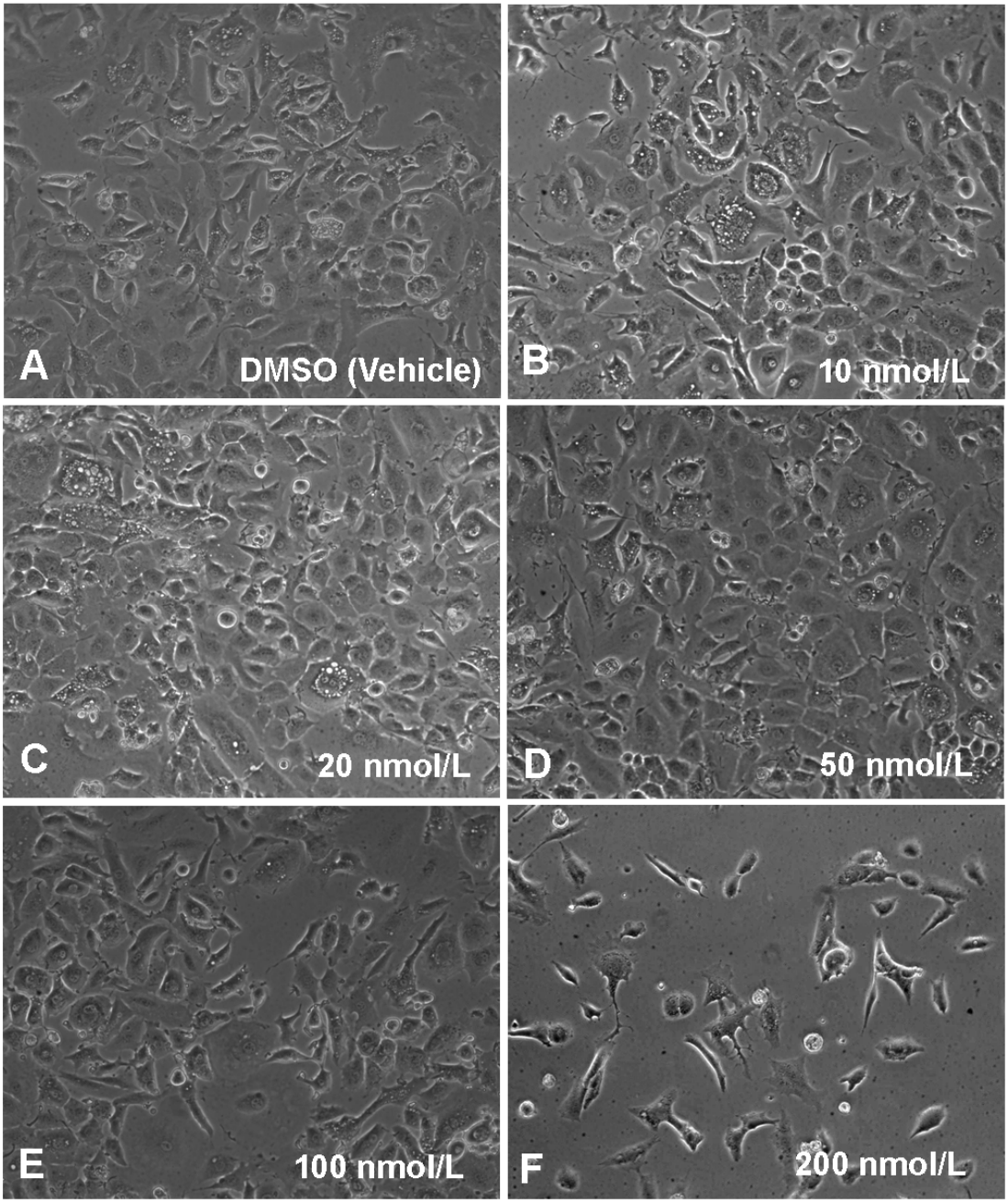

Figure 6.9 Effect of tyrphostin (AG1478) withdrawal from U-CH1 cells. The cells were grown in complete medium containing a range of concentrations of tyrphostin (AG1478), for 4 days, after which the drug was removed and the cells were grown in complete medium for another 4 days. Removal of the drug at concentrations of 50 nmol/L or less resulted in the morphology of the cells and the cell density returning to that of the control cultures (B, C, D). Cells treated with 100 nmol/L showed partial restoration of morphology and cell density (E), and cells treated with 200 nmol/L showed little reversibility of the drug effects (F). The experiment was performed three times in triplicates. Images are from one representative experiment. Magnification is 100X.

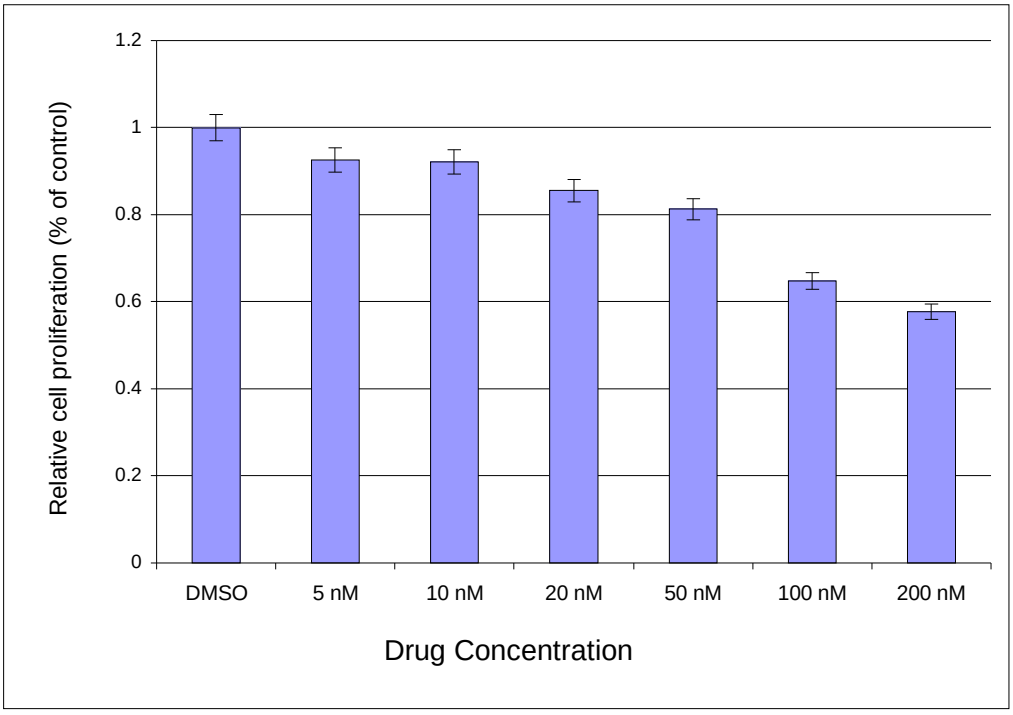

Figure 6.10 MTS assay of U-CH1 cells after withdrawal of tyrphostin (AG1478) cells. The cells were treated with the drug for 4 days after which the drug was withdrawn and cells were grown for another 4 days. There is restoration of up to 85% of the activity of cells treated with concentrations equal to or less than 50 nmol/L compared to the vehicle (DMSO) control. The concentrations of 100 and 200 nmol/L showed only partial restoration of the MTS processing activity.

6.2.5.3 The effect of tyrphostin (AG1478) on tyrosine phosphorylation of EGFR

The effect of tyrphostin (AG1478) on the expression of p-EGFR in U-CH1 cells was investigated using pEGFR-specific membranes. When the cells were exposed to vehicle (DMSO) alone the membranes showed phosphorylation of EGFR at three sites Tyr^{845}, Tyr^{1086} and Tyr^{1173}, whereas phosphorylation of these sites was clearly diminished when the membranes were exposed to tyrphostin (AG1478) in drug concentration as low as 20 nmol/L (Figure 6.11). The results of the EGFR phosphorylation

antibody array membranes were confirmed by Western blot analyses which also showed a dose-dependent response (Figure 6.12).

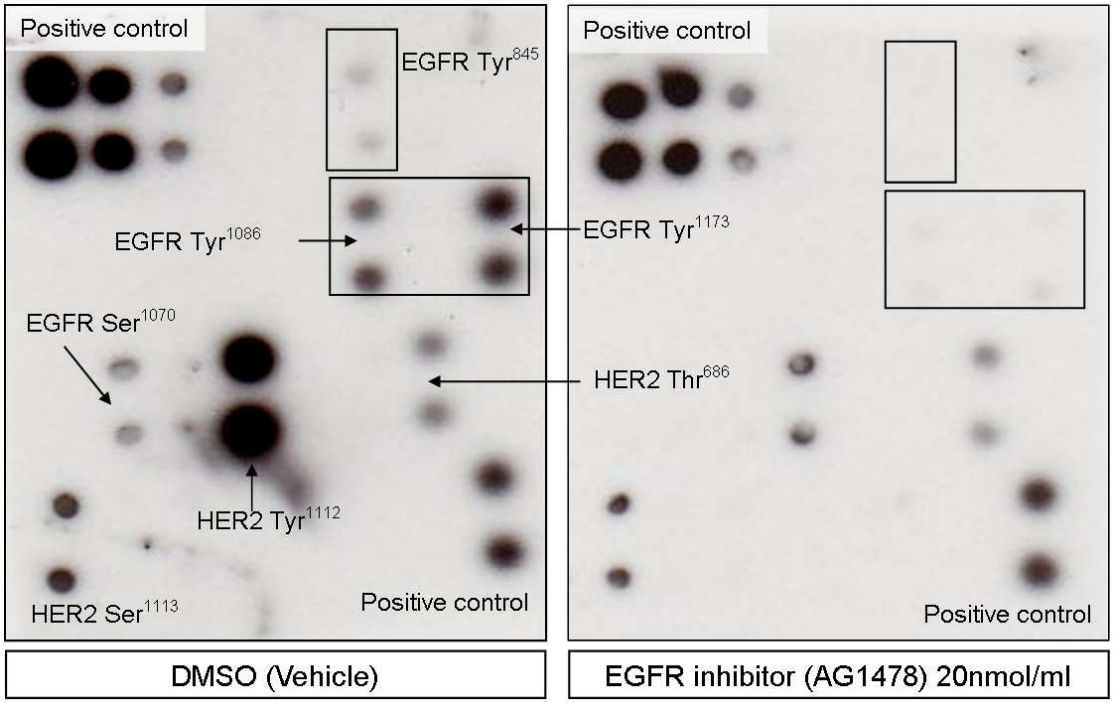

Figure 6.11 EGFR phosphorylation of U-CH1 cells in the presence and absence of tyrphostin (AG1478) using p-EGFR antibody array membranes. The cells treated with vehicle (DMSO) on the right side showed EGFR phosphorylation at the sites Tyr^{845}, Tyr^{1086}, Tyr^{1173} while cells treated with 20 nmol/L of tyrphostin (AG1478) showed marked reduction of these phosphorylation sites.

6.2.5.4 Effect of tyrphostin (AG1478) on activation of MAPK and AKT downstream targets of EGFR signalling

Activation of EGFR leads to proliferation of cells mainly by inducing downstream signalling through RAS/RAF/MEK/ERK and PI3K/AKT pathways. To test whether AG1478 could inhibit activation of these downstream pathways, U-CH1 cells were treated with a range of concentrations of AG1478 and the expression of p-AKT and p-ERK1/2 was determined by Western blot analysis using phospho-specific antibodies

directed against p-AKT (Ser^{473}) and p-ERK 1/2 (Thr^{202}/Tyr^{204}) respectively. The results showed that p-AKT and p-ERK decreased significantly after treatment with AG1478 with 200 nmol/L (Figure 6.12).

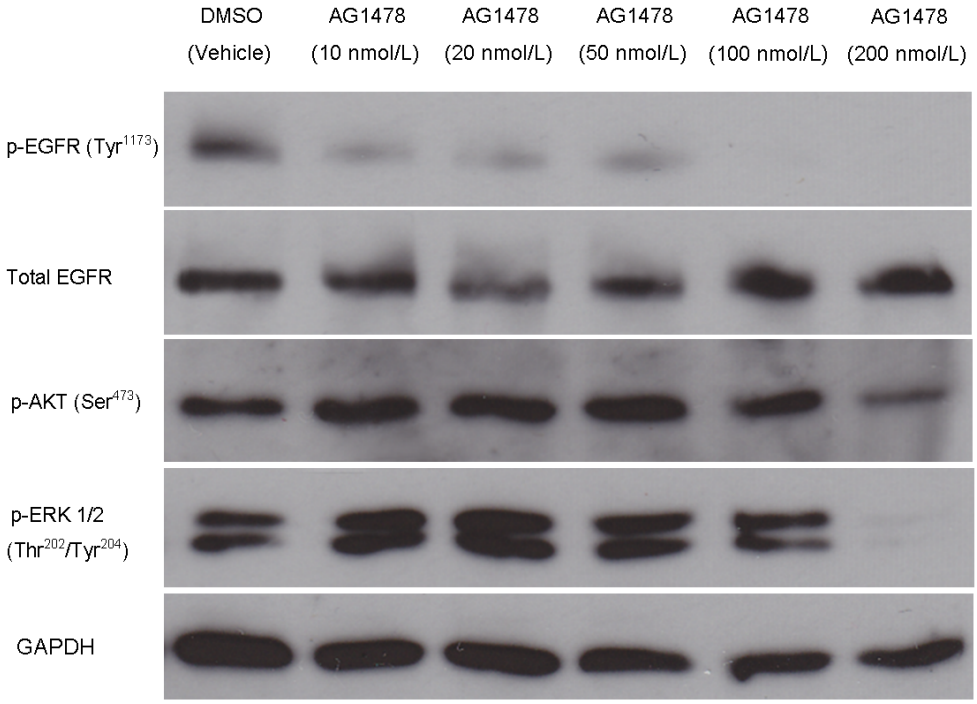

Figure 6.12 Western blot analysis of the effect of various concentrations of tyrphostin (AG1478) on U-CH1 cells. The upper panel shows a gradual reduction of the expression of p-EGFR in response to increasing concentrations of the drug. The expression of p-AKT and p-ERK1/2 shows a marked decrease at the concentration of 200 nmol/L while being nearly constant at the lower concentrations. The membrane was probed with anti-GAPDH antibody as a loading control.

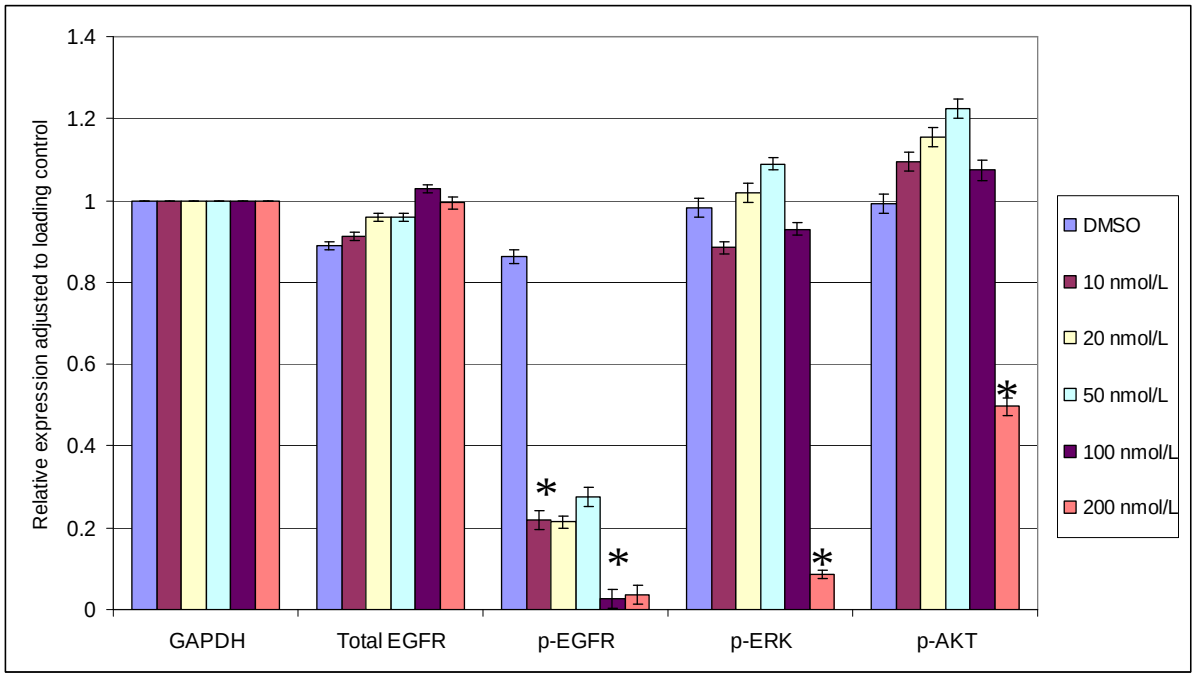

Figure 6.13 Densitometric measurements of Western blot analysis of the effect of various concentrations of tyrphostin (AG1478) on U-CH1 cells. The total EGFR expression is not significantly affected by addition of the drug. The p-EGFR showed marked reduction with nearly with almost absent expression at concentrations of 100 and 200 nmol/L. p-ERK and p-AKT were significantly reduced with the concentration of 200 nmol/L. The expression was adjusted to GAPDH expression as a loading control. The experiment was performed three separate times and each variable was analysed in triplicates. Error bars represent standard deviation. * $p < 0.05$.

6.3 DISCUSSION

EGFR represents an important candidate for molecular targeted therapy as it plays an essential role in the growth of many types of solid tumours especially non-small cell lung cancer, colon cancer, head and neck and pancreatic cancers (Roberts et al., 2002). Some EGFR inhibitors are already in clinical use for management of some of these tumours (Rocha-Lima et al., 2007).

The few reports which have described the expression of EGFR in chordomas using immunohistochemical techniques show a wide range of immunoreactivity from 61% to 100% (Tamayama et al., 1990; Weinberger et al., 2005; Fasig et al., 2008; Ptaszynski et al., 2009). In comparison, the results presented here revealed EGFR expression in 64% of the examined cases. The difference in the expression levels reported can be attributed to different immunohistochemical techniques employed including different antibodies, and the use of TMAs compared to whole tissue sections, the differences in scoring systems adopted and the size of the examined cohort. The results presented in this part of the project are closest to the 67% reported by Fasig et al., (2008) who also used TMA and adopted a similar scoring system and only included a positive result when a minimum of 10% of the lesional cells were immunoreactive (Karamouzis et al., 2007; Fasig et al., 2008). The expression of EGFR, as determined by immunohistochemistry, is associated with a poor prognosis in many cancers including gastric, esophageal and breast carcinomas compared to

EGFR negative tumours, although this is not the case for lung carcinoma (Kris and Tonato, 2002; DiGiovanna et al., 2005; Gibault et al., 2005). However, most of the studies and clinical trials found that expression of EGFR alone is not a robust predictor of response to therapeutic intervention with EGFR inhibitors (Bishop et al., 2002; Chung et al., 2005; Dei Tos and Ellis, 2005; Sartore-Bianchi et al., 2007). The assessment of the phospho-EGFR status in tumours in other studies has failed to show that this is a good predictor of response to anti-EGFR therapy (Rego et al., 2010).

The best evidence for predicting the response to EGFR inhibitors include *EGFR* gene dosage, somatic mutations in *EGFR*, mutations in the downstream molecules in the EGFR signalling pathway especially KRAS and the absence of PTEN expression (Frattini et al., 2007)

High level EGFR gene dosage detected by FISH either in the form of amplification or balanced polysomy has been reported to be a predictive of good response to anti-*EGFR* therapy (Cappuzzo et al., 2005; Moroni et al., 2005; van Krieken et al., 2008). Hence the finding that 45% (43 of 96) chordomas showed high level *EGFR* gene dosage either by amplification (6%) or by high level polysomy (39%) suggest that a substantial number of these tumours may respond well to anti-EGFR therapy.

Failure to detect any mutations in the exons (18-21) coding for the EGFR tyrosine kinase domain, suggests that *EGFR* mutation is not a major mechanism for EGFR activation in chordomas. However, the presence of

unreported mutations, outside the examined exons or in the introns remains a possibility. Single nucleotide polymorphisms (SNPs) represent the most common genetic variation in the human genome and they may contribute to the susceptibility to cancers. A recently reported SNP was found in 65% of the chordomas examined in this study and although little is known about the contribution of this SNP to the disease process, the possibility remains that it may have an effect on *EGFR* expression or activity (Choi et al., 2007). Another predictor of sensitivity to anti-EGFR drugs is the mutation status of the EGFR downstream molecules especially those in the RAS/RAF/MEK/ERK pathway including *KRAS, NRAS, HRAS, BRAF* and *MEK1/2*. This necessitates conducting mutational analysis of these genes in chordomas (Raponi et al., 2008), although no mutations in *KRAS*, *BRAF* were identified in 23 chordomas in this study as described in chapter 4.

The *in vitro* response of the U-CH1 chordoma-derived cell line presented in this work provides an evidence base that chordomas may be responsive for the anti-EGFR therapy. The dose-dependent inhibition of phosphorylation of EGFR as shown by the Western blot analysis and the reversibility of the morphologic changes of the cells after drug withdrawal proves that the effects seen are specific and caused mainly by inhibition of EGFR signalling. The application tyrphostin (AG1478) to a cell line that does not overexpress EGFR would be usefull as a control to exclude the possibility of the drug toxic effect, although the dose dependent effect seen

on U-CH1 cells can provide evidence that the drug is not mediating its effect through a direct toxicity. The diminished expression of p-ERK 1/2 (Thr^{202}/Tyr^{204}) and p-AKT (Ser^{473}) provides further evidence to the specificity of the drug. However, the effect on these downstream molecules is only evident with higher doses (200 nmol/L) and this suggests that the range of doses which may be required to cause the cellular effect is higher that that is required to inhibit the EGFR phosphorylation..

The detection of HER2 phosphorylation at (Tyr^{1112}) in U-CH1 cells as detected by the p-EGFR antibody array membranes and the detection of p-HER2 by the RTK antibody array membranes may be an indication of ERBB2 activation in chordomas, however, the chordomas examined in this study failed to show HER2 expression by immunohistochemistry. Further investigation of HER2 status using FISH in this tumour is required; however, it is beyond the scope of this project.

The findings of this study including the high copy number of EGFR and the response of the chordoma cell line to the EGFR inhibitor tyrphostin (AG1478) provides an evidence base for the first time for a clinical trial to be carried to test the effect of treating chordomas with EGFR inhibitors. However, as in the treatment of other tumour knowledge of the *EGFR* mutation status, the copy number and the mutations in genes involved in the downstream pathways especially *RAS* and *PTEN* genes is required if useful information is to be acquired from such a trial.

7. CONCLUSIONS AND FUTURE WORK

7.1 Conclusions

The work presented in this thesis was started with the aim of identifying the molecules and mechanisms involved in chordoma pathogenesis, and to find an evidence base on which to offer new treatments for the management of chordomas.

In the first chapter of the results, the previous reports of chordomas arising in the context of tuberous sclerosis complex syndrome stimulated investigations into whether there was activation of PI3K/AKT/TSC/mTOR pathway in chordomas and to discover if there were underlying genetic changes in *TSC1* and or *TSC2* genes. The expression of TSC proteins by most of the chordomas investigated suggested that activation of this pathway is unlikely to be due to genetic events in these two genes and directed the work towards looking for other mechanisms of activation of this pathway. The activity of PI3K/AKT/TSC/mTOR pathway was investigated using multiple techniques including immunohistochemistry with phospho-specific antibodies directed towards the active forms of molecules involved in this pathway. The results of immunohistochemistry were validated by Western blot analysis on selected cases. Mutations affecting *PI3KCA* and *RHEB* genes were not detected by direct DNA sequencing of the regions of the genes where mutations have been previously reported. The genetic status of *mTOR* (*FRAP1*), *RPS6*, *TSC1*, *TSC2* has been investigated using FISH and the allelic loss of *mTOR* and *RPS6* in some cases provided an

explanation for the loss of expression of these molecules by immunohistochemistry. The absence of allelic loss of *TSC1* and *TSC2* in all the examined cases supported the notion that abnormal genetic events in these genes are not essential for chordoma development. In conclusion, the first chapter, showed that a subset of chordomas showed activation of PI3K/AKT/TSC/mTOR pathway and therefore these would be potentially responsive to inhibition of this pathway using rapamycin and its derivatives, PI3K inhibitors, AKT inhibitors or a combination of these agents.

In the second chapter, the role of FGFR/RAS/RAF/MEK/ERK-ETS2/Brachyury signalling pathway in chordoma development was investigated. This work was based on the evidence accumulated in the literature from studies performed in the lower vertebrates and amphibians which showed that *brachyury* is regulated by FGFR signalling. Using immunohistochemistry, FGFR expression was found in most of the chordomas (> 90%) and activity of this pathway was proved by the detection of phosphorylated FRS2α by Western blot analysis. To investigate the mechanisms underlying FGFR pathway activation in chordomas, direct sequencing of genomic DNA was performed to look for the commonly reported mutations in the four *FGFR* genes. dHLPC screening was employed to look for the common mutations previously reported in *KRAS* and *BRAF*.

The failure to detect mutations in all of these genes suggests that genetic events in these genes are not a common mechanism for chordoma

development. The activation of this pathway in chordomas offers some potential therapeutic targets because FGFR and RAS are emerging as therapeutic targets for some cancers including endometrial carcinoma, urothelial carcinoma and multiple myeloma. Although direct sequencing of the *brachyury* coding exons and promoter region failed to detect any mutation, the presence of genetic changes detected by FISH in this gene provided for the first time, evidence for involvement of *brachyury* in the pathogenesis of sporadic chordomas and is concordant with the recent report implicating duplication of *brachyury* in susceptibility to the development of familial chordoma.

In the third chapter of results, further evidence for the role of *brachyury* in chordoma pathogenesis was provided by using shRNA technique to knockdown *brachyury* gene in the only available chordoma-derived cell line, U-CH1. The striking cellular changes resulted from knocking down *brachyury* in these cells provided *in vitro* evidence for a pathogenic role for *brachyury* in chordoma development and proves that it is not only expressed in chordoma cells but it also plays an essential role in the biology of these cells. The resulting effect of *brachyury* knockdown on the U-CH1 chordoma cells opens the door for the possibility of the future targeting of this gene or its downstream targets in the management of chordomas.

In the last chapter, the role of *EGFR* was investigated. The reason for investigating this gene was based on the fact that EGFR acts upstream

of the PI3K/TSC/mTOR and RAS/RAF/MEK/MAPK pathways which were shown to be activated in a subset of chordomas as proved in the first two chapters of the results.

Furthermore, there is accumulating evidence in the literature providing evidence for activation of receptor tyrosine kinases in chordomas. EGFR is an attractive molecule in the therapeutic context as inhibitors of this molecule are already in clinical use for treatment of certain cancers such as non-small cell lung carcinoma and colon carcinoma. The results in this chapter provided evidence for expression of EGFR and its phosphorylated form in more than 50% of chordomas examined by immunohistochemistry. Although, direct DNA sequencing failed to detect any mutations in the exons coding for the kinase domain of *EGFR*, the presence of gene copy number gain detected by FISH provides good evidence for the involvement of *EGFR* in the growth of chordoma cells. The presence of copy number gain also suggests that at least some chordomas are potentially responsive to anti-EGFR therapy. This concept has been also supported by the *in vitro* work performed on U-CH1 where the EGFR inhibitor tyrphostin (AG1478) induced a marked decrease in the cell numbers and cell morphology.

7.2 Future work

The data presented here provides a basis for several new projects. An area that needs more investigation is the preclinical evidence for the benefit of therapeutic agents in the management of chordoma, although, this is difficult to perform *in vivo* as there is only one cell line available for testing. However, as there is no effective treatment for this disease there is an argument that clinical trial could be undertaken using inhibitors to EGFR, mTOR and other molecules which we have found to be activated in chordomas.

Another appealing project to undertake is to investigate the downstream targets of *brachyury* which are still unknown in mammalian cells. The cells in which *brachyury* has been knocked down could be exploited for this purpose; this could be achieved by rescuing the knockdown model and looking for the expression of downstream targets by performing a gene expression microarray (GEM).

8. REFERENCE LIST

Abbas-Terki,T., Blanco-Bose,W., Deglon,N., Pralong,W., and Aebischer,P. (2002). Lentiviral-mediated RNA interference. Hum. Gene Ther. *13*, 2197-2201.

Agrawal,A. (2008). Chondroid chordoma of petrous temporal bone with extensive recurrence and pulmonary metastases. J. Cancer Res. Ther. *4*, 91-92.

Agrawal,P.P., Bahadur,A.K., Mohanta,P.K., Singh,K., and Rathi,A.K. (2006). Chordoma: 6 years' experience at a tertiary centre. Australas. Radiol. *50*, 201-205.

Ahn,N.G. (1993). The MAP kinase cascade. Discovery of a new signal transduction pathway. Mol. Cell Biochem. *127-128*, 201-209.

Almefty,K., Pravdenkova,S., Colli,B.O., Al-Mefty,O., and Gokden,M. (2007). Chordoma and chondrosarcoma: similar, but quite different, skull base tumors. Cancer *110*, 2457-2467.

Amichetti,M., Cianchetti,M., Amelio,D., Enrici,R.M., and Minniti,G. (2009). Proton therapy in chordoma of the base of the skull: a systematic review. Neurosurg. Rev. *32*, 403-416.

Arnold,S.J., Stappert,J., Bauer,A., Kispert,A., Herrmann,B.G., and Kemler,R. (2000). Brachyury is a target gene of the Wnt/beta-catenin signaling pathway. Mech. Dev. *91*, 249-258.

Arteaga,C.L. (2002). Overview of epidermal growth factor receptor biology and its role as a therapeutic target in human neoplasia. Semin. Oncol. *29*, 3-9.

Asano,S., Kawahara,N., and Kirino,T. (2003). Intradural spinal seeding of a clival chordoma. Acta Neurochir. (Wien.) *145*, 599-603.

Avruch,J., Khokhlatchev,A., Kyriakis,J.M., Luo,Z., Tzivion,G., Vavvas,D., and Zhang,X.F. (2001). Ras activation of the Raf kinase: tyrosine kinase recruitment of the MAP kinase cascade. Recent Prog. Horm. Res. *56*, 127-155.

Baratti,D., Gronchi,A., Pennacchioli,E., Lozza,L., Colecchia,M., Fiore,M., and Santinami,M. (2003). Chordoma: natural history and results in 28 patients treated at a single institution. Ann. Surg. Oncol. *10*, 291-296.

Barlund,M., Forozan,F., Kononen,J., Bubendorf,L., Chen,Y., Bittner,M.L., Torhorst,J., Haas,P., Bucher,C., Sauter,G., Kallioniemi,O.P., and Kallioniemi,A. (2000). Detecting activation of ribosomal protein S6 kinase by complementary DNA and tissue microarray analysis. J. Natl. Cancer Inst. *92*, 1252-1259.

Batsakis,J.G., Solomon,A.R., and Rice,D.H. (1980). The pathology of head and neck tumors: neoplasms of cartilage, bone, and the notochord, part 7. Head Neck Surg. *3*, 43-57.

Bergh,P., Kindblom,L.G., Gunterberg,B., Remotti,F., Ryd,W., and Meis-Kindblom,J.M. (2000). Prognostic factors in chordoma of the sacrum and mobile spine: a study of 39 patients. Cancer *88*, 2122-2134.

Bisceglia,M., D'Angelo,V.A., Guglielmi,G., Dor,D.B., and Pasquinelli,G. (2007). Dedifferentiated chordoma of the thoracic spine with rhabdomyosarcomatous

differentiation. Report of a case and review of the literature. Ann. Diagn. Pathol. *11*, 262-273.

Bishop,P.C., Myers,T., Robey,R., Fry,D.W., Liu,E.T., Blagosklonny,M.V., and Bates,S.E. (2002). Differential sensitivity of cancer cells to inhibitors of the epidermal growth factor receptor family. Oncogene *21*, 119-127.

Bjornsson,J., Wold,L.E., Ebersold,M.J., and Laws,E.R. (1993). Chordoma of the mobile spine. A clinicopathologic analysis of 40 patients. Cancer *71*, 735-740.

Borgel,J., Olschewski,H., Reuter,T., Miterski,B., and Epplen,J.T. (2001). Does the tuberous sclerosis complex include clivus chordoma? A case report. Eur. J. Pediatr. *160*, 138.

Boriani,S., Bandiera,S., Biagini,R., Bacchini,P., Boriani,L., Cappuccio,M., Chevalley,F., Gasbarrini,A., Picci,P., and Weinstein,J.N. (2006). Chordoma of the mobile spine: fifty years of experience. Spine (Phila Pa 1976.) *31*, 493-503.

Bos,J.L. (1989). ras oncogenes in human cancer: a review. Cancer Res. *49*, 4682-4689.

Bose,R., Molina,H., Patterson,A.S., Bitok,J.K., Periaswamy,B., Bader,J.S., Pandey,A., and Cole,P.A. (2006). Phosphoproteomic analysis of Her2/neu signaling and inhibition. Proc. Natl. Acad. Sci. U. S. A *103*, 9773-9778.

Boulay,A., Zumstein-Mecker,S., Stephan,C., Beuvink,I., Zilbermann,F., Haller,R., Tobler,S., Heusser,C., O'Reilly,T., Stolz,B., Marti,A., Thomas,G., and Lane,H.A. (2004). Antitumor efficacy of intermittent treatment schedules with the rapamycin derivative RAD001 correlates with prolonged inactivation of ribosomal protein S6 kinase 1 in peripheral blood mononuclear cells. Cancer Res. *64*, 252-261.

Bouropoulou,V., Bosse,A., Roessner,A., Vollmer,E., Edel,G., Wuisman,P., and Harle,A. (1989). Immunohistochemical investigation of chordomas: histogenetic and differential diagnostic aspects. Curr. Top. Pathol. *80*, 183-203.

Brandal,P., Bjerkehagen,B., and Heim,S. (2004). Molecular cytogenetic characterization of tenosynovial giant cell tumors. Neoplasia. *6*, 578-583.

Brooks,M., Kleefield,J., O'Reilly,G.V., Haykal,H.A., and MacLeod,M. (1987). Thoracic chordoma with unusual radiographic features. Comput. Radiol. *11*, 85-90.

Brummelkamp,T.R., Bernards,R., and Agami,R. (2002). A system for stable expression of short interfering RNAs in mammalian cells. Science *296*, 550-553.

Buettner,R., Mora,L.B., and Jove,R. (2002). Activated STAT signaling in human tumors provides novel molecular targets for therapeutic intervention. Clin. Cancer Res. *8*, 945-954.

Butler,M.G., Dahir,G.A., Hedges,L.K., Juliao,S.F., Sciadini,M.F., and Schwartz,H.S. (1995). Cytogenetic, telomere, and telomerase studies in five surgically managed lumbosacral chordomas. Cancer Genet. Cytogenet. *85*, 51-57.

Butler,M.G., Sciadini,M., Hedges,L.K., and Schwartz,H.S. (1996). Chromosome telomere integrity of human solid neoplasms. Cancer Genet. Cytogenet. *86*, 50-53.

Campbell,C., Goodrich,K., Casey,G., and Beatty,B. (1995). Cloning and mapping of a human gene (TBX2) sharing a highly conserved protein motif with the Drosophila omb gene. Genomics *28*, 255-260.

Cappell, D.F. (1928). Chordoma of vertebral column with 3 new cases. J. Path. Bact., *31*, 797-814.

Cappuzzo,F., Finocchiaro,G., Rossi,E., Janne,P.A., Carnaghi,C., Calandri,C., Bencardino,K., Ligorio,C., Ciardiello,F., Pressiani,T., Destro,A., Roncalli,M., Crino,L., Franklin,W.A., Santoro,A., and Varella-Garcia,M. (2008). EGFR FISH assay predicts for response to cetuximab in chemotherapy refractory colorectal cancer patients. Ann. Oncol. *19*, 717-723.

Cappuzzo,F., Hirsch,F.R., Rossi,E., Bartolini,S., Ceresoli,G.L., Bemis,L., Haney,J., Witta,S., Danenberg,K., Domenichini,I., Ludovini,V., Magrini,E., Gregorc,V., Doglioni,C., Sidoni,A., Tonato,M., Franklin,W.A., Crino,L., Bunn,P.A., Jr., and Varella-Garcia,M. (2005). Epidermal growth factor receptor gene and protein and gefitinib sensitivity in non-small-cell lung cancer. J. Natl. Cancer Inst. *97*, 643-655.

Cappuzzo,F., Ligorio,C., Toschi,L., Rossi,E., Trisolini,R., Paioli,D., Magrini,E., Finocchiaro,G., Bartolini,S., Cancellieri,A., Hirsch,F.R., Crino,L., and Varella-Garcia,M. (2007). EGFR and HER2 gene copy number and response to first-line chemotherapy in patients with advanced non-small cell lung cancer (NSCLC). J. Thorac. Oncol. *2*, 423-429.

Casali,P.G., Messina,A., Stacchiotti,S., Tamborini,E., Crippa,F., Gronchi,A., Orlandi,R., Ripamonti,C., Spreafico,C., Bertieri,R., Bertulli,R., Colecchia,M., Fumagalli,E., Greco,A., Grosso,F., Olmi,P., Pierotti,M.A., and Pilotti,S. (2004). Imatinib mesylate in chordoma. Cancer *101*, 2086-2097.

Casali,P.G., Stacchiotti,S., Sangalli,C., Olmi,P., and Gronchi,A. (2007). Chordoma. Curr. Opin. Oncol. *19*, 367-370.

Chambers,P.W. and Schwinn,C.P. (1979). Chordoma. A clinicopathologic study of metastasis. Am. J. Clin. Pathol. *72*, 765-776.

Chang,S.D., Martin,D.P., Lee,E., and Adler,J.R., Jr. (2001). Stereotactic radiosurgery and hypofractionated stereotactic radiotherapy for residual or recurrent cranial base and cervical chordomas. Neurosurg. Focus. *10*, E5.

Chattopadhyay,A., Vecchi,M., Ji,Q., Mernaugh,R., and Carpenter,G. (1999). The role of individual SH2 domains in mediating association of phospholipase C-gamma1 with the activated EGF receptor. J. Biol. Chem. *274*, 26091-26097.

Chen,G., Hohmeier,H.E., and Newgard,C.B. (2001). Expression of the transcription factor STAT-1 alpha in insulinoma cells protects against cytotoxic effects of multiple cytokines. J. Biol. Chem. *276*, 766-772.

Chen,J., Williams,I.R., Lee,B.H., Duclos,N., Huntly,B.J., Donoghue,D.J., and Gilliland,D.G. (2005). Constitutively activated FGFR3 mutants signal through PLCgamma-dependent and -independent pathways for hematopoietic transformation. Blood *106*, 328-337.

Chen,K.W., Yang,H.L., Lu,J., Liu,J.Y., and Chen,X.Q. (2010). Prognostic factors of sacral chordoma after surgical therapy: a study of 36 patients. Spinal Cord. *48*, 166-171.

Cheng,S.W., Fryer,L.G., Carling,D., and Shepherd,P.R. (2004). Thr2446 is a novel mammalian target of rapamycin (mTOR) phosphorylation site regulated by nutrient status. J. Biol. Chem. *279*, 15719-15722.

Chetty,R., Levin,C.V., and Kalan,M.R. (1991). Chordoma: a 20-year clinicopathologic review of the experience at Groote Schuur Hospital, Cape Town. J. Surg. Oncol. *46*, 261-264.

Choi,J.E., Park,S.H., Kim,K.M., Lee,W.K., Kam,S., Cha,S.I., Kim,C.H., Kang,Y.M., Kim,Y.C., Han,S.B., Jung,T.H., and Park,J.Y. (2007). Polymorphisms in the epidermal growth factor receptor gene and the risk of primary lung cancer: a case-control study. BMC. Cancer *7*, 199.

Chugh,R., Tawbi,H., Lucas,D.R., Biermann,J.S., Schuetze,S.M., and Baker,L.H. (2007). Chordoma: the nonsarcoma primary bone tumor. Oncologist. *12*, 1344-1350.

Chung,K.Y., Shia,J., Kemeny,N.E., Shah,M., Schwartz,G.K., Tse,A., Hamilton,A., Pan,D., Schrag,D., Schwartz,L., Klimstra,D.S., Fridman,D., Kelsen,D.P., and Saltz,L.B. (2005). Cetuximab shows activity in colorectal cancer patients with tumors that do not express the epidermal growth factor receptor by immunohistochemistry. J. Clin. Oncol. *23*, 1803-1810.

Ciruna,B.G., Schwartz,L., Harpal,K., Yamaguchi,T.P., and Rossant,J. (1997). Chimeric analysis of fibroblast growth factor receptor-1 (Fgfr1) function: a role for FGFR1 in morphogenetic movement through the primitive streak. Development *124*, 2829-2841.

Colli,B. and Al-Mefty,O. (2001). Chordomas of the craniocervical junction: follow-up review and prognostic factors. J. Neurosurg. *95*, 933-943.

Congdon,C.C. (1952). Proliferative lesions resembling chordoma following puncture of the nucleus pulposus in rabbits. J. Natl. Cancer Inst. *12*, 893-907.

Coutts,J.C. and Gallagher,J.T. (1995). Receptors for fibroblast growth factors. Immunol. Cell Biol. *73*, 584-589.

Crawford,T. (1958). The staining reactions of chordoma. J. Clin. Pathol. *11*, 110-113.

Crockard,H.A., Cheeseman,A., Steel,T., Revesz,T., Holton,J.L., Plowman,N., Singh,A., and Crossman,J. (2001). A multidisciplinary team approach to skull base chondrosarcomas. J. Neurosurg. *95*, 184-189.

Cullen,B.R. (2006). Enhancing and confirming the specificity of RNAi experiments. Nat. Methods *3*, 677-681.

Cunliffe,V. and Smith,J.C. (1992). Ectopic mesoderm formation in Xenopus embryos caused by widespread expression of a Brachyury homologue. Nature *358*, 427-430.

Dabska,M. (1977). Parachordoma: a new clinicopathologic entity. Cancer *40*, 1586-1592.

Dahlin,D.C. and MacCarty,C.S. (1952). Chordoma. Cancer *5*, 1170-1178.

Dahlin,D.C. and Unni,K.K. (1994). Chordoma. Arch. Pathol. Lab Med. *118*, 596-597.

Dalpra,L., Malgara,R., Miozzo,M., Riva,P., Volonte,M., Larizza,L., and Fuhrman Conti,A.M. (1999). First cytogenetic study of a recurrent familial chordoma of the clivus. Int. J. Cancer *81*, 24-30.

Dassonville,O., Bozec,A., Fischel,J.L., and Milano,G. (2007). EGFR targeting therapies: monoclonal antibodies versus tyrosine kinase inhibitors. Similarities and differences. Crit Rev. Oncol. Hematol. *62*, 53-61.

Davies,H., Bignell,G.R., Cox,C., Stephens,P., Edkins,S., Clegg,S., Teague,J., Woffendin,H., Garnett,M.J., Bottomley,W., Davis,N., Dicks,E., Ewing,R., Floyd,Y., Gray,K., Hall,S., Hawes,R., Hughes,J., Kosmidou,V., Menzies,A., Mould,C., Parker,A., Stevens,C., Watt,S., Hooper,S., Wilson,R., Jayatilake,H., Gusterson,B.A., Cooper,C., Shipley,J., Hargrave,D., Pritchard-Jones,K., Maitland,N., Chenevix-Trench,G., Riggins,G.J., Bigner,D.D., Palmieri,G., Cossu,A., Flanagan,A., Nicholson,A., Ho,J.W., Leung,S.Y., Yuen,S.T., Weber,B.L., Seigler,H.F., Darrow,T.L., Paterson,H., Marais,R., Marshall,C.J., Wooster,R., Stratton,M.R., and Futreal,P.A. (2002). Mutations of the BRAF gene in human cancer. Nature *417*, 949-954.

Davison,C. and WEIL,A. (1928). Malignant chordoma of the lumbar region. Arch Neurol Psychiatry *19*, 415-423.

De Jesus-Monge,W.E., Torres,E.A., Baez,V.M., De,J.O., Rivera,L., and Gonzalez-Keelan,C. (2004). Crohn's disease associated to chordoma: a case report. P. R. Health Sci. J. *23*, 233-236.

Debus,J., Schulz-Ertner,D., Schad,L., Essig,M., Rhein,B., Thillmann,C.O., and Wannenmacher,M. (2000). Stereotactic fractionated radiotherapy for chordomas and chondrosarcomas of the skull base. Int. J. Radiat. Oncol. Biol. Phys. *47*, 591-596.

Dei Tos,A.P. and Ellis,I. (2005). Assessing epidermal growth factor receptor expression in tumours: what is the value of current test methods? Eur. J. Cancer *41*, 1383-1392.

Deniz,M.L., Kilic,T., Almaata,I., Kurtkaya,O., Sav,A., and Pamir,M.N. (2002). Expression of growth factors and structural proteins in chordomas: basic fibroblast growth factor, transforming growth factor alpha, and fibronectin are correlated with recurrence. Neurosurgery *51*, 753-760.

Deshpande,V., Nielsen,G.P., Rosenthal,D.I., and Rosenberg,A.E. (2007). Intraosseous benign notochord cell tumors (BNCT): further evidence supporting a relationship to chordoma. Am. J. Surg. Pathol. *31*, 1573-1577.

DiFrancesco,L.M., vanzo Castillo,C.A., and Temple,W.J. (2006). Extra-axial chordoma. Arch. Pathol. Lab Med. *130*, 1871-1874.

DiGiovanna,M.P., Stern,D.F., Edgerton,S.M., Whalen,S.G., Moore,D., and Thor,A.D. (2005). Relationship of epidermal growth factor receptor expression to ErbB-2 signaling activity and prognosis in breast cancer patients. J. Clin. Oncol. *23*, 1152-1160.

Doucet,V., Peretti-Viton,P., Figarella-Branger,D., Manera,L., and Salamon,G. (1997). MRI of intracranial chordomas. Extent of tumour and contrast enhancement: criteria for differential diagnosis. Neuroradiology *39*, 571-576.

Draptchinskaia,N., Gustavsson,P., Andersson,B., Pettersson,M., Willig,T.N., Dianzani,I., Ball,S., Tchernia,G., Klar,J., Matsson,H., Tentler,D., Mohandas,N., Carlsson,B., and Dahl,N. (1999). The gene encoding ribosomal protein S19 is mutated in Diamond-Blackfan anaemia. Nat. Genet. *21*, 169-175.

Dufner,A., Andjelkovic,M., Burgering,B.M., Hemmings,B.A., and Thomas,G. (1999). Protein kinase B localization and activation differentially affect S6 kinase 1 activity and

eukaryotic translation initiation factor 4E-binding protein 1 phosphorylation. Mol. Cell Biol. *19*, 4525-4534.

Duo,S., Tiao-Dong,T., Lei,Z., Wei,W., Hong-Li,S., and Xian-Wei,D. (2009). Expression and clinical significance of tbx2 in pancreatic cancer. Asian Pac. J. Cancer Prev. *10*, 118-122.

Dutt,A., Salvesen,H.B., Chen,T.H., Ramos,A.H., Onofrio,R.C., Hatton,C., Nicoletti,R., Winckler,W., Grewal,R., Hanna,M., Wyhs,N., Ziaugra,L., Richter,D.J., Trovik,J., Engelsen,I.B., Stefansson,I.M., Fennell,T., Cibulskis,K., Zody,M.C., Akslen,L.A., Gabriel,S., Wong,K.K., Sellers,W.R., Meyerson,M., and Greulich,H. (2008). Drug-sensitive FGFR2 mutations in endometrial carcinoma. Proc. Natl. Acad. Sci. U. S. A *105*, 8713-8717.

Dutton,R.V. and Singleton,E.B. (1975). Tuberous sclerosis: a case report with aortic aneurysm and unusual rib changes. Pediatr. Radiol. *3*, 184-186.

Edwards,Y.H., Putt,W., Lekoape,K.M., Stott,D., Fox,M., Hopkinson,D.A., and Sowden,J. (1996). The human homolog T of the mouse T(Brachyury) gene; gene structure, cDNA sequence, and assignment to chromosome 6q27. Genome Res. *6*, 226-233.

Eisenberg,M.B., Woloschak,M., Sen,C., and Wolfe,D. (1997). Loss of heterozygosity in the retinoblastoma tumor suppressor gene in skull base chordomas and chondrosarcomas. Surg. Neurol. *47*, 156-160.

El-Rayes,B.F. and LoRusso,P.M. (2004). Targeting the epidermal growth factor receptor. Br. J. Cancer *91*, 418-424.

El-Salem,M., Raghunath,P.N., Marzec,M., Wlodarski,P., Tsai,D., Hsi,E., and Wasik,M.A. (2007). Constitutive activation of mTOR signaling pathway in post-transplant lymphoproliferative disorders. Lab Invest *87*, 29-39.

Elbauomy,E.S., Green,A.R., Lambros,M.B., Turner,N.C., Grainge,M.J., Powe,D., Ellis,I.O., and Reis-Filho,J.S. (2007). FGFR1 amplification in breast carcinomas: a chromogenic *in situ* hybridisation analysis. Breast Cancer Res. *9*, R23.

Ellis,A.G., Doherty,M.M., Walker,F., Weinstock,J., Nerrie,M., Vitali,A., Murphy,R., Johns,T.G., Scott,A.M., Levitzki,A., McLachlan,G., Webster,L.K., Burgess,A.W., and Nice,E.C. (2006). Preclinical analysis of the analinoquinazoline AG1478, a specific small molecule inhibitor of EGF receptor tyrosine kinase. Biochem. Pharmacol. *71*, 1422-1434.

Enin,I.P. (1964). Chordoma of the nasopharynx in 2 members of a family. Vestn. Otorinolaringol. *26*, 88-90.

Eriksson,B., Gunterberg,B., and Kindblom,L.G. (1981). Chordoma. A clinicopathologic and prognostic study of a Swedish national series. Acta Orthop. Scand. *52*, 49-58.

Erlandson,R.A., Tandler,B., Lieberman,P.H., and Higinbotham,N.L. (1968). Ultrastructure of human chordoma. Cancer Res. *28*, 2115-2125.

Fan,W., Huang,X., Chen,C., Gray,J., and Huang,T. (2004). TBX3 and its isoform TBX3+2a are functionally distinctive in inhibition of senescence and are overexpressed in a subset of breast cancer cell lines. Cancer Res. *64*, 5132-5139.

Fasig,J.H., Dupont,W.D., LaFleur,B.J., Olson,S.J., and Cates,J.M. (2008). Immunohistochemical analysis of receptor tyrosine kinase signal transduction activity in chordoma. Neuropathol. Appl. Neurobiol. *34*, 95-104.

Fasig,J.H., Dupont,W.D., Olson,S.J., LaFleur,B.J., and Cates,J.M. (2007). Steroid hormone receptor and COX-2 expression in chordoma. Am. J. Clin. Pathol. *128*, 375-381.

Feldman,M.E., Apsel,B., Uotila,A., Loewith,R., Knight,Z.A., Ruggero,D., and Shokat,K.M. (2009). Active-Site Inhibitors of mTOR Target Rapamycin-Resistant Outputs of mTORC1 and mTORC2. PLoS Biol. *7*, e38.

Ferraresi,V., Nuzzo,C., Zoccali,C., Marandino,F., Vidiri,A., Salducca,N., Zeuli,M., Giannarelli,D., Cognetti,F., and Biagini,R. (2010). Chordoma: clinical characteristics, management and prognosis of a case series of 25 patients. BMC. Cancer *10*, 22.

Firooznia,H., Golimbu,C., Rafii,M., Reede,D.L., Kricheff,I.I., and Bjorkengren,A. (1986). Computed tomography of spinal chordomas. J. Comput. Tomogr. *10*, 45-50.

Fisher,C. (2000). Parachordoma exists--but what is it? Adv. Anat. Pathol. *7*, 141-148.

Fisher,C. and Miettinen,M. (1997). Parachordoma: a clinicopathologic and immunohistochemical study of four cases of an unusual soft tissue neoplasm. Ann. Diagn. Pathol. *1*, 3-10.

Fleming,A., Keynes,R.J., and Tannahill,D. (2001). The role of the notochord in vertebral column formation. J. Anat. *199*, 177-180.

Fleming,G.F., Heimann,P.S., Stephens,J.K., Simon,M.A., Ferguson,M.K., Benjamin,R.S., and Samuels,B.L. (1993). Dedifferentiated chordoma. Response to aggressive chemotherapy in two cases. Cancer *72*, 714-718.

Foote,R.F., Ablin,G., and Hall,W.W. (1958). Chordoma in siblings. Calif. Med. *88*, 383-386.

Forbes,S., Clements,J., Dawson,E., Bamford,S., Webb,T., Dogan,A., Flanagan,A., Teague,J., Wooster,R., Futreal,P.A., and Stratton,M.R. (2006). COSMIC 2005. Br. J. Cancer *94*, 318-322.

Forsyth,P.A., Cascino,T.L., Shaw,E.G., Scheithauer,B.W., O'Fallon,J.R., Dozier,J.C., and Piepgras,D.G. (1993). Intracranial chordomas: a clinicopathological and prognostic study of 51 cases. J. Neurosurg. *78*, 741-747.

Foulds,C.E., Nelson,M.L., Blaszczak,A.G., and Graves,B.J. (2004). Ras/mitogen-activated protein kinase signaling activates Ets-1 and Ets-2 by CBP/p300 recruitment. Mol. Cell Biol. *24*, 10954-10964.

Foweraker,K.L., Burton,K.E., Maynard,S.E., Jena,R., Jefferies,S.J., Laing,R.J., and Burnet,N.G. (2007). High-dose radiotherapy in the management of chordoma and chondrosarcoma of the skull base and cervical spine: Part 1--Clinical outcomes. Clin. Oncol. (R. Coll. Radiol.) *19*, 509-516.

Franke,T.F., Kaplan,D.R., and Cantley,L.C. (1997). PI3K: downstream AKTion blocks apoptosis. Cell *88*, 435-437.

Frattini,M., Saletti,P., Romagnani,E., Martin,V., Molinari,F., Ghisletta,M., Camponovo,A., Etienne,L.L., Cavalli,F., and Mazzucchelli,L. (2007). PTEN loss of expression predicts cetuximab efficacy in metastatic colorectal cancer patients. Br. J Cancer 97, 1139-1145.

Freier,K., Schwaenen,C., Sticht,C., Flechtenmacher,C., Muhling,J., Hofele,C., Radlwimmer,B., Lichter,P., and Joos,S. (2007). Recurrent FGFR1 amplification and high FGFR1 protein expression in oral squamous cell carcinoma (OSCC). Oral Oncol. *43*, 60-66.

Gabriele,P., Macias,V., Stasi,M., Chauvie,S., Munoz,F., Delmastro,E., and Scielzo,G. (2003). Feasibility of intensity-modulated radiation therapy in the treatment of advanced cervical chordoma. Tumori *89*, 298-304.

Gao,N., Zhang,Z., Jiang,B.H., and Shi,X. (2003). Role of PI3K/AKT/mTOR signaling in the cell cycle progression of human prostate cancer. Biochem. Biophys. Res. Commun. *310*, 1124-1132.

Gay,E., Sekhar,L.N., Rubinstein,E., Wright,D.C., Sen,C., Janecka,I.P., and Snyderman,C.H. (1995). Chordomas and chondrosarcomas of the cranial base: results and follow-up of 60 patients. Neurosurgery *36*, 887-896.

Ghebranious,N., Blank,R.D., Raggio,C.L., Staubli,J., McPherson,E., Ivacic,L., Rasmussen,K., Jacobsen,F.S., Faciszewski,T., Burmester,J.K., Pauli,R.M., Boachie-Adjei,O., Glurich,I., and Giampietro,P.F. (2008). A missense T (Brachyury) mutation contributes to vertebral malformations. J. Bone Miner. Res. *23*, 1576-1583.

Gibas,Z., Miettinen,M., and Sandberg,A.A. (1992). Chromosomal abnormalities in two chordomas. Cancer Genet. Cytogenet. *58*, 169-173.

Gibault,L., Metges,J.P., Conan-Charlet,V., Lozac'h,P., Robaszkiewicz,M., Bessaguet,C., Lagarde,N., and Volant,A. (2005). Diffuse EGFR staining is associated with reduced overall survival in locally advanced oesophageal squamous cell cancer. Br. J. Cancer *93*, 107-115.

Glasker,S., Li,J., Xia,J.B., Okamoto,H., Zeng,W., Lonser,R.R., Zhuang,Z., Oldfield,E.H., and Vortmeyer,A.O. (2006). Hemangioblastomas share protein expression with embryonal hemangioblast progenitor cell. Cancer Res. *66*, 4167-4172.

Gorringe,K.L., Jacobs,S., Thompson,E.R., Sridhar,A., Qiu,W., Choong,D.Y., and Campbell,I.G. (2007). High-resolution single nucleotide polymorphism array analysis of epithelial ovarian cancer reveals numerous microdeletions and amplifications. Clin. Cancer Res. *13*, 4731-4739.

Gottschalk,D., Fehn,M., Patt,S., Saeger,W., Kirchner,T., and Aigner,T. (2001). Matrix gene expression analysis and cellular phenotyping in chordoma reveals focal differentiation pattern of neoplastic cells mimicking nucleus pulposus development. Am. J. Pathol. *158*, 1571-1578.

Graff,J.R., Konicek,B.W., Carter,J.H., and Marcusson,E.G. (2008). Targeting the eukaryotic translation initiation factor 4E for cancer therapy. Cancer Res. *68*, 631-634.

Gruneberg,H. (1958). Genetical studies on the skeleton of the mouse. XXIII. The development of brachyury and anury. J. Embryol. Exp. Morphol. *6*, 424-443.

Hadari,Y. and Schlessinger,J. (2009). FGFR3-targeted mAb therapy for bladder cancer and multiple myeloma. J. Clin. Invest *119*, 1077-1079.

Hallor,K.H., Staaf,J., Jonsson,G., Heidenblad,M., Vult von,S.F., Bauer,H.C., Ijszenga,M., Hogendoorn,P.C., Mandahl,N., Szuhai,K., and Mertens,F. (2008). Frequent deletion of the CDKN2A locus in chordoma: analysis of chromosomal imbalances using array comparative genomic hybridisation. Br. J. Cancer *98*, 434-442.

Han,S., Polizzano,C., Nielsen,G.P., Hornicek,F.J., Rosenberg,A.E., and Ramesh,V. (2009). Aberrant hyperactivation of akt and Mammalian target of rapamycin complex 1 signaling in sporadic chordomas. Clin. Cancer Res. *15*, 1940-1946.

Hanna,S.A., Aston,W.J., Briggs,T.W., Cannon,S.R., and Saifuddin,A. (2008a). Sacral chordoma: can local recurrence after sacrectomy be predicted? Clin. Orthop. Relat Res. *466*, 2217-2223.

Hanna,S.A., Tirabosco,R., Amin,A., Pollock,R.C., Skinner,J.A., Cannon,S.R., Saifuddin,A., and Briggs,T.W. (2008b). Dedifferentiated chordoma: a report of four cases arising 'de novo'. J. Bone Joint Surg. Br. *90*, 652-656.

Harada,H., Andersen,J.S., Mann,M., Terada,N., and Korsmeyer,S.J. (2001). p70S6 kinase signals cell survival as well as growth, inactivating the pro-apoptotic molecule BAD. Proc. Natl. Acad. Sci. U. S. A *98*, 9666-9670.

Harrowe,D.J. and Taylor,C.R. (1981). Immunoperoxidase staining for carcinoembryonic antigen in colonic carcinoma, osteosarcoma, and chordoma. J. Surg. Oncol. *16*, 1-6.

Hart,K.C., Robertson,S.C., Kanemitsu,M.Y., Meyer,A.N., Tynan,J.A., and Donoghue,D.J. (2000). Transformation and Stat activation by derivatives of FGFR1, FGFR3, and FGFR4. Oncogene *19*, 3309-3320.

Hayflick,L. and Moorhead,P.S. (1961). The serial cultivation of human diploid cell strains. Exp. Cell Res. *25*, 585-621.

Heffelfinger,M.J., Dahlin,D.C., MacCarty,C.S., and Beabout,J.W. (1973). Chordomas and cartilaginous tumors at the skull base. Cancer *32*, 410-420.

Heitman,J., Movva,N.R., Hiestand,P.C., and Hall,M.N. (1991). FK 506-binding protein proline rotamase is a target for the immunosuppressive agent FK 506 in Saccharomyces cerevisiae. Proc. Natl. Acad. Sci. U. S. A *88*, 1948-1952.

Henderson,F.C., McCool,K., Seigle,J., Jean,W., Harter,W., and Gagnon,G.J. (2009). Treatment of chordomas with CyberKnife: georgetown university experience and treatment recommendations. Neurosurgery *64*, A44-A53.

Henderson,S.R., Guiliano,D., Presneau,N., McLean,S., Frow,R., Vujovic,S., Anderson,J., Sebire,N., Whelan,J., Athanasou,N., Flanagan,A.M., and Boshoff,C. (2005). A molecular map of mesenchymal tumors. Genome Biol. *6*, R76.

Hengstschlager,M., Rodman,D.M., Miloloza,A., Hengstschlager-Ottnad,E., Rosner,M., and Kubista,M. (2001). Tuberous sclerosis gene products in proliferation control. Mutat. Res. *488*, 233-239.

Henning L (1900). Uber congenitale echte Sakraltumoren. Beitz Z Path Anat UZ Allg Path 593.

Hernandez,S., de,M.S., Agell,L., Juanpere,N., Esgueva,R., Lorente,J.A., Mojal,S., Serrano,S., and Lloreta,J. (2009). FGFR3 mutations in prostate cancer: association with low-grade tumors. Mod. Pathol. *22*, 848-856.

Herrmann,B.G. and Kispert,A. (1994). The T genes in embryogenesis. Trends Genet. *10*, 280-286.

Herrmann,B.G., Labeit,S., Poustka,A., King,T.R., and Lehrach,H. (1990). Cloning of the T gene required in mesoderm formation in the mouse. Nature *343*, 617-622.

Higinbotham,N.L., Phillips,R.F., Farr,H.W., and Hustu,H.O. (1967). Chordoma. Thirty-five-year study at Memorial Hospital. Cancer *20*, 1841-1850.

Hof,H., Welzel,T., and Debus,J. (2006). Effectiveness of cetuximab/gefitinib in the therapy of a sacral chordoma. Onkologie *29*, 572-574.

Hoffmann,A., Czichos,S., Kaps,C., Bachner,D., Mayer,H., Kurkalli,B.G., Zilberman,Y., Turgeman,G., Pelled,G., Gross,G., and Gazit,D. (2002b). The T-box transcription factor Brachyury mediates cartilage development in mesenchymal stem cell line C3H10T1/2. J. Cell Sci. *115*, 769-781.

Holton,J.L., Steel,T., Luxsuwong,M., Crockard,H.A., and Revesz,T. (2000). Skull base chordomas: correlation of tumour doubling time with age, mitosis and Ki67 proliferation index. Neuropathol. Appl. Neurobiol. *26*, 497-503.

Horiguchi,H., Sano,T., Qian,Z.R., Hirokawa,M., Kagawa,N., Yamaguchi,T., Hirose,T., and Nagahiro,S. (2004). Expression of cell adhesion molecules in chordomas: an immunohistochemical study of 16 cases. Acta Neuropathol. *107*, 91-96.

Hruban,R.H., Traganos,F., Reuter,V.E., and Huvos,A.G. (1990). Chordomas with malignant spindle cell components. A DNA flow cytometric and immunohistochemical study with histogenetic implications. Am. J. Pathol. *137*, 435-447.

Hsieh CK and Hsieh HH (1936). Roentgenologic study of sacro- coccygeal chordoma. Radiology 101.

Hsu,T., Trojanowska,M., and Watson,D.K. (2004). Ets proteins in biological control and cancer. J. Cell Biochem. *91*, 896-903.

Hug,E.B. (2001). Review of skull base chordomas: prognostic factors and long-term results of proton-beam radiotherapy. Neurosurg. Focus. *10*, E11.

Hug,E.B., Loredo,L.N., Slater,J.D., DeVries,A., Grove,R.I., Schaefer,R.A., Rosenberg,A.E., and Slater,J.M. (1999). Proton radiation therapy for chordomas and chondrosarcomas of the skull base. J. Neurosurg. *91*, 432-439.

Husain,F. (1960). Chordoma of the thoracic spine. Report of a case. J. Bone Joint Surg. Br. *42-B*, 560-564.

Ikeda,H., Honjo,J., Sakurai,H., Mitsuhashi,N., Fukuda,T., and Niibe,H. (1997). Dedifferentiated chordoma arising in irradiated sacral chordoma. Radiat. Med. *15*, 109-111.

Imai,R., Kamada,T., Tsuji,H., Sugawara,S., Serizawa,I., Tsujii,H., and Tatezaki,S.I. (2009). Effect of Carbon Ion Radiotherapy for Sacral Chordoma: Results of Phase I-II and Phase II Clinical Trials. Int. J. Radiat. Oncol. Biol. Phys.

Inoki,K., Li,Y., Zhu,T., Wu,J., and Guan,K.L. (2002). TSC2 is phosphorylated and inhibited by Akt and suppresses mTOR signalling. Nat. Cell Biol. *4*, 648-657.

Inoki,K., Ouyang,H., Li,Y., and Guan,K.L. (2005). Signaling by target of rapamycin proteins in cell growth control. Microbiol. Mol. Biol. Rev. *69*, 79-100.

Isaacs,H.V., Pownall,M.E., and Slack,J.M. (1994). eFGF regulates Xbra expression during Xenopus gastrulation. EMBO J. *13*, 4469-4481.

Ishida,T. and Dorfman,H.D. (1994). Chondroid chordoma versus low-grade chondrosarcoma of the base of the skull: can immunohistochemistry resolve the controversy? J. Neurooncol. *18*, 199-206.

Jacobs,J.J., Keblusek,P., Robanus-Maandag,E., Kristel,P., Lingbeek,M., Nederlof,P.M., van,W.T., van,d., V, Koh,E.Y., Daley,G.Q., and van,L.M. (2000). Senescence bypass screen identifies TBX2, which represses Cdkn2a (p19(ARF)) and is amplified in a subset of human breast cancers. Nat. Genet. *26*, 291-299.

Jaeschke,A., Hartkamp,J., Saitoh,M., Roworth,W., Nobukuni,T., Hodges,A., Sampson,J., Thomas,G., and Lamb,R. (2002). Tuberous sclerosis complex tumor suppressor-mediated S6 kinase inhibition by phosphatidylinositide-3-OH kinase is mTOR independent. J. Cell Biol. *159*, 217-224.

Jensen,L.E., Barbaux,S., Hoess,K., Fraterman,S., Whitehead,A.S., and Mitchell,L.E. (2004). The human T locus and spina bifida risk. Hum. Genet. *115*, 475-482.

Jones,D.T., Kocialkowski,S., Liu,L., Pearson,D.M., Backlund,L.M., Ichimura,K., and Collins,V.P. (2008). Tandem duplication producing a novel oncogenic BRAF fusion gene defines the majority of pilocytic astrocytomas. Cancer Res. *68*, 8673-8677.

Jones,P.M., Salmon,D.M., and Howell,S.L. (1988). Protein phosphorylation in electrically permeabilized islets of Langerhans. Effects of Ca2+, cyclic AMP, a phorbol ester and noradrenaline. Biochem. J. *254*, 397-403.

Kaiser,T.E., Pritchard,D.J., and Unni,K.K. (1984). Clinicopathologic study of sacrococcygeal chordoma. Cancer *53*, 2574-2578.

Karamouzis,M.V., Konstantinopoulos,P.A., and Papavassiliou,A.G. (2007). Intriguing issues of EGFR targeting in head and neck cancer. Ann. Oncol. *18*, 962.

Kawachi,K., Masuyama,N., and Nishida,E. (2003). Essential role of the transcription factor Ets-2 in Xenopus early development. J. Biol. Chem. *278*, 5473-5477.

Kelley,M.J., Korczak,J.F., Sheridan,E., Yang,X., Goldstein,A.M., and Parry,D.M. (2001). Familial chordoma, a tumor of notochordal remnants, is linked to chromosome 7q33. Am. J. Hum. Genet. *69*, 454-460.

Kerr,W.A., Allen,K.L., Haynes,D.R., and Sellars,S.L. (1975). Letter: Familial nasopharyngeal chordoma. S. Afr. Med. J. *49*, 1584.

Klebs,E. (1864). Ein Fall Von Ecchondrosis spheno-occipital mylacea. Virchow's Arch, f. , Path. Anat. 396.

Klingler,L., Shooks,J., Fiedler,P.N., Marney,A., Butler,M.G., and Schwartz,H.S. (2000). Microsatellite instability in sacral chordoma. J. Surg. Oncol. *73*, 100-103.

Klingler,L., Trammell,R., Allan,D.G., Butler,M.G., and Schwartz,H.S. (2006). Clonality studies in sacral chordoma. Cancer Genet. Cytogenet. *171*, 68-71.

Knowles,M.A. (2008). Novel therapeutic targets in bladder cancer: mutation and expression of FGF receptors. Future. Oncol. *4*, 71-83.

Kouhara,H., Hadari,Y.R., Spivak-Kroizman,T., Schilling,J., Bar-Sagi,D., Lax,I., and Schlessinger,J. (1997). A lipid-anchored Grb2-binding protein that links FGF-receptor activation to the Ras/MAPK signaling pathway. Cell *89*, 693-702.

Kris,M.G. and Tonato,M. (2002). New approaches in the treatment of non-small cell lung cancer: taxanes in the treatment of NSCLC: pathways to progress. Lung Cancer *38 Suppl 4*, 1-3.

Krishnan,K., Bruce,B., Hewitt,S., Thomas,D., Khanna,C., and Helman,L.J. (2006). Ezrin mediates growth and survival in Ewing's sarcoma through the AKT/mTOR, but not the MAPK, signaling pathway. Clin. Exp. Metastasis *23*, 227-236.

Kunii,K., Davis,L., Gorenstein,J., Hatch,H., Yashiro,M., Di,B.A., Elbi,C., and Lutterbach,B. (2008). FGFR2-amplified gastric cancer cell lines require FGFR2 and Erbb3 signaling for growth and survival. Cancer Res. *68*, 2340-2348.

Kurien,B.T. and Scofield,R.H. (2003). Protein blotting: a review. J. Immunol. Methods *274*, 1-15.

Kwabi-Addo,B., Wang,J., Erdem,H., Vaid,A., Castro,P., Ayala,G., and Ittmann,M. (2004). The expression of Sprouty1, an inhibitor of fibroblast growth factor signal transduction, is decreased in human prostate cancer. Cancer Res. *64*, 4728-4735.

Larizza,L., Mortini,P., and Riva,P. (2005). Update on the cytogenetics and molecular genetics of chordoma. Hered. Cancer Clin. Pract. *3*, 29-41.

Laskowski J.Zarysonkologii (1955). In Pathology of Tumors, Kolodziejska H, ed. (Warsaw: PZWL), pp. 91-99.

Lee,H.S., Cho,H.H., Kim,H.K., Bae,Y.C., Baik,H.S., and Jung,J.S. (2007). Tbx3, a transcriptional factor, involves in proliferation and osteogenic differentiation of human adipose stromal cells. Mol. Cell Biochem. *296*, 129-136.

Lee-Fruman,K.K., Kuo,C.J., Lippincott,J., Terada,N., and Blenis,J. (1999). Characterization of S6K2, a novel kinase homologous to S6K1. Oncogene *18*, 5108-5114.

Lee-Jones,L., Aligianis,I., Davies,P.A., Puga,A., Farndon,P.A., Stemmer-Rachamimov,A., Ramesh,V., and Sampson,J.R. (2004). Sacrococcygeal chordomas in patients with tuberous sclerosis complex show somatic loss of TSC1 or TSC2. Genes Chromosomes Cancer *41*, 80-85.

Leproux,F., de,T.B., Aesch,B., and Cotty,P. (1993). MRI of cranial chordomas: the value of gadolinium. Neuroradiology *35*, 543-545.

Li,D.M. and Sun,H. (1998). PTEN/MMAC1/TEP1 suppresses the tumorigenicity and induces G1 cell cycle arrest in human glioblastoma cells. Proc. Natl. Acad. Sci. U. S. A *95*, 15406-15411.

Linden,O., Stenberg,L., and Kjellen,E. (2009). Regression of cervical spinal cord compression in a patient with chordoma following treatment with cetuximab and gefitinib. Acta Oncol. *48*, 158-159.

Liu,Z., Xu,J., Colvin,J.S., and Ornitz,D.M. (2002). Coordination of chondrogenesis and osteogenesis by fibroblast growth factor 18. Genes Dev. *16*, 859-869.

Llauger,J., Palmer,J., Amores,S., Bague,S., and Camins,A. (2000). Primary tumors of the sacrum: diagnostic imaging. AJR Am. J. Roentgenol. *174*, 417-424.

Lombardo,C.R., Consler,T.G., and Kassel,D.B. (1995). *In vitro* phosphorylation of the epidermal growth factor receptor autophosphorylation domain by c-src: identification of phosphorylation sites and c-src SH2 domain binding sites. Biochemistry *34*, 16456-16466.

Lountzis,N.I., Hogarty,M.D., Kim,H.J., and Junkins-Hopkins,J.M. (2006a). Cutaneous metastatic chordoma with concomitant tuberous sclerosis. J. Am. Acad. Dermatol. *55*, S6-10.

Luschka,H. (1856). Die Altersveränderungen der Zwischenwirbelknorpel. Archiv für Pathologische Anatomie, *9*, 311.

MacKenzie,A.R. and von Mehren,M. (2007). Mechanisms of mammalian target of rapamycin inhibition in sarcoma: present and future. Expert. Rev. Anticancer Ther. *7*, 1145-1154.

Magrini,S.M., Papi,M.G., Marletta,F., Tomaselli,S., Cellai,E., Mungai,V., and Biti,G. (1992). Chordoma-natural history, treatment and prognosis. The Florence Radiotherapy Department experience (1956-1990) and a critical review of the literature. Acta Oncol. *31*, 847-851.

Mamane,Y., Petroulakis,E., Rong,L., Yoshida,K., Ler,L.W., and Sonenberg,N. (2004). eIF4E--from translation to transformation. Oncogene *23*, 3172-3179.

Marshall,J. (2006). Clinical implications of the mechanism of epidermal growth factor receptor inhibitors. Cancer *107*, 1207-1218.

Martin,J.H., Fay,M.F., and Ungerer,J.P. (2009). eGFR--use beyond the evidence. Med. J. Aust. *190*, 197-199.

Mass,R.D. (2004). The HER receptor family: a rich target for therapeutic development. Int. J. Radiat. Oncol. Biol. Phys. *58*, 932-940.

Matsumoto,J., Kumano,G., and Nishida,H. (2007). Direct activation by Ets and Zic is required for initial expression of the Brachyury gene in the ascidian notochord. Dev. Biol. *306*, 870-882.

Matsuno,A. and Nagashima,T. (2000). Radiation therapy for chordomas. J. Neurosurg. *93*, 157.

Matsuno,A., Sasaki,T., Nagashima,T., Matsuura,R., Tanaka,H., Hirakawa,M., Murakami,M., and Kirino,T. (1997). Immunohistochemical examination of proliferative potentials and the expression of cell cycle-related proteins of intracranial chordomas. Hum. Pathol. *28*, 714-719.

McMaster,M.L., Goldstein,A.M., Bromley,C.M., Ishibe,N., and Parry,D.M. (2001). Chordoma: incidence and survival patterns in the United States, 1973-1995. Cancer Causes Control *12*, 1-11.

McPherson,C.M., Suki,D., McCutcheon,I.E., Gokaslan,Z.L., Rhines,L.D., and Mendel,E. (2006). Metastatic disease from spinal chordoma: a 10-year experience. J. Neurosurg. Spine *5*, 277-280.

Meakin,S.O., MacDonald,J.I., Gryz,E.A., Kubu,C.J., and Verdi,J.M. (1999). The signaling adapter FRS-2 competes with Shc for binding to the nerve growth factor receptor TrkA. A model for discriminating proliferation and differentiation. J. Biol. Chem. *274*, 9861-9870.

Mehra,R., Tomlins,S.A., Shen,R., Nadeem,O., Wang,L., Wei,J.T., Pienta,K.J., Ghosh,D., Rubin,M.A., Chinnaiyan,A.M., and Shah,R.B. (2007). Comprehensive assessment of TMPRSS2 and ETS family gene aberrations in clinically localized prostate cancer. Mod. Pathol. *20*, 538-544.

Mehta,P., Robson,C.N., Neal,D.E., and Leung,H.Y. (2000). Fibroblast growth factor receptor-2 mutation analysis in human prostate cancer. BJU. Int. *86*, 681-685.

Meis,J.M., Raymond,A.K., Evans,H.L., Charles,R.E., and Giraldo,A.A. (1987). "Dedifferentiated" chordoma. A clinicopathologic and immunohistochemical study of three cases. Am. J. Surg. Pathol. *11*, 516-525.

Meisler,M. (1997). Mutation watch. Mamm. Genome *8*, 305-306.

Mendelsohn,J. (2001). The epidermal growth factor receptor as a target for cancer therapy. Endocr. Relat Cancer *8*, 3-9.

Mendelsohn,J. and Baselga,J. (2003). Status of epidermal growth factor receptor antagonists in the biology and treatment of cancer. J. Clin. Oncol. *21*, 2787-2799.

Mertens,F., Kreicbergs,A., Rydholm,A., Willen,H., Carlen,B., Mitelman,F., and Mandahl,N. (1994). Clonal chromosome aberrations in three sacral chordomas. Cancer Genet. Cytogenet. *73*, 147-151.

Miozzo,M., Dalpra,L., Riva,P., Volonta,M., Macciardi,F., Pericotti,S., Tibiletti,M.G., Cerati,M., Rohde,K., Larizza,L., and Fuhrman Conti,A.M. (2000). A tumor suppressor locus in familial and sporadic chordoma maps to 1p36. Int. J. Cancer *87*, 68-72.

Mirra JM, Della Rocca C, Nelson SD, and Mertens F (2002). In Pathology and genetics of tumours of soft tissue and bone, Fletcher CDM, Unni KK, and Mertens F, eds. (Lyon: IARC Press), pp. 316-317.

Missiaglia,E., Selfe,J., Hamdi,M., Williamson,D., Schaaf,G., Fang,C., Koster,J., Summersgill,B., Messahel,B., Versteeg,R., Pritchard-Jones,K., Kool,M., and Shipley,J. (2009). Genomic imbalances in rhabdomyosarcoma cell lines affect expression of genes frequently altered in primary tumors: an approach to identify candidate genes involved in tumor development. Genes Chromosomes. Cancer *48*, 455-467.

Mitchell,A., Scheithauer,B.W., Unni,K.K., Forsyth,P.J., Wold,L.E., and McGivney,D.J. (1993). Chordoma and chondroid neoplasms of the spheno-occiput. An immunohistochemical study of 41 cases with prognostic and nosologic implications. Cancer *72*, 2943-2949.

Mizoe,J.E., Hasegawa,A., Takagi,R., Bessho,H., Onda,T., and Tsujii,H. (2009). Carbon ion radiotherapy for skull base chordoma. Skull. Base. *19*, 219-224.

Mori,K., Chano,T., Kushima,R., Hukuda,S., and Okabe,H. (2002). Expression of E-cadherin in chordomas: diagnostic marker and possible role of tumor cell affinity. Virchows Arch. *440*, 123-127.

Morimitsu,Y., Aoki,T., Yokoyama,K., and Hashimoto,H. (2000). Sarcomatoid chordoma: chordoma with a massive malignant spindle-cell component. Skeletal Radiol. *29*, 721-725.

Moroni,M., Veronese,S., Benvenuti,S., Marrapese,G., Sartore-Bianchi,A., Di,N.F., Gambacorta,M., Siena,S., and Bardelli,A. (2005). Gene copy number for epidermal growth factor receptor (EGFR) and clinical response to antiEGFR treatment in colorectal cancer: a cohort study. Lancet Oncol. *6*, 279-286.

Muenke,M., Gripp,K.W., Donald-McGinn,D.M., Gaudenz,K., Whitaker,L.A., Bartlett,S.P., Markowitz,R.I., Robin,N.H., Nwokoro,N., Mulvihill,J.J., Losken,H.W., Mulliken,J.B., Guttmacher,A.E., Wilroy,R.S., Clarke,L.A., Hollway,G., Ades,L.C., Haan,E.A., Mulley,J.C., Cohen,M.M., Jr., Bellus,G.A., Francomano,C.A., Moloney,D.M., Wall,S.A., Wilkie,A.O., and . (1997). A unique point mutation in the fibroblast growth factor receptor 3 gene (FGFR3) defines a new craniosynostosis syndrome. Am. J. Hum. Genet. *60*, 555-564.

Muenke,M., Schell,U., Hehr,A., Robin,N.H., Losken,H.W., Schinzel,A., Pulleyn,L.J., Rutland,P., Reardon,W., Malcolm,S., and . (1994). A common mutation in the fibroblast growth factor receptor 1 gene in Pfeiffer syndrome. Nat. Genet. *8*, 269-274.

Müller, H (1858). Ueber das Vorkommen von Resten der Chorda dorsalis bei Menschen nach der Geburt und über ihr Verhültniss zu den Gallertgeschwülsten am Clivus. Z Rationelle Med 202-229.

Muller,C.W. and Herrmann,B.G. (1997). Crystallographic structure of the T domain-DNA complex of the Brachyury transcription factor. Nature *389*, 884-888.

Munzenrider,J.E. and Liebsch,N.J. (1999). Proton therapy for tumors of the skull base. Strahlenther. Onkol. *175 Suppl 2*, 57-63.

Murad,T.M. and Murthy,M.S. (1970). Ultrastructure of a chordoma. Cancer *25*, 1204-1215.

Murphy,J.M., Wallis,F., Toland,J., Toner,M., and Wilson,G.F. (1998). CT and MRI appearances of a thoracic chordoma. Eur. Radiol. *8*, 1677-1679.

Muthukumar,N., Kondziolka,D., Lunsford,L.D., and Flickinger,J.C. (1998). Stereotactic radiosurgery for chordoma and chondrosarcoma: further experiences. Int. J. Radiat. Oncol. Biol. Phys. *41*, 387-392.

Naka,T., Boltze,C., Kuester,D., Schulz,T.O., Samii,A., Herold,C., Ostertag,H., and Roessner,A. (2004). Expression of matrix metalloproteinase (MMP)-1, MMP-2, MMP-9, cathepsin B, and urokinase plasminogen activator in non-skull base chordoma. Am. J. Clin. Pathol. *122*, 926-930.

Naka,T., Boltze,C., Kuester,D., Schulz,T.O., Schneider-Stock,R., Kellner,A., Samii,A., Herold,C., Ostertag,H., and Roessner,A. (2005). Alterations of G1-S checkpoint in chordoma: the prognostic impact of p53 overexpression. Cancer *104*, 1255-1263.

Naka,T., Boltze,C., Samii,A., Herold,C., Ostertag,H., Iwamoto,Y., Oda,Y., Tsuneyoshi,M., Kuester,D., and Roessner,A. (2003). Skull base and nonskull base chordomas: clinicopathologic and immunohistochemical study with special reference to nuclear pleomorphism and proliferative ability. Cancer *98*, 1934-1941.

Naka,T., Fukuda,T., Chuman,H., Iwamoto,Y., Sugioka,Y., Fukui,M., and Tsuneyoshi,M. (1996). Proliferative activities in conventional chordoma: a clinicopathologic, DNA flow cytometric, and immunohistochemical analysis of 17 specimens with special reference to anaplastic chordoma showing a diffuse proliferation and nuclear atypia. Hum. Pathol. *27*, 381-388.

Naka,T., Kuester,D., Boltze,C., Scheil-Bertram,S., Samii,A., Herold,C., Ostertag,H., Krueger,S., and Roessner,A. (2008). Expression of hepatocyte growth factor and c-MET in skull base chordoma. Cancer *112*, 104-110.

Naka,T., Oda,Y., Iwamoto,Y., Shinohara,N., Chuman,H., Fukui,M., and Tsuneyoshi,M. (2001). Immunohistochemical analysis of E-cadherin, alpha-catenin, beta-catenin, gamma-catenin, and neural cell adhesion molecule (NCAM) in chordoma. J. Clin. Pathol. *54*, 945-950.

Nakatani,Y., Yasuo,H., Satoh,N., and Nishida,H. (1996). Basic fibroblast growth factor induces notochord formation and the expression of As-T, a Brachyury homolog, during ascidian embryogenesis. Development *122*, 2023-2031.

Nojima,H., Tokunaga,C., Eguchi,S., Oshiro,N., Hidayat,S., Yoshino,K., Hara,K., Tanaka,N., Avruch,J., and Yonezawa,K. (2003). The mammalian target of rapamycin (mTOR) partner, raptor, binds the mTOR substrates p70 S6 kinase and 4E-BP1 through their TOR signaling (TOS) motif. J. Biol. Chem. *278*, 15461-15464.

Nucera,C., Goldfarb,M., Hodin,R., and Parangi,S. (2009). Role of B-RafV600E in differentiated thyroid cancer and preclinical validation of compounds against B-RafV600E. Biochimica et Biophysica Acta (BBA) - Reviews on Cancer *1795*, 152-161.

O'Connell,J.X., Renard,L.G., Liebsch,N.J., Efird,J.T., Munzenrider,J.E., and Rosenberg,A.E. (1994a). Base of skull chordoma. A correlative study of histologic and clinical features of 62 cases. Cancer *74*, 2261-2267.

O'Donnell,P., Tirabosco,R., Vujovic,S., Bartlett,W., Briggs,T.W., Henderson,S., Boshoff,C., and Flanagan,A.M. (2007). Diagnosing an extra-axial chordoma of the proximal tibia with the help of brachyury, a molecule required for notochordal differentiation. Skeletal Radiol. *36*, 59-65.

Ornitz,D.M. and Marie,P.J. (2002). FGF signaling pathways in endochondral and intramembranous bone development and human genetic disease. Genes Dev. *16*, 1446-1465.

Osaka,S., Matsuzaki,H., Osaka,E., Yoshida,Y., and Ryu,J. (2008). A comparative study for wide excision of malignant tumors distal to S2. Anticancer Res. *28*, 4143-4147.

Ostroumov,E. and Hunter,C.J. (2008). Identifying mechanisms for therapeutic intervention in chordoma: c-Met oncoprotein. Spine (Phila Pa 1976.) *33*, 2774-2780.

Park,J.B., Lee,C.K., Koh,J.S., Lee,J.K., Park,E.Y., and Riew,K.D. (2007). Overexpressions of nerve growth factor and its tropomyosin-related kinase A receptor on chordoma cells. Spine (Phila Pa 1976.) *32*, 1969-1973.

Park,L., Delaney,T.F., Liebsch,N.J., Hornicek,F.J., Goldberg,S., Mankin,H., Rosenberg,A.E., Rosenthal,D.I., and Suit,H.D. (2006). Sacral chordomas: Impact of high-dose proton/photon-beam radiation therapy combined with or without surgery for primary versus recurrent tumor. Int. J. Radiat. Oncol. Biol. Phys. *65*, 1514-1521.

Persson,S., Kindblom,L.G., and Angervall,L. (1991). Classical and chondroid chordoma. A light-microscopic, histochemical, ultrastructural and immunohistochemical analysis of the various cell types. Pathol. Res. Pract. *187*, 828-838.

Perzin,K.H. and Pushparaj,N. (1986). Nonepithelial tumors of the nasal cavity, paranasal sinuses, and nasopharynx. A clinicopathologic study. XIV: Chordomas. Cancer *57*, 784-796.

Peyssonnaux,C. and Eychene,A. (2001). The Raf/MEK/ERK pathway: new concepts of activation. Biol. Cell *93*, 53-62.

Plas,D.R. and Thompson,C.B. (2003). Akt activation promotes degradation of tuberin and FOXO3a via the proteasome. J. Biol. Chem. *278*, 12361-12366.

Pollock,P.M., Gartside,M.G., Dejeza,L.C., Powell,M.A., Mallon,M.A., Davies,H., Mohammadi,M., Futreal,P.A., Stratton,M.R., Trent,J.M., and Goodfellow,P.J. (2007). Frequent activating FGFR2 mutations in endometrial carcinomas parallel germline mutations associated with craniosynostosis and skeletal dysplasia syndromes. Oncogene *26*, 7158-7162.

Ptaszynski,K., Szumera-Cieckiewicz,A., Owczarek,J., Mrozkowiak,A., Pekul,M., Baranska,J., and Rutkowski,P. (2009). Epidermal growth factor receptor (EGFR) status in chordoma. Pol. J. Pathol. *60*, 81-87.

Radu,A., Neubauer,V., Akagi,T., Hanafusa,H., and Georgescu,M.M. (2003). PTEN induces cell cycle arrest by decreasing the level and nuclear localization of cyclin D1. Mol. Cell Biol. *23*, 6139-6149.

Raffel,C., Wright,D.C., Gutin,P.H., and Wilson,C.B. (1985). Cranial chordomas: clinical presentation and results of operative and radiation therapy in twenty-six patients. Neurosurgery *17*, 703-710.

Raponi,M., Winkler,H., and Dracopoli,N.C. (2008). KRAS mutations predict response to EGFR inhibitors. Curr. Opin. Pharmacol. *8*, 413-418.

Raught,B., Peiretti,F., Gingras,A.C., Livingstone,M., Shahbazian,D., Mayeur,G.L., Polakiewicz,R.D., Sonenberg,N., and Hershey,J.W. (2004). Phosphorylation of eucaryotic translation initiation factor 4B Ser422 is modulated by S6 kinases. EMBO J. *23*, 1761-1769.

Raul,P. and Diss,A. (1924). Chordome maIin de Ia colonne vertebrale lombaire. Bull. et. Mem. Soc. Anat. de Paris 395-402.

Rego,R.L., Foster,N.R., Smyrk,T.C., Le,M., O'Connell,M.J., Sargent,D.J., Windschitl,H., and Sinicrope,F.A. (2010). Prognostic effect of activated EGFR expression in human colon carcinomas: comparison with EGFR status. Br. J. Cancer *102*, 165-172.

Reis-Filho,J.S., Simpson,P.T., Turner,N.C., Lambros,M.B., Jones,C., Mackay,A., Grigoriadis,A., Sarrio,D., Savage,K., Dexter,T., Iravani,M., Fenwick,K., Weber,B., Hardisson,D., Schmitt,F.C., Palacios,J., Lakhani,S.R., and Ashworth,A. (2006). FGFR1

emerges as a potential therapeutic target for lobular breast carcinomas. Clin. Cancer Res. *12*, 6652-6662.

Ribbert H (1894). Ueber die Eccchondrosys physaliphora sphenooccipitalis. Zentralbl Allg Pathol 457-461.

Ribbert H (1895). Ueber die experimentelle Erzeugugng einer Ecchondrosis Physaliphora. Verh Dtsch Kongr Int Med 455-464.

Rich,T.A., Schiller,A., Suit,H.D., and Mankin,H.J. (1985). Clinical and pathologic review of 48 cases of chordoma. Cancer *56*, 182-187.

Richardson,C.J., Broenstrup,M., Fingar,D.C., Julich,K., Ballif,B.A., Gygi,S., and Blenis,J. (2004). SKAR is a specific target of S6 kinase 1 in cell growth control. Curr. Biol. *14*, 1540-1549.

Riemenschneider,M.J., Betensky,R.A., Pasedag,S.M., and Louis,D.N. (2006). AKT activation in human glioblastomas enhances proliferation via TSC2 and S6 kinase signaling. Cancer Res. *66*, 5618-5623.

Risinger,J.I., Hayes,A.K., Berchuck,A., and Barrett,J.C. (1997). PTEN/MMAC1 mutations in endometrial cancers. Cancer Res. *57*, 4736-4738.

Riva,P., Crosti,F., Orzan,F., Dalpra,L., Mortini,P., Parafioriti,A., Pollo,B., Fuhrman Conti,A.M., Miozzo,M., and Larizza,L. (2003). Mapping of candidate region for chordoma development to 1p36.13 by LOH analysis. Int. J. Cancer *107*, 493-497.

Roberts,R.B., Min,L., Washington,M.K., Olsen,S.J., Settle,S.H., Coffey,R.J., and Threadgill,D.W. (2002). Importance of epidermal growth factor receptor signaling in establishment of adenomas and maintenance of carcinomas during intestinal tumorigenesis. Proc. Natl. Acad. Sci. U. S. A *99*, 1521-1526.

Rocha-Lima,C.M., Soares,H.P., Raez,L.E., and Singal,R. (2007). EGFR targeting of solid tumors. Cancer Control *14*, 295-304.

Rojo,F., Najera,L., Lirola,J., Jimenez,J., Guzman,M., Sabadell,M.D., Baselga,J., and Cajal,S. (2007). 4E-binding protein 1, a cell signaling hallmark in breast cancer that correlates with pathologic grade and prognosis. Clin. Cancer Res. *13*, 81-89.

Romeo,S. and Hogendoorn,P.C. (2006). Brachyury and chordoma: the chondroid-chordoid dilemma resolved? J. Pathol. *209*, 143-146.

Rosenberg,A.E., Brown,G.A., Bhan,A.K., and Lee,J.M. (1994). Chondroid chordoma--a variant of chordoma. A morphologic and immunohistochemical study. Am. J. Clin. Pathol. *101*, 36-41.

Rosenberg,A.E., Nielsen,G.P., Keel,S.B., Renard,L.G., Fitzek,M.M., Munzenrider,J.E., and Liebsch,N.J. (1999). Chondrosarcoma of the base of the skull: a clinicopathologic study of 200 cases with emphasis on its distinction from chordoma. Am. J. Surg. Pathol. *23*, 1370-1378.

Ross,D.E., Buchanan,R.W., Medoff,D., Lahti,A.C., and Thaker,G.K. (1998). Association between eye tracking disorder in schizophrenia and poor sensory integration. Am. J. Psychiatry *155*, 1352-1357.

Rosty,C., Aubriot,M.H., Cappellen,D., Bourdin,J., Cartier,I., Thiery,J.P., Sastre-Garau,X., and Radvanyi,F. (2005). Clinical and biological characteristics of cervical neoplasias with FGFR3 mutation. Mol. Cancer *4*, 15.

Roux,P.P., Ballif,B.A., Anjum,R., Gygi,S.P., and Blenis,J. (2004). Tumor-promoting phorbol esters and activated Ras inactivate the tuberous sclerosis tumor suppressor complex via p90 ribosomal S6 kinase. Proc. Natl. Acad. Sci. U. S. A *101*, 13489-13494.

Rozeman,L.B., Szuhai,K., Schrage,Y.M., Rosenberg,C., Tanke,H.J., Taminiau,A.H., Cleton-Jansen,A.M., Bovee,J.V., and Hogendoorn,P.C. (2006). Array-comparative genomic hybridization of central chondrosarcoma: identification of ribosomal protein S6 and cyclin-dependent kinase 4 as candidate target genes for genomic aberrations. Cancer *107*, 380-388.

Ruvinsky,I. and Meyuhas,O. (2006). Ribosomal protein S6 phosphorylation: from protein synthesis to cell size. Trends Biochem. Sci. *31*, 342-348.

Ruvinsky,I., Sharon,N., Lerer,T., Cohen,H., Stolovich-Rain,M., Nir,T., Dor,Y., Zisman,P., and Meyuhas,O. (2005). Ribosomal protein S6 phosphorylation is a determinant of cell size and glucose homeostasis. Genes Dev. *19*, 2199-2211.

Saad,A.G. and Collins,M.H. (2005). Prognostic value of MIB-1, E-cadherin, and CD44 in pediatric chordomas. Pediatr. Dev. Pathol. *8*, 362-368.

Sabatini,D.M., Erdjument-Bromage,H., Lui,M., Tempst,P., and Snyder,S.H. (1994). RAFT1: a mammalian protein that binds to FKBP12 in a rapamycin-dependent fashion and is homologous to yeast TORs. Cell *78*, 35-43.

Sacchi,N., Watson,D.K., Guerts van Kessel,A.H., Hagemeijer,A., Kersey,J., Drabkin,H.D., Patterson,D., and Papas,T.S. (1986). Hu-ets-1 and Hu-ets-2 genes are transposed in acute leukemias with (4;11) and (8;21) translocations. Science *231*, 379-382.

Saito,A., Hasegawa,T., Shimoda,T., Toda,G., Hirohashi,S., Tajima,G., and Moriya,Y. (1998). Dedifferentiated chordoma: a case report. Jpn. J. Clin. Oncol. *28*, 766-771.

Salisbury,J.R. (1993). The pathology of the human notochord. J. Pathol. *171*, 253-255.

Salisbury,J.R., Deverell,M.H., Cookson,M.J., and Whimster,W.F. (1993). Three-dimensional reconstruction of human embryonic notochords: clue to the pathogenesis of chordoma. J. Pathol. *171*, 59-62.

Salisbury,J.R. and Isaacson,P.G. (1985). Demonstration of cytokeratins and an epithelial membrane antigen in chordomas and human fetal notochord. Am. J. Surg. Pathol. *9*, 791-797.

Santarius,T., Shipley,J., Brewer,D., Stratton,M.R., and Cooper,C.S. (2010). A census of amplified and overexpressed human cancer genes. Nat. Rev. Cancer *10*, 59-64.

Sarbassov,D.D., Ali,S.M., Kim,D.H., Guertin,D.A., Latek,R.R., Erdjument-Bromage,H., Tempst,P., and Sabatini,D.M. (2004). Rictor, a novel binding partner of mTOR, defines a rapamycin-insensitive and raptor-independent pathway that regulates the cytoskeleton. Curr. Biol. *14*, 1296-1302.

Sarbassov,D.D., Guertin,D.A., Ali,S.M., and Sabatini,D.M. (2005). Phosphorylation and regulation of Akt/PKB by the rictor-mTOR complex. Science *307*, 1098-1101.

Sartore-Bianchi,A., Moroni,M., Veronese,S., Carnaghi,C., Bajetta,E., Luppi,G., Sobrero,A., Barone,C., Cascinu,S., Colucci,G., Cortesi,E., Nichelatti,M., Gambacorta,M., and Siena,S. (2007). Epidermal growth factor receptor gene copy number and clinical outcome of metastatic colorectal cancer treated with panitumumab. J. Clin. Oncol. *25*, 3238-3245.

Sato,T., Seyama,K., Fujii,H., Maruyama,H., Setoguchi,Y., Iwakami,S., Fukuchi,Y., and Hino,O. (2002). Mutation analysis of the TSC1 and TSC2 genes in Japanese patients with pulmonary lymphangioleiomyomatosis. J. Hum. Genet. *47*, 20-28.

Sawyer,J.R., Husain,M., and Al-Mefty,O. (2001). Identification of isochromosome 1q as a recurring chromosome aberration in skull base chordomas: a new marker for aggressive tumors? Neurosurg. Focus. *10*, E6.

Saxena,N., Lahiri,S.S., Hambarde,S., and Tripathi,R.P. (2008). RAS: target for cancer therapy. Cancer Invest *26*, 948-955.

Scheil,S., Bruderlein,S., Liehr,T., Starke,H., Herms,J., Schulte,M., and Moller,P. (2001). Genome-wide analysis of sixteen chordomas by comparative genomic hybridization and cytogenetics of the first human chordoma cell line, U-CH1. Genes Chromosomes. Cancer *32*, 203-211.

Scheper,M.A., Chaisuparat,R., Nikitakis,N.G., and Sauk,J.J. (2008). Expression and alterations of the PTEN / AKT / mTOR pathway in ameloblastomas. Oral Dis. *14*, 561-568.

Schlessinger,J. (2000). Cell signaling by receptor tyrosine kinases. Cell *103*, 211-225.

Schroeder,B.A., Wells,R.G., Starshak,R.J., and Sty,J.R. (1987). Clivus chordoma in a child with tuberous sclerosis: CT and MR demonstration. J. Comput. Assist. Tomogr. *11*, 195-196.

Schulte-Merker,S. and Smith,J.C. (1995). Mesoderm formation in response to Brachyury requires FGF signalling. Curr. Biol. *5*, 62-67.

Schulz-Ertner,D., Nikoghosyan,A., Didinger,B., Karger,C.P., Jakel,O., Wannenmacher,M., and Debus,J. (2003a). Treatment planning intercomparison for spinal chordomas using intensity-modulated photon radiation therapy (IMRT) and carbon ions. Phys. Med. Biol. *48*, 2617-2631.

Schulz-Ertner,D., Nikoghosyan,A., Thilmann,C., Haberer,T., Jakel,O., Karger,C., Scholz,M., Kraft,G., Wannenmacher,M., and Debus,J. (2003b). Carbon ion radiotherapy for chordomas and low-grade chondrosarcomas of the skull base. Results in 67 patients. Strahlenther. Onkol. *179*, 598-605.

Schwab,J., Antonescu,C., Boland,P., Healey,J., Rosenberg,A., Nielsen,P., Iafrate,J., Delaney,T., Yoon,S., Choy,E., Harmon,D., Raskin,K., Yang,C., Mankin,H., Springfield,D., Hornicek,F., and Duan,Z. (2009a). Combination of PI3K/mTOR inhibition demonstrates efficacy in human chordoma. Anticancer Res. *29*, 1867-1871.

Schwab,J.H., Boland,P.J., Agaram,N.P., Socci,N.D., Guo,T., O'Toole,G.C., Wang,X., Ostroumov,E., Hunter,C.J., Block,J.A., Doty,S., Ferrone,S., Healey,J.H., and Antonescu,C.R. (2009b). Chordoma and chondrosarcoma gene profile: implications for immunotherapy. Cancer Immunol. Immunother. *58*, 339-349.

Scimeca,P.G., James-Herry,A.G., Black,K.S., Kahn,E., and Weinblatt,M.E. (1996). Chemotherapeutic treatment of malignant chordoma in children. J. Pediatr. Hematol. Oncol. *18*, 237-240.

Scolyer,R.A., Bonar,S.F., Palmer,A.A., Barr,E.M., Wills,E.J., Stalley,P., Schatz,J., Soper,J., Li,L.X., and McCarthy,S.W. (2004). Parachordoma is not distinguishable from axial chordoma using immunohistochemistry. Pathol. Int. *54*, 364-370.

Shin,E.Y., Lee,B.H., Yang,J.H., Shin,K.S., Lee,G.K., Yun,H.Y., Song,Y.J., Park,S.C., and Kim,E.G. (2000). Up-regulation and co-expression of fibroblast growth factor receptors in human gastric cancer. J. Cancer Res. Clin. Oncol. *126*, 519-528.

Showell,C., Binder,O., and Conlon,F.L. (2004). T-box genes in early embryogenesis. Dev. Dyn. *229*, 201-218.

Sinclair,C.S., Adem,C., Naderi,A., Soderberg,C.L., Johnson,M., Wu,K., Wadum,L., Couch,V.L., Sellers,T.A., Schaid,D., Slezak,J., Fredericksen,Z., Ingle,J.N., Hartmann,L., Jenkins,R.B., and Couch,F.J. (2002). TBX2 is preferentially amplified in B. Cancer Res. *62*, 3587-3591.

Sinclair,C.S., Rowley,M., Naderi,A., and Couch,F.J. (2003). The 17q23 amplicon and breast cancer. Breast Cancer Res. Treat. *78*, 313-322.

Singhal,N., Kotasek,D., and Parnis,F.X. (2009). Response to erlotinib in a patient with treatment refractory chordoma. Anticancer Drugs *20*, 953-955.

Smith,J.C., Price,B.M., Green,J.B., Weigel,D., and Herrmann,B.G. (1991). Expression of a Xenopus homolog of Brachyury (T) is an immediate-early response to mesoderm induction. Cell *67*, 79-87.

Smolders,D., Wang,X., Drevelengas,A., Vanhoenacker,F., and De Schepper,A.M. (2003). Value of MRI in the diagnosis of non-clival, non-sacral chordoma. Skeletal Radiol. *32*, 343-350.

Song,R.X., McPherson,R.A., Adam,L., Bao,Y., Shupnik,M., Kumar,R., and Santen,R.J. (2002). Linkage of rapid estrogen action to MAPK activation by ERalpha-Shc association and Shc pathway activation. Mol. Endocrinol. *16*, 116-127.

SPJUT,H.J. and LUSE,S.A. (1964). CHORDOMA: AN ELECTRON MICROSCOPIC STUDY. Cancer *17*, 643-656.

Stacchiotti,S., Casali,P.G., Lo,V.S., Mariani,L., Palassini,E., Mercuri,M., Alberghini,M., Pilotti,S., Zanella,L., Gronchi,A., and Picci,P. (2010). Chordoma of the mobile spine and sacrum: a retrospective analysis of a series of patients surgically treated at two referral centers. Ann. Surg. Oncol. *17*, 211-219.

Stacchiotti S, Ferrari S, Ferraresi V, Grignani F, Crippa A, Messina A, Spreafico C, Tamborini E, Gronchi A, and Casali PG. (2007). Imatinib mesylate in advanced chordoma: a multicenter phase II study [Abstract]. J Clin Oncol. *255(Suppl 18)*, 10003.

Stacchiotti,S., Marrari,A., Tamborini,E., Palassini,E., Virdis,E., Messina,A., Crippa,F., Morosi,C., Gronchi,A., Pilotti,S., and Casali,P.G. (2009). Response to imatinib plus sirolimus in advanced chordoma. Ann. Oncol. *20*, 1886-1894.

Stemple,D.L. (2005). Structure and function of the notochord: an essential organ for chordate development. Development *132*, 2503-2512.

Stepanek,J., Cataldo,S.A., Ebersold,M.J., Lindor,N.M., Jenkins,R.B., Unni,K., Weinshenker,B.G., and Rubenstein,R.L. (1998). Familial chordoma with probable autosomal dominant inheritance. Am. J. Med. Genet. *75*, 335-336.

Stephens,L., Anderson,K., Stokoe,D., Erdjument-Bromage,H., Painter,G.F., Holmes,A.B., Gaffney,P.R., Reese,C.B., McCormick,F., Tempst,P., Coadwell,J., and Hawkins,P.T. (1998). Protein kinase B kinases that mediate phosphatidylinositol 3,4,5-trisphosphate-dependent activation of protein kinase B. Science *279*, 710-714.

Sundaresan,N. (1986). Chordomas. Clin. Orthop. Relat Res. 135-142.

Sundaresan,N., Huvos,A.G., Krol,G., Lane,J.M., and Brennan,M. (1987). Surgical treatment of spinal chordomas. Arch. Surg. *122*, 1479-1482.

Sze,G., Uichanco,L.S., III, Brant-Zawadzki,M.N., Davis,R.L., Gutin,P.H., Wilson,C.B., Norman,D., and Newton,T.H. (1988). Chordomas: MR imaging. Radiology *166*, 187-191.

Takahashi,S., Kawase,T., Yoshida,K., Hasegawa,A., and Mizoe,J.E. (2009). Skull base chordomas: efficacy of surgery followed by carbon ion radiotherapy. Acta Neurochir. (Wien.) *151*, 759-769.

Tamayama,C., Miyauchi,M., and Maruyama,K. (1990). [Expression of embryonal and differentiational proteins in chordomas and in the notochord]. Gan No Rinsho *36*, 7-12.

Tamborini,E., Miselli,F., Negri,T., Lagonigro,M.S., Staurengo,S., Dagrada,G.P., Stacchiotti,S., Pastore,E., Gronchi,A., Perrone,F., Carbone,A., Pierotti,M.A., Casali,P.G., and Pilotti,S. (2006). Molecular and biochemical analyses of platelet-derived growth factor receptor (PDGFR) B, PDGFRA, and KIT receptors in chordomas. Clin. Cancer Res. *12*, 6920-6928.

Taniguchi,K., Tateishi,A., Higaki,S., Igarashi,M., Hayashi,V., Inoue,S., and Shoji,H. (1984). Type of collagen in chordoma. Nippon Seikeigeka Gakkai Zasshi *58*, 829-834.

Thatcher,N., Faivre-Finn,C., and Lorigan,P. (2005). Management of small-cell lung cancer. Ann. Oncol. *16 Suppl 2*, ii235-ii239.

Thieblemont,C., Biron,P., Rocher,F., Bouhour,D., Bobin,J.Y., Gerard,J.P., and Blay,J.Y. (1995). Prognostic factors in chordoma: role of postoperative radiotherapy. Eur. J. Cancer *31A*, 2255-2259.

Tirabosco,R., Mangham,D.C., Rosenberg,A.E., Vujovic,S., Bousdras,K., Pizzolitto,S., De,M.G., den Bakker,M.A., Di,F.L., Kalil,R.K., Athanasou,N.A., O'Donnell,P., McCarthy,E.F., and Flanagan,A.M. (2008). Brachyury expression in extra-axial skeletal and soft tissue chordomas: a marker that distinguishes chordoma from mixed tumor/myoepithelioma/parachordoma in soft tissue. Am. J. Surg. Pathol. *32*, 572-580.

Tkaczyk,C., Metcalfe,D.D., and Gilfillan,A.M. (2002). Determination of protein phosphorylation in Fc epsilon RI-activated human mast cells by immunoblot analysis requires protein extraction under denaturing conditions. J. Immunol. Methods *268*, 239-243.

Toker,A. and Newton,A.C. (2000). Cellular signaling: pivoting around PDK-1. Cell *103*, 185-188.

Tomlinson,D.C., Baldo,O., Harnden,P., and Knowles,M.A. (2007). FGFR3 protein expression and its relationship to mutation status and prognostic variables in bladder cancer. J. Pathol. *213*, 91-98.

Torres,M.A., Chang,E.L., Mahajan,A., Lege,D.G., Riley,B.A., Zhang,X., Lii,M., Kornguth,D.G., Pelloski,C.E., and Woo,S.Y. (2009). Optimal treatment planning for skull base chordoma: photons, protons, or a combination of both? Int. J. Radiat. Oncol. Biol. Phys. *74*, 1033-1039.

Tost,J. and Gut,I.G. (2007). DNA methylation analysis by pyrosequencing. Nat. Protoc. *2*, 2265-2275.

Trudel,S., Stewart,A.K., Rom,E., Wei,E., Li,Z.H., Kotzer,S., Chumakov,I., Singer,Y., Chang,H., Liang,S.B., and Yayon,A. (2006). The inhibitory anti-FGFR3 antibody, PRO-001, is cytotoxic to t(4;14) multiple myeloma cells. Blood *107*, 4039-4046.

Ueda,Y., Oda,Y., Kawashima,A., Tsuchiya,H., Tomita,K., and Nakanishi,I. (1992). Collagenous and basement membrane proteins of chordoma: immunohistochemical analysis. Histopathology *21*, 345-352.

Ulich,T.R. and Mirra,J.M. (1982). Ecchordosis physaliphora vertebralis. Clin. Orthop. Relat Res. 282-289.

Ullrich,A., Coussens,L., Hayflick,J.S., Dull,T.J., Gray,A., Tam,A.W., Lee,J., Yarden,Y., Libermann,T.A., Schlessinger,J., and . (1984). Human epidermal growth factor receptor cDNA sequence and aberrant expression of the amplified gene in A431 epidermoid carcinoma cells. Nature *309*, 418-425.

Ullrich,A. and Schlessinger,J. (1990). Signal transduction by receptors with tyrosine kinase activity. Cell *61*, 203-212.

van Akkooi,A.C., van Geel,A.N., Bessems,J.H., and den Bakker,M.A. (2006). Extra-axial chordoma. J. Bone Joint Surg. Br. *88*, 1232-1234.

van Krieken,J.H., Jung,A., Kirchner,T., Carneiro,F., Seruca,R., Bosman,F.T., Quirke,P., Flejou,J.F., Plato,H.T., de,H.G., Jares,P., Langner,C., Hoefler,G., Ligtenberg,M., Tiniakos,D., Tejpar,S., Bevilacqua,G., and Ensari,A. (2008). KRAS mutation testing for predicting response to anti-EGFR therapy for colorectal carcinoma: proposal for an European quality assurance program. Virchows Arch. *453*, 417-431.

van Rhijn,B.W., van Tilborg,A.A., Lurkin,I., Bonaventure,J., de,V.A., Thiery,J.P., van der Kwast,T.H., Zwarthoff,E.C., and Radvanyi,F. (2002). Novel fibroblast growth factor receptor 3 (FGFR3) mutations in bladder cancer previously identified in non-lethal skeletal disorders. Eur. J. Hum. Genet. *10*, 819-824.

van,S.M., de,H.R., Hermans,C., Nellist,M., Janssen,B., Verhoef,S., Lindhout,D., van den,O.A., Halley,D., Young,J., Burley,M., Jeremiah,S., Woodward,K., Nahmias,J., Fox,M., Ekong,R., Osborne,J., Wolfe,J., Povey,S., Snell,R.G., Cheadle,J.P., Jones,A.C., Tachataki,M., Ravine,D., Sampson,J.R., Reeve,M.P., Richardson,P., Wilmer,F., Munro,C., Hawkins,T.L., Sepp,T., Ali,J.B., Ward,S., Green,A.J., Yates,J.R., Kwiatkowska,J., Henske,E.P., Short,M.P., Haines,J.H., Jozwiak,S., and Kwiatkowski,D.J. (1997). Identification of the tuberous sclerosis gene TSC1 on chromosome 9q34. Science *277*, 805-808.

Varella-Garcia,M., Diebold,J., Eberhard,D.A., Geenen,K., Hirschmann,A., Kockx,M., Nagelmeier,I., Ruschoff,J., Schmitt,M., Arbogast,S., and Cappuzzo,F. (2009). EGFR fluorescence *in situ* hybridisation assay: guidelines for application to non-small-cell lung cancer. J. Clin. Pathol. *62*, 970-977.

Vega,F., Medeiros,L.J., Leventaki,V., Atwell,C., Cho-Vega,J.H., Tian,L., Claret,F.X., and Rassidakis,G.Z. (2006). Activation of mammalian target of rapamycin signaling pathway contributes to tumor cell survival in anaplastic lymphoma kinase-positive anaplastic large cell lymphoma. Cancer Res. *66*, 6589-6597.

Vergara,G., Belinchon,B., Valcarcel,F., Veiras,M., Zapata,I., and de la,T.A. (2008). Metastatic disease from chordoma. Clin. Transl. Oncol. *10*, 517-521.

Vignot,S., Faivre,S., Aguirre,D., and Raymond,E. (2005). mTOR-targeted therapy of cancer with rapamycin derivatives. Ann. Oncol. *16*, 525-537.

Virchow RLK (1857). Untersuchungen über des Schüdelgrundes im gesunden und krankhaften Zustande und über den Einfluss derselben auf Sch◌̈delform. In Gesichbildung und Gehirnbau, G Reimer, ed. (Berlin: p. 128.

Vivanco,I. and Sawyers,C.L. (2002). The phosphatidylinositol 3-Kinase AKT pathway in human cancer. Nat. Rev. Cancer *2*, 489-501.

Volpe,R. and Mazabraud,A. (1983). A clinicopathologic review of 25 cases of chordoma (a pleomorphic and metastasizing neoplasm). Am. J. Surg. Pathol. *7*, 161-170.

Vujovic,S., Henderson,S., Presneau,N., Odell,E., Jacques,T.S., Tirabosco,R., Boshoff,C., and Flanagan,A.M. (2006). Brachyury, a crucial regulator of notochordal development, is a novel biomarker for chordomas. J. Pathol. *209*, 157-165.

Walker,W.P., Landas,S.K., Bromley,C.M., and Sturm,M.T. (1991). Immunohistochemical distinction of classic and chondroid chordomas. Mod. Pathol. *4*, 661-666.

Wang,T.J., Shu,S.H., Lin,C.W., Chen,L.F., Lin,T.C., Chang Chien,H.S., Chan,K.Y., Lee,M.Y., Wang,Y.A., Huang,C.J., and Liu,C.C. (2008). Thoracic chordoma: an unusual presentation of the spinal tumor. Am. J. Med. Sci. *335*, 239-241.

Weber,A.L., Brown,E.W., Hug,E.B., and Liebsch,N.J. (1995). Cartilaginous tumors and chordomas of the cranial base. Otolaryngol. Clin. North Am. *28*, 453-471.

Weinberger,P.M., Yu,Z., Kowalski,D., Joe,J., Manger,P., Psyrri,A., and Sasaki,C.T. (2005). Differential expression of epidermal growth factor receptor, c-Met, and HER2/neu in chordoma compared with 17 other malignancies. Arch. Otolaryngol. Head Neck Surg. *131*, 707-711.

Wilkinson,D.G., Bhatt,S., and Herrmann,B.G. (1990). Expression pattern of the mouse T gene and its role in mesoderm formation. Nature *343*, 657-659.

Xu,Y., Fang,Y., Chen,J., and Prestwich,G.D. (2004). Activation of mTOR signaling by novel fluoromethylene phosphonate analogues of phosphatidic acid. Bioorg. Med. Chem. Lett. *14*, 1461-1464.

Yamaguchi,T., Iwata,J., Sugihara,S., McCarthy,E.F., Jr., Karita,M., Murakami,H., Kawahara,N., Tsuchiya,H., and Tomita,K. (2008). Distinguishing benign notochordal cell tumors from vertebral chordoma. Skeletal Radiol. *37*, 291-299.

Yamaguchi,T., Suzuki,S., Ishiiwa,H., Shimizu,K., and Ueda,Y. (2004a). Benign notochordal cell tumors: A comparative histological study of benign notochordal cell tumors, classic chordomas, and notochordal vestiges of fetal intervertebral discs. Am. J. Surg. Pathol. *28*, 756-761.

Yamaguchi,T., Suzuki,S., Ishiiwa,H., and Ueda,Y. (2004b). Intraosseous benign notochordal cell tumours: overlooked precursors of classic chordomas? Histopathology *44*, 597-602.

Yamaguchi,T., Yamato,M., and Saotome,K. (2002). First histologically confirmed case of a classic chordoma arising in a precursor benign notochordal lesion: differential diagnosis of benign and malignant notochordal lesions. Skeletal Radiol. *31*, 413-418.

Yang,C., Schwab,J.H., Schoenfeld,A.J., Hornicek,F.J., Wood,K.B., Nielsen,G.P., Choy,E., Mankin,H., and Duan,Z. (2009a). A novel target for treatment of chordoma: signal transducers and activators of transcription 3. Mol. Cancer Ther. *8*, 2597-2605.

Yang,X.R., Ng,D., Alcorta,D.A., Liebsch,N.J., Sheridan,E., Li,S., Goldstein,A.M., Parry,D.M., and Kelley,M.J. (2009b). T (brachyury) gene duplication confers major susceptibility to familial chordoma. Nat. Genet. *41*, 1176-1178.

Yarden,Y. and Sliwkowski,M.X. (2001). Untangling the ErbB signalling network. Nat. Rev. Mol. Cell Biol. *2*, 127-137.

Yarden,Y. and Ullrich,A. (1988). Growth factor receptor tyrosine kinases. Annu. Rev. Biochem. *57*, 443-478.

Yarosh,W., Barrientos,T., Esmailpour,T., Lin,L., Carpenter,P.M., Osann,K., nton-Culver,H., and Huang,T. (2008). TBX3 is overexpressed in breast cancer and represses p14 ARF by interacting with histone deacetylases. Cancer Res. *68*, 693-699.

York,J.E., Kaczaraj,A., bi-Said,D., Fuller,G.N., Skibber,J.M., Janjan,N.A., and Gokaslan,Z.L. (1999). Sacral chordoma: 40-year experience at a major cancer center. Neurosurgery *44*, 74-79.

Yoshimura,N., Sano,H., Hashiramoto,A., Yamada,R., Nakajima,H., Kondo,M., and Oka,T. (1998). The expression and localization of fibroblast growth factor-1 (FGF-1) and FGF receptor-1 (FGFR-1) in human breast cancer. Clin. Immunol. Immunopathol. *89*, 28-34.

Zhang,X. and Chang,A. (2008). Molecular predictors of EGFR-TKI sensitivity in advanced non-small cell lung cancer. Int. J. Med. Sci. *5*, 209-217.

Zhao,X., Wang,X., Zhou,C., Peng,R., Yan,S., and Wu,M. (1995). Abrupt reduction of c-myc expression by antisense RNA inducing terminal differentiation and apoptosis of a human esophageal cancer cell line. Sci. China B *38*, 580-589.

Zhu,X.F., Liu,Z.C., Xie,B.F., Li,Z.M., Feng,G.K., Yang,D., and Zeng,Y.X. (2001). EGFR tyrosine kinase inhibitor AG1478 inhibits cell proliferation and arrests cell cycle in nasopharyngeal carcinoma cells. Cancer Lett. *169*, 27-32.

Zorlu,F., Gurkaynak,M., Yildiz,F., Oge,K., and Atahan,I.L. (2000). Conventional external radiotherapy in the management of clivus chordomas with overt residual disease. Neurol. Sci. *21*, 203-207.